Quantitative dynamics of auxin signaling proteins in Marchantia polymorpha

Shubhajit Das

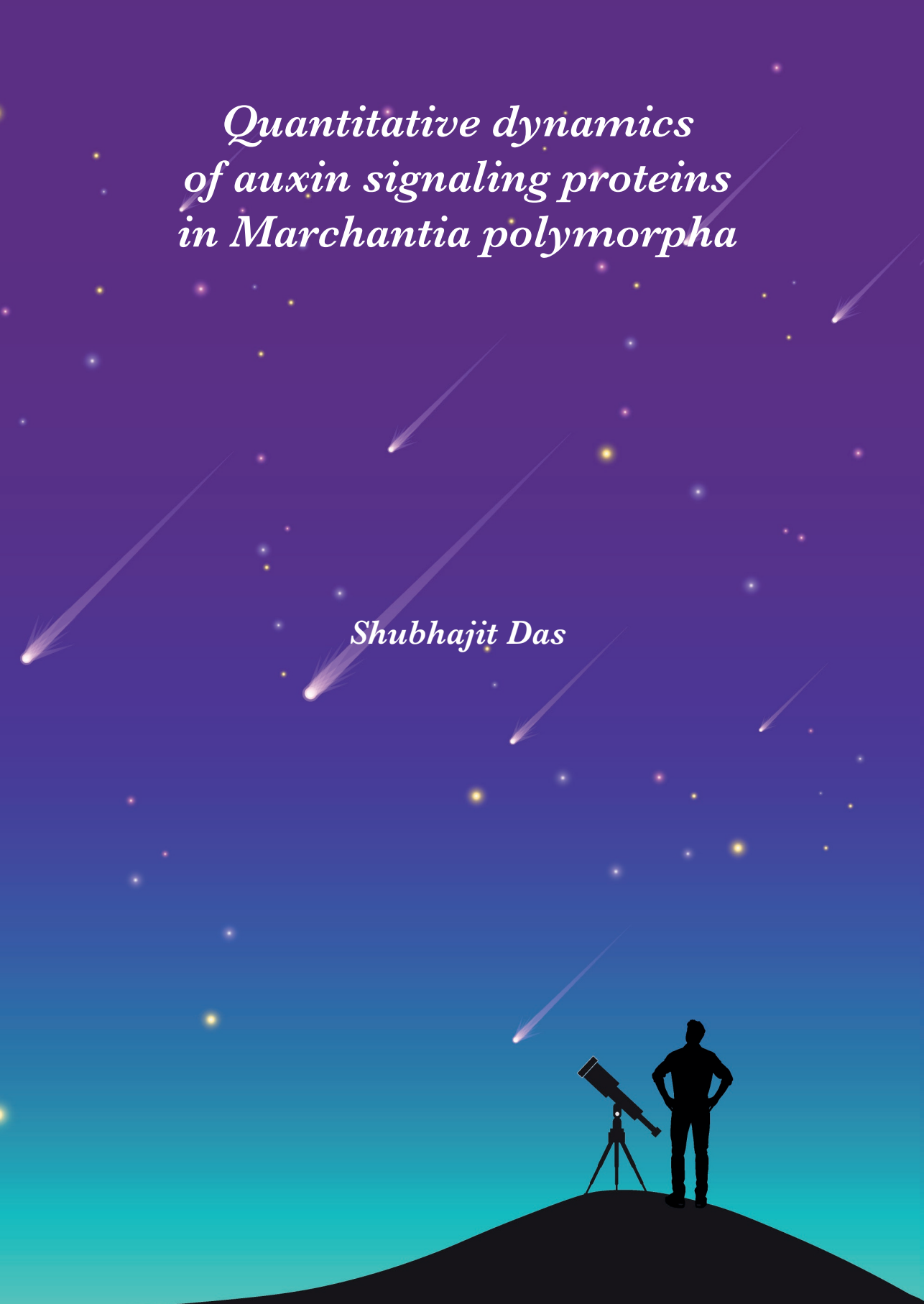

Propositions

1. Insights into relative accumulation patterns of auxin response factors is necessary to predict transcriptional auxin response in *Marchantia polymorpha*.
   (this thesis)

2. ARF2 degron occlusion in the dimer interface permits ARF2 binding only to inverted repeat auxin response elements.
   (this thesis)

3. Early career researcher job security may have adverse effects on scientific output.

4. Science progresses faster by competition than cooperation between research groups.

5. Increased public outreach of scientists will provide better role models among youth.

6. Ministry-specific higher education should be mandatory for all ministers.

Propositions belonging to the thesis, entitled "Quantitative analysis of auxin signaling proteins in *Marchantia polymorpha"*

Shubhajit Das
Wageningen, 3 May 2023

Quantitative dynamics of auxin signaling proteins in Marchantia polymorpha

Shubhajit Das

Thesis committee

Promotor
Prof. Dr Dolf Weijers
Personal Chair at the Laboratory of Biochemistry
Wageningen University & Research

Co-promotor
Dr. Jan Willem Borst
Assistant Professor, Laboratory of Biochemistry
Wageningen University & Research

Other members
Prof. Dr Leonie Bentsink, Wageningen University & Research
Prof. Dr Malcolm Bennett, University of Nottingham, UK
Prof. Dr Dorus Gadella, University of Amsterdam
Dr Isabel Monte, University of Tübingen, Germany

This research was conducted under the auspices of the Graduate School of Experimental Plant Sciences.

Quantitative dynamics of auxin signaling proteins in *Marchantia polymorpha*

Shubhajit Das

Thesis
submitted in fulfilment of the requirements for the degree of doctor
at Wageningen University
by the authority of the Rector Magnificus
Prof. Dr A.P.J. Mol,
in the presence of the
Thesis Committee appointed by the Academic Board
to be defended in public
on Wednesday 3 May 2023
at 11 a.m. in the Omnia Auditorium.

Shubhajit Das
Quantitative dynamics of auxin signaling proteins in *Marchantia polymorpha*
158 pages.

Ph.D. thesis, Wageningen University, Wageningen, the Netherlands (2023)
With references, with summary in English
ISBN: 978-94-6447-561-6
DOI: 10.18174/585707

Table of Contents

Chapter 1 **7**
Introduction

Chapter 2 **21**
Auxin response by the numbers

Chapter 3 **41**
Illuminating the nuclear auxin signaling network of *Marchantia polymorpha*

Chapter 4 **63**
Dynamic regulation of MpARF stoichiometry is required for gemma development

Chapter 5 **87**
Selective degradation of ARF2 monomers controls auxin response in Marchantia

Chapter 6 **109**
Dynamics of input and output of the auxin response system in early gemma development

Chapter 7 **135**
General Discussion

Summary **146**

Acknowledgements **149**

Curriculum Vitae **153**

Publications **154**

Educational Statement **155**

Chapter 1

Introduction

Auxin signaling in plant development

The plant hormone auxin is a key regulator of growth and development of all land plants[1,2]. A major form of naturally occurring auxin is indole-3-acetic acid (IAA), which is synthesized by a tryptophan-dependent indole pyruvic acid pathway[3]. Almost a century of research has been conducted to understand how auxin elicits a myriad of physiological and transcriptional responses. Among the multiple known routes of auxin response, the nuclear auxin signaling pathway (NAP) contributes to most of the long-term responses via transcriptional regulation[4]. Within this transcriptional auxin response system, at low auxin concentrations, Aux/IAA (Auxin/INDOLE-3-ACETIC ACID) repressors interact with ARF (AUXIN RESPONSE FACTOR) transcription factors and thereby prevent transcription of auxin-regulated genes[5–8] (Figure 1). At higher auxin concentrations, auxin is perceived by an F-box receptor protein TIR1/AFB (TRANSPORT INHIBITOR RESPONSE/AUXIN SIGNALING F-BOX) which upon auxin binding interacts with Aux/IAA repressors[9–11]. Auxin-dependent TIR1/AFB-Aux/IAA interaction results in ubiquitination of Aux/IAA by the ubiquitin ligase complexes that encompass TIR1/AFB proteins, followed by proteasomal degradation of this repressor[12]. Removal of Aux/IAA releases ARFs to control transcription of their target genes[4]. Such targets genes are marked by having auxin responsive element (AuxRE) DNA motifs present in the gene promoters[13–15].

Each of the TIR1/AFB, Aux/IAA and ARF proteins are represented by gene families in land plants[16–18]. While TIR1/AFB and Aux/IAA proteins are critical requirements for auxin-triggered gene regulatory changes, they do not appear to contribute substantially to the selectivity of gene regulation[19–21]. Instead, as the DNA-binding components, ARFs are important regulatory proteins defining which genes are subject to nuclear auxin signaling. The angiosperm *Arabidopsis thaliana* has 23 ARF transcription factors in its genome[22]. Based on phylogeny across land plants[23], ARFs have been divided into three classes: A, B and C. Functional characterization of ARFs in Arabidopsis suggests that class-A ARFs mostly act as transcriptional activators whereas class-B and C are considered as repressors[24].

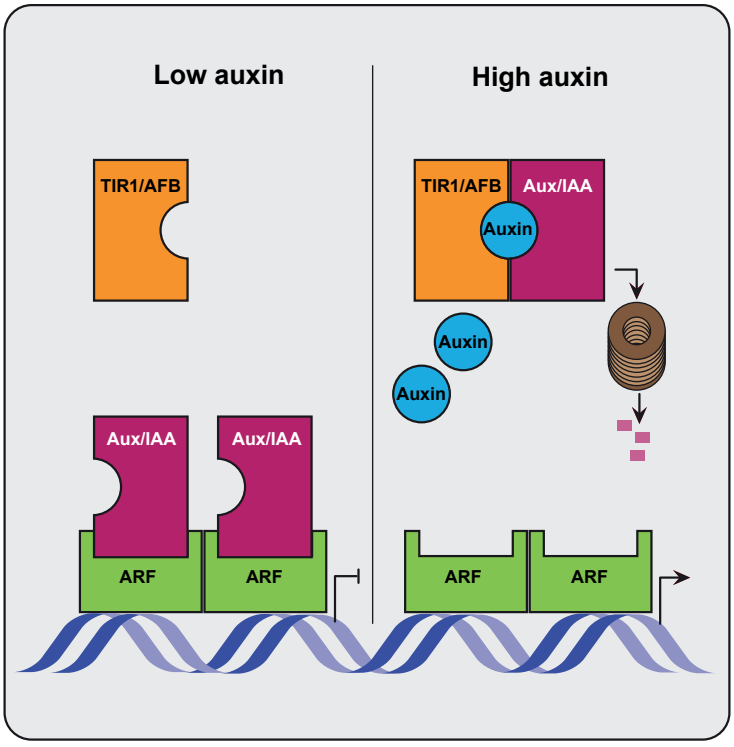

Figure 1: Simplified schematic diagram of the nuclear auxin signaling pathway (NAP). At low auxin concentrations, Aux/IAA repressors interact with ARF transcription factors and repress transcription of auxin responsive genes. At higher auxin concentrations, auxin is perceived by TIR1/AFB receptors which enhance TIR1/AFB-Aux/IAA interaction affinity. TIR1/AFB ubiquitinates Aux/IAA and targets it to proteasome for degradation. Removal of Aux/IAA allow ARFs to activate transcription of auxin responsive genes.

ARFs are composed of two structured domains; an N-terminal DNA binding domain (DBD) required for contact with DNA and a C-terminal Phox and Bem1 (PB1) domain for oligomerization and interaction with Aux/IAA proteins[7]. Flanked by these two domains, ARFs have a variable, middle region (MR) that connects the DBD and PB1 domains and is predicted to be disordered[25]. Variable amino acid composition of the MR is thought to determine the activator or repressor activity of ARFs[26]. ARFs mostly function as dimers or oligomers[13]. Dimerization of ARFs is cooperatively facilitated by the single PB1 oligomerization domain and the two dimerization domains within the DBD[27,28]. Given that these dimerization domains are conserved across ARF classes, different combinations of ARF dimers are in principle possible. In angiosperms, both homotypic and heterotypic ARF dimerization have been

reported[5,29], although the exact differences in functions of these types of interactions are not yet delineated. Moreover, most of these interactions were studied in non-physiological concentrations of these proteins in heterologous systems[5,29,30]. Whether these interactions are biologically meaningful, depends on their occurrence at endogenous concentration of each protein.

ARFs bind to DNA and selectively regulate transcription of auxin-responsive genes[14,15,31]. DNA binding by ARFs is highly specific, largely due to their function as dimers[13,27]. Using DNA-binding assays and DNA-ARF co-crystal structural analysis, ARF homodimers have been shown to bind to a tandem TGTC(TC/GG) AuxRE motif with variable spacing preference for different ARFs[27,28,32]. The repetitive binding sites together with variable spacing preference among ARFs, creates a gene regulatory system where a set of ARFs can either co-regulate a set of common genes or bind selectively to genes that have unique spacing between AuxREs. Class-A and -B ARFs were found to have similar DNA-binding preference[28]. Based on their similar affinity for TGTC(TC/GG) motif, class-A and -B ARFs have been proposed to compete for binding to AuxRE sites[28]. This competitive ARF-DNA binding has been supported by experimental evidence from multiple plant species[28,33]. Since two different classes of ARFs have similar DNA affinity, it is considered that the relative concentration of competing ARFs play a major part in determination of DNA occupancy. Given that the endogenous relative ARF concentrations are unknown in plants, the impact of differences of ARF concentration in auxin response is yet unclear.

The seemingly simple NAP controls nearly every step of plant life[2,34] beginning with seed germination[35], shoot and root development[36–39], flowering[40], stress response[41,42] to senescence[42]. How such a simple signaling system can influence plant development so broadly has been investigated for the past two decades[43]. Biochemical analysis of individual NAP components has revealed their functions and genetic analysis have helped to decipher their biological relevance. Together, these results have established the working model of NAP discussed above. However, the current NAP model describes two distinct scenarios of high -and low auxin, to predict the transcriptional output solely based on auxin concentration (Figure 1). It is important to realize that the output can be regulated at any level of signaling. For instance, even if high auxin concentrations trigger Aux/IAA degradation, a low ARF concentration may dampen the output. Therefore, it is important to consider the native dynamics of auxin and each signaling protein of the NAP while predicting the output.

This is a daunting goal to achieve in angiosperms given their large gene families. In Arabidopsis, there are in total 58 NAP proteins and there are thousands of possible interaction combinations among these. Additionally, there is no efficient tool to determine endogenous protein levels in angiosperms. Therefore, it would be ideal to study NAP in a simpler genetic network with the possibility to determine endogenous protein concentrations. With recent advancements in whole genome sequencing an early diverging plant species *Marchantia polymorpha* has emerged, which perfectly fits the idea of a simpler NAP and therefore promises an exploration of the endogenous status of NAP[44,45].

(Re)emergence of the bryophyte model *Marchantia polymorpha*

The bryophyte *Marchantia polymorpha* is a historic model plant[46]. Since the 18th century, Marchantia has been used to study the bryophyte life cycle. Much before angiosperm model plants like *Arabidopsis thaliana* came to use, plant anatomy, physiology, and cell biology were studied in Marchantia. Despite its early emergence as a model species, molecular genetic tools were unavailable until the early 21st century, while angiosperm research flourished in this period. Completion of the Marchantia genome sequencing in 2017 revealed an astonishing simplicity of genetics which reinstated interest in bryophyte research[44]. In particular, genome sequencing revealed that most biological signaling pathways including the NAP consists of the minimal number of genetic components in Marchantia[44,45,47]. This relatively reduced protein network offered a clear advantage in investigating the fundamental rules of auxin signaling.

Due to its "weedy" nature, Marchantia grows in any moist, shady areas in nature and thus maintaining this plant species in laboratory conditions is not demanding. Marchantia has a (haploid) gametophyte-dominant life cycle[48]. The complete sexual life cycle of Marchantia is short and takes approximately three months. The gametophytic generation begins with microscopic spores being released after sexual reproduction. Under favourable light conditions and nutrient sources, spores can germinate and form a prothallus which further develop into a flat thallus, which is the main photosynthetic tissue. Growth under indirect sunlight rich in far-red wavelengths, induces thallus to form gametangiophores, the specialized organs for sexual reproduction. Since Marchantia is a dioecious plant, male and female plants develop separate gametangiophores. In nature, sexual reproduction is often facilitated by rain splash that disperse motile sperm cells from male to female gametan-

giophores. Successful fertilization leads to development of a diploid zygote that marks the onset of the sporophyte generation. A zygote matures to form a sporophyte of thousands of spore mother cells that each undergo meiosis to produce spore cells. This marks the end of the short sporophyte generation. In controlled growth conditions with far-red light, it is possible to induce sporophyte generation and perform desired crosses for genetic analysis which is simplified by the haploid genome. Millions of spores produced by the sporophyte generation are a great resource, as they can be transformed by Agrobacterium[49]. In particular, spore transformation is useful to scale up low efficiency transformation such as the homologous recombination-based gene knock-in or knock-out[50]. Taking advantage of spore transformation and homologous recombination it will be possible to fluorescently tag the native proteins of NAP and determine their concentrations and dynamics *in vivo*. Recently developed monomeric fluorophores such as mNeonGreen[51] and mScarlet-I[52] with high molecular brightness allows for a quantitative imaging-based investigation of the NAP in Marchantia.

Marchantia gemma as a model to study auxin signaling

The asexual lifecycle of Marchantia is based on development and propagation of the vegetative tissue called gemmae[53]. The body plan of Marchantia is composed of thallus, a flat leaf-like tissue that grows horizontally on soil. On the dorsal side, at each bifurcation-point of thallus, a cup like structure called gemma cup is formed[53]. At the floor of gemma cups, a single epidermal cell elongates and divide asymmetrically to produce small, disc-shaped tissue called gemma, which are stored in stacks inside gemmae cups. Gemmae are asexual clones of the parent plant and remain dormant when they are stored inside gemma cups. Auxin has been proposed as a key signal in maintaining dormancy inside gemmae cups[54]. Removal of gemmae from the cup which naturally occurs by rain splash, induces gemma germination. Upon germination, gemmae start to grow and develop into a mature plant genetically identical to its parent.

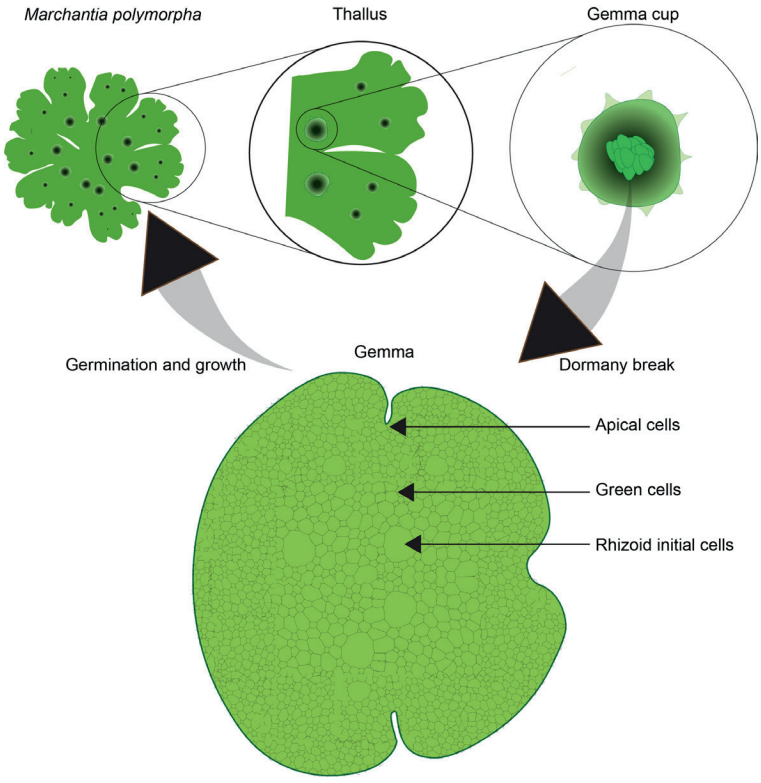

Figure 2: Vegetative lifecycle of *Marchantia polymorpha*. Mature plants produce gemma cups on the dorsal side of thallus. Gemma cups store stacks of disc-shaped gemmae and keep them dormant. On removal of gemmae from the cups, they being to germinate and grow into another mature plant that is genetically identical to the parent plant. Both male and female Marchantia plants have the same asexual lifecycle. The gemmae tissue is composed of two oppositely positioned apical notches where apical stem cells are present. Near the center of gemma a few rhizoid initial cells give rise to rhizoids upon germination. These cells are easily identified their relatively larger size and low chlorophyll content. Rest of the gemmae is made of green cells with higher chlorophyll content.

The use of Marchantia gemmae offers many unique advantages for experimental purposes. Anatomically, dormant gemmae are thin discoid tissue with the center of gemma being 5 cell layers thick and the tapered edges having 1-2 cell layers[53]. This is particularly advantageous for non-invasive microscopic imaging of live tissue. Gemmae are composed of both meristematic and differentiated cells. The meristem cells also known as apical cells are located at the center of two oppositely positioned apical notches in gemmae (Figure 2). Upon germination, the apical cells start to divide and add more cells to allow growth. At the center of gemmae, the rhizoid initial cells are formed. There are only a few of these cells which are identified by their relatively large size, lower chlorophyll content and they are specified to develop rhizoid cells af-

ter germination. The entire region between the apical notch and the rhizoid cells are composed of green cells, mainly identified by their high chlorophyll content. Apart from these three main cell types, some specialized oil cells are observed around the periphery of gemmae and are considered as storage sites for secondary metabolites. Thus, in the small tissue of gemmae it is possible to study both stem cells and differentiated cells. From the auxin signaling perspective, this is highly useful as auxin plays a major role in cell differentiation and stem cell maintenance[55].

Dormant gemmae lack any dorsiventral polarity until germination is initiated. This feature can be utilized to study establishment of photo- or gravitropism, both of which are highly auxin-dependent. Another remarkable feature of gemmae and thallus is their strong regeneration ability. While this property helps in faster vegetative propagation in laboratory, it can also be a great model to investigate auxin-dependent tissue regeneration. Gemmae remain dormant inside the cup and germination can be manually induced by simply placing gemmae on appropriate growth medium. Thus, it is easy to induce a major developmental transition and follow the natural dynamics of auxin signaling during growth. These unique qualities of Marchantia gemmae makes it an excellent model to study auxin mediated plant development.

Scope of this thesis

Molecular genetic analysis in angiosperms have enriched our vision of NAP functions. In this thesis, we extended this qualitative vision by a holistic investigation of the native dynamics of auxin input and output signals during development and present a quantitative vision of auxin signaling.

To provide a theoretical background, in **chapter 2** we briefly reviewed the state of the art of the qualitative NAP model and discussed prospects of using Marchantia NAP for a quantitative investigation. We highlight the key parameters that would be the building blocks of a quantitative model. Possible tools and resources to determine these parameters are also discussed.

In **chapter 3**, we took the first steps towards a native view of Marchantia NAP. We developed fluorescent genomic knock-in lines of all NAP proteins and described their native expression patterns in dormant gemmae. We also analysed MpARF co-expression patterns in double genomic knock-in lines.

To understand the dynamics of the ARF proteins, in **chapter 4** we followed protein accumulation patterns of the three MpARFs in germinating gemmae. We quantified ARF expression dynamics and found both MpARF1 and MpARF2 levels to decline whereas MpARF3 levels remained similar after germination. We further demonstrate that MpARF concentration decline is a result of proteasomal degradation of the proteins. We assessed the biological importance of MpARF2 degradation by computational simulations and *in vivo* manipulation of MpARF2 expression levels.

Realizing the importance ARF degradation, we focused on understanding the mechanism of MpARF2 degradation. In **chapter 5**, we systematically dissected MpARF2 domains and identified a degron region within dimerization domain 2 of DNA-binding domain. Mutation in this degron caused a strong auxin insensitivity and highlighted the importance of MpARF2 degradation. Based on an inaccessible position of the degron in MpARF2 dimer structure we explored the possibility of monomer-specific degradation. Mutation analysis indeed showed an enhanced instability of MpARF2 when dimerization is disrupted. We demonstrate the negative impact of stable monomeric ARF2 in plant growth.

In **chapter 6**, we explored the dynamics of the single auxin receptor MpTIR1, single transcriptional repressor MpAux/IAA and auxin concentration itself. We analysed how these input signals from TIR-Aux/IAA together with ARF function, result in a dynamic transcriptional output during germination.

Finally in **chapter 7,** we integrated the key conclusions of this thesis and discussed the results from a broader context of plant development, followed by a future outlook.

References

1. Benjamins, R. & Scheres, B. Auxin: The Looping Star in Plant Development. *Annu Rev Plant Biol* **59**, 443–465 (2008).
2. Vanneste, S. & Friml, J. Auxin: A Trigger for Change in Plant Development. *Cell* vol. 136 Preprint at https://doi.org/10.1016/j.cell.2009.03.001 (2009).
3. Mashiguchi, K. *et al.* The main auxin biosynthesis pathway in Arabidopsis. *Proc Natl Acad Sci U S A* **108**, (2011).
4. Weijers, D. & Wagner, D. Transcriptional Responses to the Auxin Hormone. *Annu Rev Plant Biol* **67**, 539–574 (2016).
5. Piya, S., Shrestha, S. K., Binder, B., Neal Stewart, C. & Hewezi, T. Protein-protein interaction and gene co-expression maps of ARFs and Aux/IAAs in Arabidopsis. *Front Plant Sci* **5**, (2014).
6. Ulmasov, T., Murfett, J., Hagen, G. & Guilfoyle, T. J. Aux/IAA proteins repress expression of reporter genes containing natural and highly active synthetic auxin response elements. *Plant Cell* **9**, (1997).
7. Guilfoyle, T. J. The PB1 domain in auxin response factor and aux/IAA proteins: A versatile protein interaction module in the auxin response. *Plant Cell* **27**, 33–43 (2015).
8. Han, M. *et al.* Structural basis for the auxin-induced transcriptional regulation by Aux/IAA17. *Proc Natl Acad Sci U S A* **111**, (2014).
9. Dharmasiri, N., Dharmasiri, S. & Estelle, M. The F-box protein TIR1 is an auxin receptor. *Nature* **435**, 441–445 (2005).
10. Tan, X. *et al.* Mechanism of auxin perception by the TIR1 ubiquitin ligase. *Nature* **446**, 640–645 (2007).
11. Kepinski, S. & Leyser, O. The Arabidopsis F-box protein TIR1 is an auxin receptor. *Nature* **435**, 446–451 (2005).
12. Gray, W. M., Kepinski, S., Rouse, D., Leyser, O. & Estelle, M. Auxin regulates SCFTIR1-dependent degradation of AUX/IAA proteins. *Nature* **414**, 271–276 (2001).
13. Ulmasov, T., Hagen, G. & Guilfoyle, T. J. Dimerization and DNA binding of auxin response factors. *Plant Journal* **19**, (1999).
14. Galli, M. *et al.* The DNA binding landscape of the maize AUXIN RESPONSE FACTOR family. *Nat Commun* **9**, (2018).
15. Stigliani, A. *et al.* Capturing Auxin Response Factors Syntax Using DNA Binding Models. *Mol Plant* **12**, 822–832 (2019).
16. Parry, G. *et al.* Complex regulation of the TIR1/AFB family of auxin receptors. *Proc Natl Acad Sci U S A* **106**, 22540–22545 (2009).
17. Guilfoyle, T. J., Ulmasov, T. & Hagen, G. The ARF family of transcription factors and their role in plant hormone-responsive transcription. *Cellular and Molecular Life Sciences* vol. 54 Preprint at https://doi.org/10.1007/s000180050190 (1998).
18. Luo, J., Zhou, J. J. & Zhang, J. Z. Aux/IAA gene family in plants: Molecular structure, regulation, and function. *International Journal of Molecular Sciences* vol. 19 Preprint at https://doi.org/10.3390/ijms19010259 (2018).
19. Muto, H., Watahiki, M. K., Nakamoto, D., Kinjo, M. & Yamamoto, K. T. Specificity and similarity of functions of the Aux/IAA genes in auxin signaling of arabidopsis revealed by promoter-exchange experiments among MSG2/IAA19, AXR2/IAA7, and SLR/IAA14. *Plant Physiol* **144**, (2007).
20. Prigge, M. J. *et al.* Genetic analysis of the arabidopsis TIR1/AFB auxin receptors reveals both overlapping and specialized functions. *Elife* **9**, (2020).

21. Weijers, D. *et al.* Developmental specificity of auxin response by pairs of ARF and Aux/IAA transcriptional regulators. *EMBO Journal* **24**, 1874–1885 (2005).
22. Roosjen, M., Paque, S. & Weijers, D. Auxin Response Factors: Output control in auxin biology. *J Exp Bot* **69**, 179–188 (2018).
23. Finet, C., Berne-Dedieu, A., Scutt, C. P. & Marlétaz, F. Evolution of the ARF gene family in land plants: Old domains, new tricks. *Mol Biol Evol* **30**, (2013).
24. Ulmasov, T., Hagen, G. & Guilfoyle, T. J. Activation and repression of transcription by auxin-response factors. *Proc Natl Acad Sci U S A* **96**, (1999).
25. Powers, S. K. *et al.* Nucleo-cytoplasmic Partitioning of ARF Proteins Controls Auxin Responses in Arabidopsis thaliana. *Mol Cell* **76**, 177-190.e5 (2019).
26. Tiwari, S. B., Hagen, G. & Guilfoyle, T. The roles of auxin response factor domains in auxin-responsive transcription. *Plant Cell* **15**, (2003).
27. Boer, D. R. *et al.* Structural basis for DNA binding specificity by the auxin-dependent ARF transcription factors. *Cell* **156**, 577–589 (2014).
28. Kato, H. *et al.* Design principles of a minimal auxin response system. *Nat Plants* **6**, (2020).
29. Vernoux, T. *et al.* The auxin signalling network translates dynamic input into robust patterning at the shoot apex. *Mol Syst Biol* **7**, (2011).
30. Rios, A. F., Radoeva, T., de Rybel, B., Weijers, D. & Borst, J. W. Fret-flim for visualizing and quantifying protein interactions in live plant cells. in *Methods in Molecular Biology* vol. 1497 (2017).
31. Ulmasov, T., Hagen, G. & Guilfoyle, T. J. ARF1, a transcription factor that binds to auxin response elements. *Science (1979)* **276**, 1865–1868 (1997).
32. Freire-Rios, A. *et al.* Architecture of DNA elements mediating ARF transcription factor binding and auxin-responsive gene expression in Arabidopsis. *Proc Natl Acad Sci U S A* **117**, (2020).
33. Lavy, M. *et al.* Constitutive auxin response in Physcomitrella reveals complex interactions between Aux/IAA and ARF proteins. *Elife* **5**, (2016).
34. Kepinski, S. & Leyser, O. Plant development: Auxin in loops. *Current Biology* vol. 15 Preprint at https://doi.org/10.1016/j.cub.2005.03.012 (2005).
35. Liu, X. *et al.* Auxin controls seed dormancy through stimulation of abscisic acid signaling by inducing ARF-mediated ABI3 activation in Arabidopsis. *Proc Natl Acad Sci U S A* **110**, (2013).
36. Ding, Z. & Friml, J. Auxin regulates distal stem cell differentiation in Arabidopsis roots. *Proc Natl Acad Sci U S A* **107**, (2010).
37. Billou, I. *et al.* The PIN auxin efflux facilitator network controls growth and patterning in Arabidopsis roots. *Nature* **433**, 39–44 (2005).
38. Lavenus, J. *et al.* Lateral root development in Arabidopsis: Fifty shades of auxin. *Trends in Plant Science* vol. 18 Preprint at https://doi.org/10.1016/j.tplants.2013.04.006 (2013).
39. Schlereth, A. *et al.* MONOPTEROS controls embryonic root initiation by regulating a mobile transcription factor. *Nature* **464**, 913–916 (2010).
40. Cucinotta, M., Cavalleri, A., Chandler, J. W. & Colombo, L. Auxin and flower development: A blossoming field. *Cold Spring Harb Perspect Biol* **13**, (2021).
41. Korver, R. A., Koevoets, I. T. & Testerink, C. Out of Shape During Stress: A Key Role for Auxin. *Trends in Plant Science* vol. 23 Preprint at https://doi.org/10.1016/j.tplants.2018.05.011 (2018).

42. Ellis, C. M. *et al.* AUXIN RESPONSE FACTOR1 and AUXIN RESPONSE FACTOR2 regulate senescence and floral organ abscission in Arabidopsis thaliana. *Development* **132**, (2005).
43. Friml, J. Fourteen Stations of Auxin. *Cold Spring Harbor perspectives in biology* vol. 14 Preprint at https://doi.org/10.1101/cshperspect.a039859 (2022).
44. Bowman, J. L. *et al.* Insights into Land Plant Evolution Garnered from the Marchantia polymorpha Genome. *Cell* **171**, (2017).
45. Flores-Sandoval, E., Eklund, D. M. & Bowman, J. L. A Simple Auxin Transcriptional Response System Regulates Multiple Morphogenetic Processes in the Liverwort Marchantia polymorpha. *PLoS Genet* **11**, 1–26 (2015).
46. Bowman, J. L., Araki, T. & Kohchi, T. Marchantia: Past, present and future. *Plant Cell Physiol* **57**, 205–209 (2016).
47. Kato, H. *et al.* The roles of the sole activator-type auxin response factor in pattern formation of marchantia polymorpha. *Plant Cell Physiol* **58**, 1642–1651 (2017).
48. Shimamura, M. Marchantia polymorpha: Taxonomy, phylogeny and morphology of a model system. *Plant Cell Physiol* **57**, 230–256 (2016).
49. Ishizaki, K., Chiyoda, S., Yamato, K. T. & Kohchi, T. Agrobacterium-mediated transformation of the haploid liverwort Marchantia polymorpha L., an emerging model for plant biology. *Plant Cell Physiol* **49**, 1084–1091 (2008).
50. Ishizaki, K., Johzuka-Hisatomi, Y., Ishida, S., Iida, S. & Kohchi, T. Homologous recombination-mediated gene targeting in the liverwort Marchantia polymorpha L. *Sci Rep* **3**, 1–6 (2013).
51. Shaner, N. C. *et al.* A bright monomeric green fluorescent protein derived from Branchiostoma lanceolatum. *Nat Methods* **10**, (2013).
52. Bindels, D. S. *et al.* MScarlet: A bright monomeric red fluorescent protein for cellular imaging. *Nat Methods* **14**, (2016).
53. Kato, H., Yasui, Y. & Ishizaki, K. Gemma cup and gemma development in Marchantia polymorpha. *New Phytologist* vol. 228 Preprint at https://doi.org/10.1111/nph.16655 (2020).
54. Eklund, D. M. *et al.* Auxin produced by the indole-3-pyruvic acid pathway regulates development and gemmae dormancy in the liverwort marchantia polymorpha. *Plant Cell* **27**, 1650–1669 (2015).
55. Ma, Y. *et al.* WUSCHEL acts as an auxin response rheostat to maintain apical stem cells in Arabidopsis. *Nat Commun* **10**, (2019).

Chapter 2

Auxin response by the numbers

Shubhajit Das, Dolf Weijers and Jan Willem Borst
Laboratory of Biochemistry, Wageningen University, the Netherlands

A modified version of this chapter has been published as:
Das S., Weijers D. and Borst JW (2021) Auxin response by the numbers. Trends in Plant Sciences. 26 (5), 442-451. DOI: 10.1016/j.tplants.2020.12.017

Abstract
Auxin is fundamental to growth and development of land plants, and acts in large part through the control of gene activity. Genetic and biochemical analysis of the nuclear auxin signaling pathway (NAP) has led to the establishment of a generic model for auxin-dependent gene regulation. However, to understand how this dynamic system operates in living cells, quantitative data are needed. We describe how the use of the liverwort *Marchantia polymorpha* with its limited number of NAP components, combined with experimental approaches to determine concentrations, binding affinities, and turnover rates, will enable a new, quantitative view on the mechanisms that allow auxin to control plant growth and development.

The Nuclear Auxin Signaling Pathway

Auxin-induced physiological and transcriptional responses are at the heart of land plant growth and development[1–3]. Auxin is perceived by TIR1/AFB (TRANSPORT INHIBITOR RESPONSE1/AUXIN-BINDING F-BOX) an F-box protein in the **$SCF^{TIR1/AFB}$ complex** (see Glossary)[4,5], and its Aux/IAA (Auxin/INDOLE-3-ACETIC ACID) substrate[6,7]. At low cellular auxin concentration, Aux/IAA repressors interact with DNA-binding ARFs (AUXIN RESPONSE FACTORS) via their shared **PB1 domain** and prevent ARF-driven transcription. At high auxin level, the $SCF^{TIR1/AFB}$ complex initiates ubiquitination and degradation of Aux/IAA repressors, allowing ARFs to regulate gene transcription[8,9]. Based on phylogeny, ARFs are divided into three classes: class-A, B and C. Transient assays have shown that A-ARFs tend to activate transcription, whereas B/C-ARFs are considered repressors[7].

In the last two decades, fluorescent transcriptional and translational reporters have been used to map the activity of the NAP genes and proteins in various plant tissues[10–12]. In addition, the network of protein-protein and protein-DNA interactions among the response components has been established[13–16]. These investigations provided a qualitative view of the functions of each signaling protein family and a generic mechanistic model for auxin-driven gene activation. However, it is well known that responses to auxin in plant tissues are extremely diverse, e.g. high auxin inhibits root growth, yet promotes hypocotyl growth[17–19]. This demonstrates that qualitative information alone is not sufficient to explain differential auxin sensitivities and cell/tissue-specific responses. The dynamics and diversity of auxin responses could be encrypted in cellular protein abundance, protein-protein/DNA interaction affinities, complex stoichiometry, turnover rates etc. Here, we argue that systematic quantitative analysis of auxin response is the next frontier in auxin research.

The Arabidopsis Auxin Response Network: A Tangled Web of Paralogs

Whole genome duplications have played a central role in the evolution of land plants. From **Charophytes** through **Angiosperms**, genome duplications have inflated gene families with multiple **paralogs** and allowed their **sub/neofunctionalization** thereby expanding genome complexity, spurring physiological innovations[20]. Higher paralog numbers in Angiosperms gave rise to multiple auxin signaling proteins with overlapping, or in cases non-redundant functions[21]. In *Arabidopsis thaliana*, 6 AtTIR1, 23 AtARFs and 29 AtAux/IAAs constitute the NAP[22]. These 58 proteins create thousands of possible interaction combinations which makes it nearly impossible to quantitatively

describe the system. However, a qualitative AtARF-Aux/IAA interaction network has been obtained with **yeast-2-hybrid** assays (see text box1) showing that AtAux/IAAs can homodimerize and also heterodimerize with class-A ARFs while interactions are more limited with class-B/C ARFs[23,24]. These studies provided a static, binary interactome for AtARF-Aux/IAA interactions, but lack binding affinities and interaction dynamics.

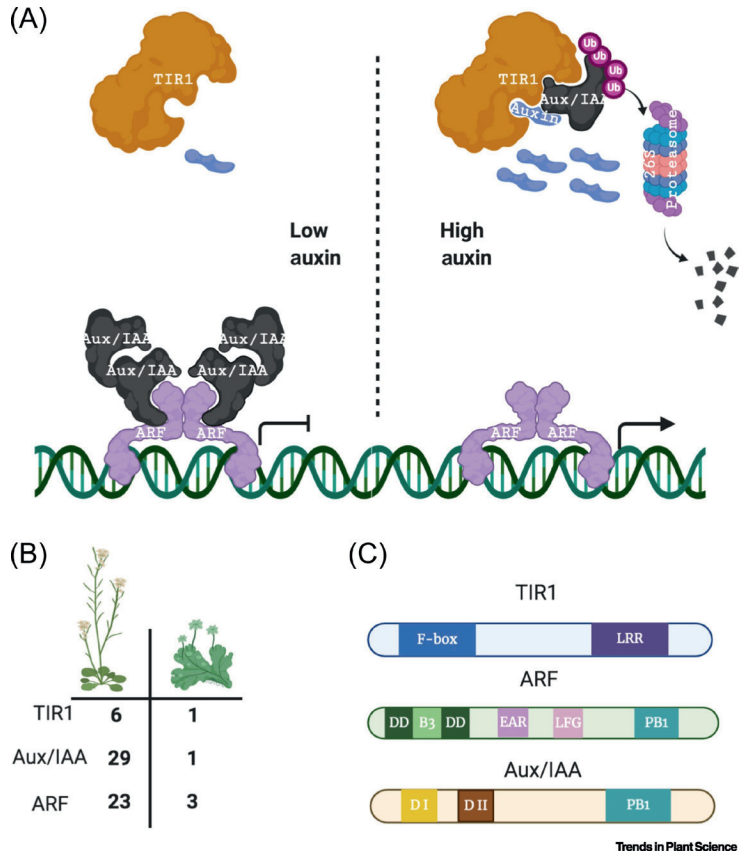

Figure 1: (a) Schematic representation of the Nuclear Auxin signaling Pathway (NAP). At low cellular auxin level, the hormone is not perceived by the TIR1 receptor allowing the Aux/IAA repressors to persist and bind to ARF transcription factors. This interaction prevents ARFs from driving gene transcription. At high cellular auxin concentration, the hormone is perceived by the TIR1-Aux/IAA co-receptor complex which is followed by ubiquitination and proteasomal degradation of Aux/IAA proteins. In absence of Aux/IAA repressors, ARFs activate auxin induced gene transcription. (b) *Arabidopsis thaliana* harbours multiple auxin response proteins whereas *Marchantia polymorpha* has only one response protein of each family. Domain architecture of auxin response proteins: (c) TIR1 receptor has an N-terminal F-box domain for interaction with other SCF complex subunits. A C-terminal leucine-rich-repeat (LRR) domain mediates binding to auxin and Aux/IAA repressors. ARF TFs have a B3 DNA-binding domain inserted between two halves of a dimerization domain (DD) at the N-terminus. The unstructured middle region (MR) of ARFs has class-dependent amino acid composition. Class-A ARFs have glutamine-rich MR, whereas Class-B

and C ARFs have a proline/serine-rich MR. Some ARFs have EAR and LFG motifs for the interaction with TPL. The C-terminal end of ARFs and Aux/IAA have a Phox and Bem1(PB1) domain for ARF-ARF and ARF-Aux/IAA oligomerization. At N-terminus of Aux/IAA repressors, a domain 1 (DI) mediates TPL recruitment while domain 2 (DII) harbours a degron motif for recognition and degradation of Aux/IAA by TIR1-SCF complex. A C-terminal PB1 domain allows oligomerization. This figure was created using BioRender.

Auxin has strong influence on plant growth and therefore any mutation in key signaling genes is expected to manifest into a phenotype. However, due to the high genetic redundancy, single mutations in AtTIR1/AFB genes do not cause strong defects[25]. Likewise, only a few loss of function mutants of AtAux/IAA (IAA3, 7, 28) with growth defects have been reported[26–29]. Out of the 23 At-ARFs, only 5 show strong phenotypes as single mutants[30], which impedes the dissection of individual function of each NAP proteins. In all these families, higher-order mutants do reveal biological function[11], supporting the notions of functional redundancy.

Beyond redundancy, partial functional diversification among paralogous proteins in Arabidopsis generates a complex set of cell-specific auxin response systems. It is well understood that intracellular auxin perception results in liberation of ARFs from Aux/IAAs allowing activation of auxin responsive genes. However, this activation model does not clarify the roles of the different ARF classes. Recently, analysis of the minimal auxin response system of *Marchantia polymorpha* (hereafter Marchantia) provided insight into these roles[31].

The Marchantia Auxin Response System: A Rudimentary Design

The liverwort *Marchantia polymorpha*[32] has an auxin response network operating with the least possible number of signaling components: one copy of MpTIR1 and MpAux/IAA, and three MpARFs representing each phylogenetic classes[33,34]. Out of the 3 MpARFs, MpARF1 acts as an activator, while MpARF2 and MpARF3 are repressors[31,33]. This simple network dramatically reduces the number of protein interaction combinations and opens an opportunity for *in vivo* quantitative research.

While Marchantia has been a model bryophyte for almost a century, modern genetic tools for this species were unavailable until recently. Progress in T-DNA transformation methods, CRISPR/Cas gene editing and homologous recombination have paved the way for modern genetics and genomics on this haploid model[35–41]. Therefore, Marchantia represents an epitome of a model system for both evolutionary and quantitative auxin research.

Protein Concentrations Define Response Output

A long-standing hypothesis on auxin signaling is the competition between class-A and B ARFs for binding similar **AuxRE**[23,31,42]. Distinct intracellular ARF concentrations could rationalize this hypothesis as contrasting levels of class-A and B ARFs could dictate which ARF binds an AuxRE. Differing expression profiles of MpARFs in genomic knock-in translational fusion lines further endorsed this notion[31]. Additionally, auxin sensitivity could be highly dependent on the concentration of TIR1, as low concentrations of this receptor could dampen auxin response. At high auxin levels, the Aux/IAA concentration depletes and favours ARF dimerization. Therefore, concentration of these proteins within the cell is a determinant of homo-heteromer or monomer-oligomer equilibria. However, determining native protein concentrations from a single plant cell is unattainable due to technical limitations, which has caused our sparse understanding of how response protein abundance modulates auxin signaling. Utilizing the simplicity of Marchantia NAP, and if all auxin signaling proteins are fluorescently labelled at endogenous locus, quantification of absolute protein concentrations would be possible with Fluorescence Correlation Spectroscopy **(FCS**) and Raster Image Correlation Spectroscopy **(RICS)** methods[43]**,** but these approaches remain very challenging in plants. Furthermore, a key modulator of the native protein concentration is the **turnover rate** of a protein, which in turn can depend on post-translational modifications (PTM) and its cooperative stability in a complex. Most NAP components are reported to undergo PTM[44,45] and oligomerization[46–49]. Hence, it is imperative to learn how native protein concentrations are affected by these modifications.

Binding Affinities Define the Response Network

The auxin response network is defined by protein-protein and protein-DNA interactions. For example, ARFs and Aux/IAAs have a shared C-terminal PB1 domain which mediates their homo- and heterotypic interactions[13,14]. Crystallography studies on wildtype and mutated PB1 domains of AtARF5, AtARF7 and AtIAA17 have shown the presence of opposite electrostatic interfaces in this domain which may facilitate oligomerization[46,47].

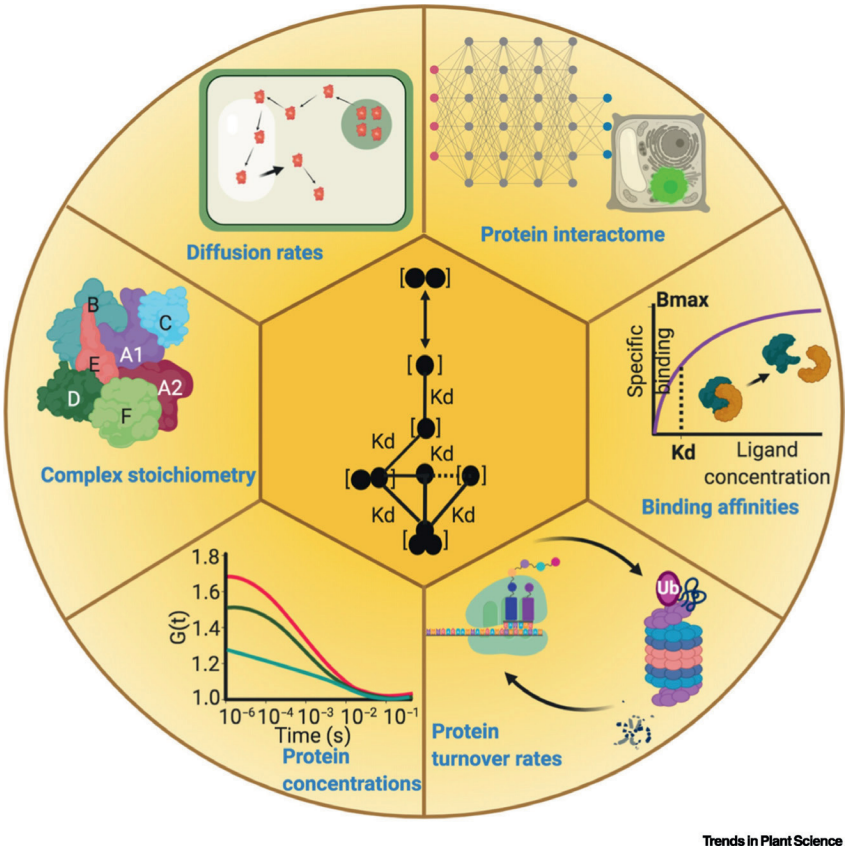

Figure 2: Key quantitative parameters that can regulate nuclear auxin signaling. Determination and integration of these parameters will allow development of a quantitative mathematical model for output prediction of auxin signaling network. This figure was created using BioRender.

To understand the logic behind preferential binding and stable/transient complex formation, it is essential to determine **dissociation constants (Kd)** of all biomolecular interactions in NAP. Quantification of Kds of purified proteins or isolated protein domains can be performed using biophysical methods like isothermal titration calorimetry (**ICT**), Microscale Thermophoresis (**MST**), Surface Plasmon Resonance (**SPR**), Single Molecule Förster Resonance Energy Transfer (**smFRET**) and FCS**.**

In Arabidopsis, binding affinities of different TIR1/AFB-Aux/IAA co-receptor members were determined using SPR[50]. The results showed that all AtAux/IAA degron peptides have very rapid dissociation rates from AtAFB5 (K_{off} ranging 1.1 to 1.9 × 10^{-2} s^{-1}) as compared to AtTIR1 (K_{off} ranging 3.3 to 5.8×10^{-3} s^{-1})[50]. ITC experiments with PB1 domains of ARF and Aux/IAA have shown that PB1 heterodimerization of ARF5-Aux/IAA17 has a higher affinity (Kd ~0.07 μM) than either ARF5 (Kd 0.2-0.9 μM) or Aux/IAA17 (Kd 6.5 μM) homodimerization, and values of ARF7 homodimerization support these differences[51–53]. However, it should be noted that these distinct affinities for homo- versus heterotypic PB1 interactions, derived from a few Aux/IAA and ARF proteins in Arabidopsis, may not reflect the typical behaviour of these protein families. Apart from the PB1 domain, the N-terminal DNA binding domain (**DBD**) can also facilitate AtARF1 and AtARF5 dimerization[16]. Hence, the binding constant of full length ARFs and Aux/IAAs is required to understand the significance of divergent interaction affinities.

In addition to variable protein-protein interaction (PPI) affinities, ARF-DNA affinity is another important regulatory module. ARFs can bind AuxRE motif as dimers[16,54]. Differential DNA binding affinities among ARFs influence which ARF dimer forms and binds to the promoter to regulate transcription. Two well-known ARF binding DNA motifs are TGTCTC[16,55] and TGTCGG[16] both known to be bound by class-A and class-B ARFs. However, there are experimental evidences that different ARF classes may have different preferences for AuxREs. For example, in genome-wide DAPseq experiments, class-A ARFs showed higher enrichment for the TGTCGG motif whereas class-B ARFs were enriched for TGTCTC[42]. Additionally, ARFs may have non-overlapping DNA binding sites between different classes, further suggesting variable ARF-DNA binding preferences. Recent bioinformatics analysis of *cis* elements showed that auxin induced genes may have other TGTCNN motifs in their promoter besides the two hexameric consensus motifs[55–57]. Identification of novel AuxRE elements and determination of ARF-AuxRE binding affinities could explain the basis for specificity of ARF induced gene regulation. To determine ARF-AuxRE affinities, smFRET would be the method of choice as this tool can track binding and unbinding dynamics. Recently, smFRET analysis revealed that MpARF1-DBD (Kd ~12nM) has higher AuxRE binding affinity than MpARF2-DBD (Kd ~61nM), suggesting competitive advantage for ARF1[31]. A similar mode of binding affinities were found in smFRET with AtARF1 (class-B) and AtARF5 (class-A), where class-A AtARF5 binds to DR5 and IR8 motifs with higher affinity than class-B AtARF1[58].

These independent observations encourage a systematic survey of protein-protein/DNA interaction analysis to understand auxin response. Due to the lack of adaptable *in vivo* Kd determination tools, most studies have been using *in vitro* methods as discussed above. These *in vitro* Kd values are good starting points, but it is important to note that *in vivo* Kd values can be affected by PTMs, presence of binding competitor and intracellular crowding etc. and thus could be different than known *in vitro* Kd values.

Regulation of NAP by Dynamic Stoichiometry of protein complexes

In auxin signaling, most protein interactions are transient, context-specific and restricted in specific tissues, cell types or even in organelles[59]. Therefore, imaging-based PPI assays offering dynamic analysis, can illuminate these interactions. Recently, the interaction between overexpressed MpTOPLESS (MpTPL) and MpARF1 andMpARF2 was tested in Arabidopsis protoplasts using FRET- Fluorescence Lifetime Microscopy (**FRET-FLIM**). MpTPL and MpARF1 did not interact whereas a clear interaction between MpTPL and MpARF2 was observed. Interestingly, the interaction was abrogated in the MpARF2 **LFG motif** mutant, indicating a role of this motif in MpTPL-MpARF2 association[31]. Future FRET-FLIM studies with natively expressed signaling proteins would allow spatial resolution of protein interactions and enrichment of quantitative models for tissue-specific output prediction.

Although many protein complexes within the core auxin response network are known, the stoichiometry of those complexes remains unclear. Crystal structure analysis of the N-terminus of AtTPL suggested that it might form tetramers. This observation was corroborated by a protoplast based repression assay where impaired TPL tetramerization by mutation showed higher **DR5 reporter** activity[49]. However, the functional significance of TPL oligomerization is still unknown. Likewise, crystallography of Aux/IAA proteins[46,47] and bimolecular fluorescence complementation (**BiFC**)**,** Y2H assays of TIR1[48] suggests possible oligomerisation of these auxin signaling proteins. Having multiple signaling proteins that can oligomerize, raises a question -what is their actual stoichiometry in a transcriptional regulatory complex and how important are these oligomerizations in auxin output? Therefore, dissection of protein complexes with all constituting proteins expressed at endogenous level is essential. An emerging mechanism of ARF complex formation is their condensate formation by liquid liquid phase separation (**LLPS**)**.** Arabidopsis ARF7 and ARF19 have been shown to phase separate in the cytoplasm of differentiated root cells, as a partitioning mechanism to diminish auxin re-

sponse[60]. Whether condensate formation is a conserved phenomenon among MpARFs would be the next question to address. Nuclear condensate formation of ARFs could regulate transcriptional complex stoichiometry and act as a transcriptional hub of auxin response genes.

Protein Diffusion As a Parameter

Subcellular protein abundance, protein-protein/DNA interactions are limited by protein diffusion rates. Transcription factors (TF) like ARFs may diffuse freely within the nucleus in a 3-dimensional (3D) motion or be facilitated by the electrostatic attraction between DNA and TFs. The facilitated form of diffusion includes 1D sliding motion along the DNA length, intersegmental transfer and hopping of TFs[61,62]. Due to slow 3D diffusion, TFs get access to the entire genome, whereas facilitated diffusion allows TFs to rapidly switch between genes during a quick transcriptional response. Another important purpose served by random 3D diffusion, is the continuous collision between various proteins, thereby allowing to find interaction partners and form protein complexes. Calculating diffusion dynamics of proteins can provide a better insight of their oligomerisation status, ARF-DNA binding dynamics and probability of interaction . Relatively fast or slow diffusion rates of auxin signaling proteins could give an indication whether it is part of a large protein complex or a free monomer. Based on variable diffusion rates of ARFs, one could differentiate DNA-bound and freely diffusing ARFs. It is important to note that the intracellular environment is nonhomogeneous and therefore diffusion rates of a protein can differ based on its subcellular location, the temperature, molecular weight, concentration etc. **Diffusion coefficients** can be measured *in vivo* using **FRAP**, **FCS/FCCS**, and **RICS** and pair correlation function **(pCF)** allows to track the path of movement/diffusion of a labelled molecule. In contrast to measuring protein concentrations (see above), the use of RICS to determine diffusion does not suffer significantly from autofluorescence, and is therefore a promising approach.

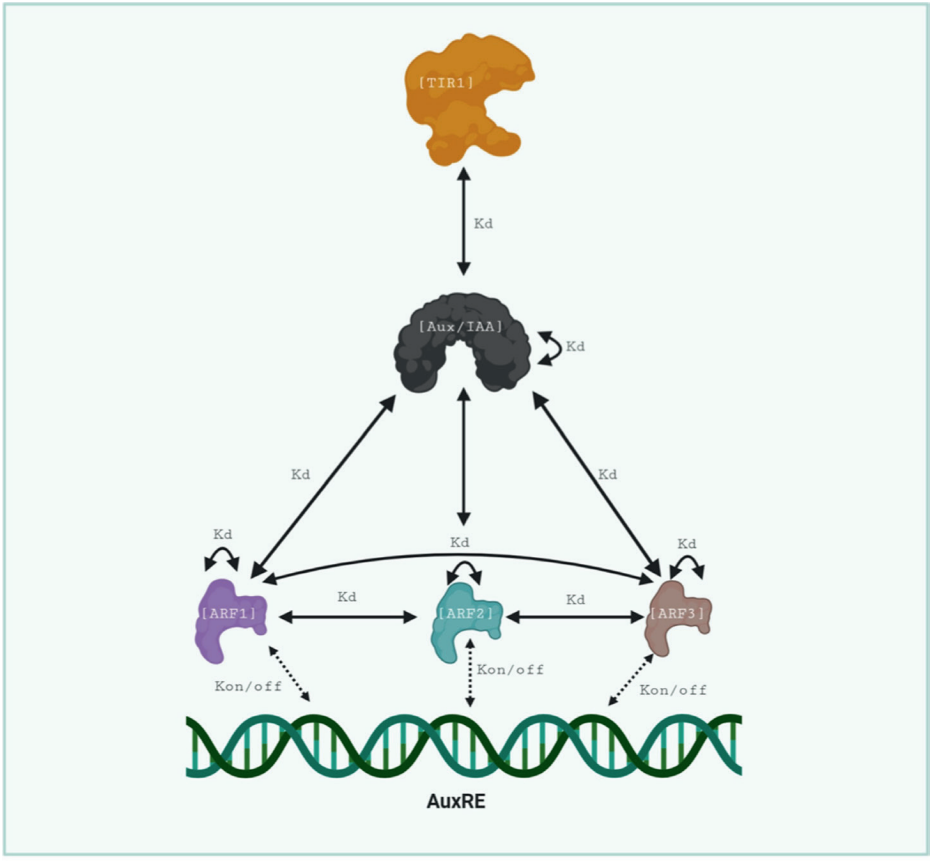

Figure 3: A hypothetical quantitative model of auxin response protein network of *Marchantia polymorpha.* This figure was created using BioRender.

Concluding Remarks

For almost a century, plant biologists have been intrigued by the incredible functional diversity of the small auxin molecule. Even though extensive qualitative research has been conducted, the entire operational complexity of the NAP is still a conundrum. Recent genome analysis and phylogenetic studies have indicated the presence of simple auxin signaling network in Marchantia, which has opened up opportunities to explore auxin signaling from a quantitative perspective.

Employing genetic and biochemical approaches we have substantial qualitative background to proceed towards a quantitative investigation of auxin signaling. Semi-quantitatively visualising auxin response has become pos-

sible with the development of fluorescent reporters for auxin activity such as **DR5**, **DII-Venus**, **DR5v2** and **R2D2**[63,64]. These reporters revealed differences in auxin sensitivity and transcriptional responses across plant tissues. Simultaneous advancements in hardware technologies and implementation of functional imaging modalities has promoted quantitative analysis in auxin biology.

Determination of protein-protein/DNA interaction affinities will explain how structural features of these proteins contribute to a dynamic and specific auxin response. Estimation of *in vivo* ARF concentrations can clarify how competition for same DNA motif binding between different ARFs is regulated. Protein turnover and diffusion rates will reflect on how local concentration of response proteins are maintained within a cell. ARF protein complex stoichiometry analysis will help determining actual constituents of auxin induced transcriptional activator or repressor complexes. Beyond these properties, it will also be critical to determine how post-translational modifications of NAP components influence activity and response output. The various microscopy tools mentioned above will aid in achieving these goals. To deal with the multitude of quantitative data generated, interdisciplinary collaborations will be required that will lead to an integrative mathematical auxin response model. Mathematical models will help us answer biological questions that are difficult to address experimentally. In the past decade, several mathematical models have been developed to understand aspects of auxin and other plant hormone signaling[65,66]. Such models can describe various scales, from the molecular to the cellular and tissue level. Each allows addressing different questions and requires a different level of detail and granulation. The simplicity of Marchantia anatomy would hopefully bring us closer to integrating these scales in multi-level models. Since auxin signaling is wired tightly with other plant hormone signaling pathways, a complete mathematical model of the auxin system grounded in measurement of most (or all) possible parameters may also be a starting point to address how the auxin system connects to other hormone signalling pathways. Finally, in foreseeable future the challenge will be to develop quantitative models for other plant hormone signaling pathways and their amalgamation into one unified model of plant development.

Glossary:

Angiosperms: seed-bearing flowering plants with a complete vascular system.

Auxin responsive elements (AuxRE): sequence-specific DNA motifs present in the promoter of auxin-regulated genes; these serve as ARF binding sites.

Charophytes: extant group of green algae that are sister to land plants.

DII-Venus: an auxin reporter based on the Aux/IAA DII degron motif fused to a Venus fluorophore. In presence of auxin this reporter protein is degraded, and it thus serves as a "negative" sensor for the presence of auxin .

Diffusion coefficient: the proportionality constant between molar flux and concentration gradient.

Direct Repeat5 (DR5): a synthetic reporter designed with a tandem direct repeat of an 11 bp region containing the AuxRE TGTCTC, used to visualise cells with high auxin response.

Dissociation constant (Kd): an equilibrium constant to signify reversible dissociation rate of a multimeric complex.

DNA binding domain (DBD): the specific protein domain in a transcription factor that allows DNA binding.

DR5v2:a version of the DR5 promoter with the high-affinity ARF binding site TGTCGG as the AuxRE sequence.

Fluorescence lifetime: the fluorophore-specific time elapsed between fluorophore excitation and return to ground state by emission of photons.

LFG motif: a TOPLESS binding motif conserved in class-B ARFs.

Liquid-liquid phase separation (LLPS): spontaneous demixing of a homogeneous protein solution into membrane-less condensed liquid like droplets which may function as storage, partitioning or active transcriptional sites.

Neofunctionalization: acquisition of a completely new function by a paralog after gene duplication.

Paralogs: copies of the same gene generated by genome duplications.

PB1 domain: a conserved oligomerization domain present in both animal and plant kingdoms; a C-terminal PB1 domain mediates homo- and heterotypic ARF and Aux/IAA interactions.

Ratiometric version of 2 D2s (R2D2): a semiquantitative reporter of auxin activity; it is composed of a mutant DII-ntdTomato and DII-n3xVenus.

SCF complex: a E3 ubiquitin ligase complex composed of Skp, Cullin and F-box proteins. It catalyses ubiquitination of proteins and targets them for degradation by the 26S proteasome.

Subfunctionalization: changes in paralogous genes leading to each paralog

retaining a subset of the ancestral gene function
Turnover rate: the continuous balance between protein synthesis and degradation rates.

Text Box:
Yeast-2-hybrid assay (Y2H) is a genetic tool based on transcriptional activation of a reporter gene upon reconstitution of two transcription factor domains, each fused to a bait or prey protein. Upon interaction between the bait and prey proteins, the split transcription factor is reconstituted, activating a reporter gene.
Fluorescence Correlation Spectroscopy (FCS) is a single molecule technique that tracks fluorescent molecules in a small diffraction limited confocal volume ($<10^{-15}$ L). Due to diffusion, fluorescent molecules cause fluorescence fluctuation signals, which are auto-correlated in time. The generated autocorrelation curve can inform about the diffusion coefficient.
Isothermal Titration Calorimetry (ITC) is a label-free technique that utilizes the thermodynamic principle of heat exchange during a molecular binding reaction to determine dissociation constant (Kd), stoichiometry, cooperativity of protein-protein or protein-DNA interactions in a titration-based protocol.
Microscale thermophoresis (MST) is an infrared laser-based optical method that allows Kd measurements in buffer solutions or cell lysates. This immobilization-free technique requires fluorescent protein labelling, and tracks fluorescence changes due to temperature and thermophoresis.
Surface Plasmon Resonance (SPR) uses the principle of resonance angle change of refracted polarized light due to the refractive index change of a metal (gold or silver) surface by the binding/unbinding of an analyte (e.g. protein) to immobilized ligand (e.g. DNA/protein).
Single Molecule Förster Resonance Energy Transfer (smFRET) is a technique that enables the study of protein interaction, conformational dynamics, intramolecular distance, and protein complex stoichiometry at single-molecule resolution. It relies on non-radiative resonance energy transfer between donor and acceptor fluorophores which have overlapping emission and absorption spectra.
Fluorescence Lifetime Microscopy (FLIM) is a fluorescence lifetime-based quantification method of FRET efficiency between fluorophores.
Bimolecular Fluorescence Complementation (BiFC) is a protein complementation assay based on reconstituting a fluorescent protein from two split fragments, upon interaction of the proteins fused to each half.
Fluorescence Recovery After Photobleaching (FRAP) can be used to de-

duce protein diffusion rates based on the fluorescence recovery rate within a photobleached region in a cell.
FCCS is a dual fluorophore version of FCS that allows us to probe dynamic protein interactions.
Pair Correlation Function (pCF) is used to track the path of diffusion of a labelled molecule by correlating intensity fluctuations at multiple points in an image.

Acknowledgements
This work was supported by grants from the Netherlands Organization for Scientific Research (NWO) (VICI 865.14.001 to D.W. and ALWOP.402 to JWB).

References
1. Leyser, O. Auxin signaling. *Plant Physiol* **176**, 465–479 (2018).
2. Weijers, D. & Wagner, D. Transcriptional Responses to the Auxin Hormone. *Annu Rev Plant Biol* **67**, 539–574 (2016).
3. Vanneste, S. & Friml, J. Auxin: A Trigger for Change in Plant Development. *Cell* vol. 136 Preprint at https://doi.org/10.1016/j.cell.2009.03.001 (2009).
4. Dharmasiri, N., Dharmasiri, S. & Estelle, M. The F-box protein TIR1 is an auxin receptor. *Nature* **435**, 441–445 (2005).
5. Kepinski, S. & Leyser, O. The Arabidopsis F-box protein TIR1 is an auxin receptor. *Nature* **435**, 446–451 (2005).
6. Tan, X. *et al.* Mechanism of auxin perception by the TIR1 ubiquitin ligase. *Nature* **446**, 640–645 (2007).
7. Gray, W. M., Kepinski, S., Rouse, D., Leyser, O. & Estelle, M. Auxin regulates SCFTIR1-dependent degradation of AUX/IAA proteins. *Nature* **414**, 271–276 (2001).
8. Tiwari, S. B., Wang, X. & Guilfoyle, T. J. AUX / IAA Proteins Are Active Repressors , and Their Stability and Activity Are Modulated by Auxin Author (s): Shiv B . Tiwari , Xiao-Jun Wang , Gretchen Hagen and Tom J . Guilfoyle Published by : American Society of Plant Biologists (ASPB) Stable URL. *Plant Cell* **13**, 2809–2822 (2001).
9. Tiwari, S. B., Hagen, G. & Guilfoyle, T. The roles of auxin response factor domains in auxin-responsive transcription. *Plant Cell* **15**, (2003).
10. Rademacher, E. H. *et al.* A cellular expression map of the Arabidopsis AUXIN RESPONSE FACTOR gene family. *Plant Journal* **68**, 597–606 (2011).
11. Prigge, M. J. *et al.* Genetic analysis of the arabidopsis TIR1/AFB auxin receptors reveals both overlapping and specialized functions. *Elife* **9**, (2020).
12. Truskina, J. *et al.* A network of transcriptional repressors modulates auxin responses. *Nature* **589**, (2021).
13. Ulmasov, T., Murfett, J., Hagen, G. & Guilfoyle, T. J. Aux/IAA proteins repress expression of reporter genes containing natural and highly active synthetic auxin response elements. *Plant Cell* **9**, (1997).
14. Ulmasov, T., Liu, Z. bin, Hagen, G. & Guilfoyle, T. J. Composite structure of auxin response elements. *Plant Cell* **7**, (1995).

15. Kim, J., Harter, K. & Theologis, A. Protein-protein interactions among the Aux/IAA proteins. *Proc Natl Acad Sci U S A* **94**, (1997).
16. Boer, D. R. *et al.* Structural basis for DNA binding specificity by the auxin-dependent ARF transcription factors. *Cell* **156**, 577–589 (2014).
17. Chadwick, A. v. & Burg, S. P. An Explanation of the Inhibition of Root Growth Caused by Indole-3-Acetic Acid. *Plant Physiol* **42**, (1967).
18. Sauer, M. & Kleine-Vehn, J. AUXIN BINDING PROTEIN1: The outsider. *Plant Cell* **23**, 2033–2043 (2011).
19. Sauer, M., Robert, S. & Kleine-Vehn, J. Auxin: Simply complicated. *J Exp Bot* **64**, 2565–2577 (2013).
20. Mutte, S. K. *et al.* Origin and evolution of the nuclear auxin response system. *Elife* **7**, 1–25 (2018).
21. Hardtke, C. S. *et al.* Overlapping and non-redundant functions of the Arabidopsis auxin response factors MONOPTEROS and NONPHOTOTROPIC HYPOCOTYL 4. *Development* vol. 131 Preprint at https://doi.org/10.1242/dev.00925 (2004).
22. Chapman, E. J. & Estelle, M. Mechanism of auxin-regulated gene expression in plants. *Annual Review of Genetics* vol. 43 Preprint at https://doi.org/10.1146/annurev-genet-102108-134148 (2009).
23. Vernoux, T. *et al.* The auxin signalling network translates dynamic input into robust patterning at the shoot apex. *Mol Syst Biol* **7**, (2011).
24. Piya, S., Shrestha, S. K., Binder, B., Neal Stewart, C. & Hewezi, T. Protein-protein interaction and gene co-expression maps of ARFs and Aux/IAAs in Arabidopsis. *Front Plant Sci* **5**, (2014).
25. Dharmasiri, N. *et al.* Plant development is regulated by a family of auxin receptor F box proteins. *Dev Cell* **9**, 109–119 (2005).
26. Wang, C., Liu, Y., Li, S. S. & Han, G. Z. Insights into the origin and evolution of the plant hormone signaling machinery. *Plant Physiol* **167**, (2015).
27. Overvoorde, P. J. *et al.* Functional genomic analysis of the AUXIN/INDOLE-3-ACETIC ACID gene family members in Arabidopsis thaliana. *Plant Cell* **17**, (2005).
28. Nagpal, P. *et al.* AXR2 encodes a member of the Aux/IAA protein family. *Plant Physiol* **123**, (2000).
29. Tian, Q. & Reed, J. W. Control of auxin-regulated root development by the Arabidopsis thaliana SHY2/AA3 gene. *Development* **126**, (1999).
30. Okushima, Y. *et al.* Functional genomic analysis of the AUXIN RESPONSE FACTOR gene family members in Arabidopsis thaliana: Unique and overlapping functions of ARF7 and ARF19. *Plant Cell* **17**, (2005).
31. Kato, H. *et al.* Design principles of a minimal auxin response system. *Nat Plants* **6**, (2020).
32. Bowman, J. L. *et al.* Insights into Land Plant Evolution Garnered from the Marchantia polymorpha Genome. *Cell* **171**, (2017).
33. Flores-Sandoval, E., Eklund, D. M. & Bowman, J. L. A Simple Auxin Transcriptional Response System Regulates Multiple Morphogenetic Processes in the Liverwort Marchantia polymorpha. *PLoS Genet* **11**, 1–26 (2015).
34. Kato, H. *et al.* Auxin-Mediated Transcriptional System with a Minimal Set of Components Is Critical for Morphogenesis through the Life Cycle in Marchantia polymorpha. *PLoS Genet* **11**, (2015).
35. Ishizaki, K., Nishihama, R., Yamato, K. T. & Kohchi, T. Molecular genetic tools and

techniques for marchantia polymorpha research. *Plant Cell Physiol* **57**, 262–270 (2016).
36. Ishizaki, K., Chiyoda, S., Yamato, K. T. & Kohchi, T. Agrobacterium-mediated transformation of the haploid liverwort Marchantia polymorpha L., an emerging model for plant biology. *Plant Cell Physiol* **49**, 1084–1091 (2008).
37. Kubota, A., Ishizaki, K., Hosaka, M. & Kohchi, T. Efficient Agrobacterium-mediated transformation of the liverwort Marchantia polymorpha using regenerating thalli. *Biosci Biotechnol Biochem* **77**, 167–172 (2013).
38. Ishizaki, K., Johzuka-Hisatomi, Y., Ishida, S., Iida, S. & Kohchi, T. Homologous recombination-mediated gene targeting in the liverwort Marchantia polymorpha L. *Sci Rep* **3**, 1–6 (2013).
39. Tsuboyama, S., Nonaka, S., Ezura, H. & Kodama, Y. Improved G-AgarTrap: A highly efficient transformation method for intact gemmalings of the liverwort Marchantia polymorpha. *Sci Rep* **8**, 1–10 (2018).
40. Nishihama, R., Ishida, S., Urawa, H., Kamei, Y. & Kohchi, T. Conditional gene expression/deletion systems for Marchantia polymorpha using its own heat-shock promoter and cre/loxP-mediated site-specific recombination. *Plant Cell Physiol* **57**, 271–280 (2016).
41. Ishizaki, K. *et al.* Development of gateway binary vector series with four different selection markers for the liverwort marchantia polymorpha. *PLoS One* **10**, (2015).
42. Galli, M. *et al.* The DNA binding landscape of the maize AUXIN RESPONSE FACTOR family. *Nat Commun* **9**, (2018).
43. Digman, M. A. *et al.* Fluctuation correlation spectroscopy with a laser-scanning microscope: Exploiting the hidden time structure. *Biophys J* **88**, (2005).
44. Cho, H. *et al.* A secreted peptide acts on BIN2-mediated phosphorylation of ARFs to potentiate auxin response during lateral root development. *Nat Cell Biol* **16**, (2014).
45. Terrile, M. C. *et al.* Nitric oxide influences auxin signaling through S-nitrosylation of the Arabidopsis TRANSPORT INHIBITOR RESPONSE 1 auxin receptor. *Plant Journal* **70**, (2012).
46. Korasick, D. A. *et al.* Molecular basis for AUXIN RESPONSE FACTOR protein interaction and the control of auxin response repression. *Proc Natl Acad Sci U S A* **111**, 5427–5432 (2014).
47. Nanao, M. H. *et al.* Structural basis for oligomerization of auxin transcriptional regulators. *Nat Commun* **5**, 3617 (2014).
48. Dezfulian, M. H. *et al.* Oligomerization of SCFTIR1 Is Essential for Aux/IAA Degradation and Auxin Signaling in Arabidopsis. *PLoS Genet* **12**, (2016).
49. Martin-Arevalillo, R. *et al.* Structure of the Arabidopsis TOPLESS corepressor provides insight into the evolution of transcriptional repression. *Proc Natl Acad Sci U S A* **114**, (2017).
50. Lee, S. *et al.* Defining binding efficiency and specificity of auxins for SCF TIR1/AFB-Aux/IAA Co-receptor complex formation. *ACS Chem Biol* **9**, (2014).
51. Korasick, D. A. *et al.* Defining a two-pronged structural model for PB1 (Phox/Bem1p) domain interaction in plant auxin responses. *Journal of Biological Chemistry* **290**, (2015).
52. Dinesh, D. C. *et al.* Solution structure of the PsIAA4 oligomerization domain reveals interaction modes for transcription factors in early auxin response. *Proc Natl Acad Sci U S A* **112**, (2015).
53. Han, M. *et al.* Structural basis for the auxin-induced transcriptional regulation by Aux/IAA17. *Proc Natl Acad Sci U S A* **111**, (2014).

54. Ulmasov, T., Hagen, G. & Guilfoyle, T. J. Dimerization and DNA binding of auxin response factors. *Plant Journal* **19**, (1999).
55. Ballas, N., Wong, L. M. & Theologis, A. Identification of the auxin-responsive element, AuxRE, in the primary indoleacetic acid-inducible gene, PS-IAA4/5, of pea (Pisum sativum). *J Mol Biol* **233**, (1993).
56. Cherenkov, P. *et al.* Diversity of cis-regulatory elements associated with auxin response in Arabidopsis thaliana. *J Exp Bot* **69**, (2018).
57. Mironova, V. v., Omelyanchuk, N. A., Wiebe, D. S. & Levitsky, V. G. Computational analysis of auxin responsive elements in the Arabidopsis thaliana L. genome. *BMC Genomics* **15**, (2014).
58. Freire-Rios, A. *et al.* Architecture of DNA elements mediating ARF transcription factor binding and auxin-responsive gene expression in Arabidopsis. *Proc Natl Acad Sci U S A* **117**, (2020).
59. del Bianco, M. & Kepinski, S. Context, specificity, and self-organization in auxin response. *Cold Spring Harb Perspect Biol* **3**, (2011).
60. Powers, S. K. *et al.* Nucleo-cytoplasmic Partitioning of ARF Proteins Controls Auxin Responses in Arabidopsis thaliana. *Mol Cell* **76**, 177-190.e5 (2019).
61. Halford, S. E. & Marko, J. F. How do site-specific DNA-binding proteins find their targets? *Nucleic Acids Research* vol. 32 Preprint at https://doi.org/10.1093/nar/gkh624 (2004).
62. Berg, O. G. & von Hippel, P. H. Diffusion-controlled macromolecular interactions. *Annual review of biophysics and biophysical chemistry* vol. 14 Preprint at https://doi.org/10.1146/annurev.bb.14.060185.001023 (1985).
63. Brunoud, G. *et al.* A novel sensor to map auxin response and distribution at high spatio-temporal resolution. *Nature* **482**, 103–106 (2012).
64. Liao, C. Y. *et al.* Reporters for sensitive and quantitative measurement of auxin response. *Nat Methods* **12**, (2015).
65. Middleton, A. M., King, J. R., Bennett, M. J. & Owen, M. R. Mathematical modelling of the Aux/IAA negative feedback loop. *Bull Math Biol* **72**, 1383–1407 (2010).
66. Voß, U., Bishopp, A., Farcot, E. & Bennett, M. J. Modelling hormonal response and development. *Trends in Plant Science* vol. 19 Preprint at https://doi.org/10.1016/j.tplants.2014.02.004 (2014).

Chapter 3

Illuminating the nuclear auxin signaling network of *Marchantia polymorpha*

Shubhajit Das, Iris Nieuwland, Dolf Weijers, Jan Willem Borst
Laboratory of Biochemistry, Wageningen University, the Netherlands

Part of this chapter has been published as:

Das S., Roij M., Bellows S., Kohlen W., Farcot E., Weijers D. and Borst JW (2022) Selective degradation of ARF monomers controls auxin response in Marchantia. bioRxiv. DOI:10.1101/2022.11.04.515187

Abstract

Auxin is a key growth regulator in all land plants. It acts in part via a nuclear signaling pathway composed of TIR1/AFB receptors, Aux/IAA repressors and ARF transcription factors. TIR1/AFBs sense auxin and promote degradation of Aux/IAA repressors, leading to activation of ARF-mediated gene transcription. Extensive functional characterization of these proteins in angiosperms has provided a comprehensive qualitative model for auxin signaling. However, given that the endogenous accumulation patterns of these proteins are unknown, a quantitative understanding is lacking. In part, this is caused by the existence of large gene families in angiosperms, and also because tools to infer true endogenous patterns are mostly lacking in angiosperms. We used the bryophyte model *Marchantia polymorpha* to overcome these limitations. Marchantia has minimal genetic redundancy in its nuclear auxin response system and allows systematic generation of fluorescent genomic knock-in lines to quantify true endogenous protein levels. We compared the native protein expression maps of each of the auxin signaling components in dormant gemmae and found a wide range of accumulation patterns. TIR1 and ncARF showed low concentrations throughout gemmae whereas Aux/IAA was not detected at all. However, the maps of the three ARFs revealed clear differences among them. Moreover, colocalization maps of activator and repressor ARFs allowed identification of cell types with different relative concentrations. Overall, this chapter presents the development of a complete set of genomic knock-ins as a valuable resource for quantitative analysis of auxin signaling proteins in Marchantia.

Introduction

Auxin is a central regulator of plant growth and development[1]. It acts mainly via a short, auxin concentration-dependent transcriptional circuit in the nucleus, the nuclear auxin signaling pathway (NAP)[2]. This signaling circuit starts with auxin perception by TIR1/AFB (TRANSPORT INHIBITOR RESPONSE/AUXIN SIGNALING F-BOX) receptors in nucleus[3]. Auxin binding to TIR1/AFBs enhances its affinity for Aux/IAA (Auxin/INDOLE-3-ACETIC ACID) repressors which otherwise engages in an inhibitory interaction with ARF (AUXIN RESPONSE FACTOR) transcription factors at low auxin concentrations[4]. Formation of the TIR1/AFB-auxin-Aux/IAA complex results in ubiquitination and degradation of Aux/IAAs, allowing transcriptional activation of genes by ARFs. Built on decades of genetic and biochemical characterizations in Arabidopsis, a qualitative model of the NAP has emerged. This model captures the general topology, modes of NAP operations, and explains genetic interactions (Figure 1.A). However, it is important to keep in mind that any biomolecular interaction will depend on both intrinsic affinity and on concentrations of both partners. Therefore, to truly understand and predict the output of the NAP, quantitative information on binding affinities and *in vivo* protein concentrations are needed. The current view of the NAP lacks such quantitative information. It is therefore imperative to develop tools to quantify these parameters and advance the qualitative model[5].

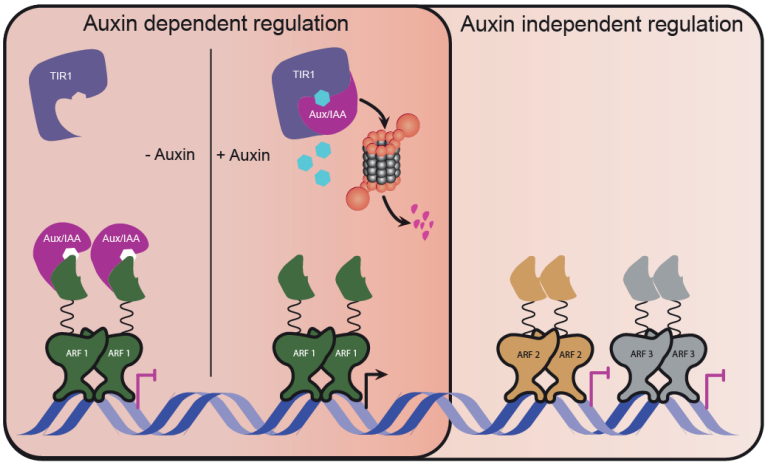

Figure 1: Schematic representation of nuclear auxin signaling pathway (NAP) in *Marchantia polymorpha*. MpARF1 is an auxin dependent transcriptional activator that is inhibited by MpAux/IAA at low auxin concentration. At high auxin concentration, TIR1 binding to auxin enhances TIR1-auxin-Aux/IAA interaction, resulting in degradation of Aux/IAA by $TIR1^{SCF}$ proteasomal complex. This allows activation of gene transcription by free MpARF1. MpARF2 and MpARF3 act as transcriptional repressors, independent of auxin concentration in cell.

One possible approach to quantitatively analysis the NAP is by visualization of the endogenous protein levels *in vivo*. Previously, visualization of translationally fused auxin signaling proteins in *Arabidopsis thaliana* have revealed their nuclear and, in some cases, cytoplasmic localization. For instance, Arabidopsis TIR1 was shown to express primarily in the nucleus whereas the four other members of TIR1/AFB family, namely AFB2, AFB3, AFB4 and AFB5 expressed in both the cytoplasm and nucleus. AFB1, the sixth member of the TIR1/AFB family, was reported as a cytoplasmic protein[6]. Likewise, expression of most ARFs in Arabidopsis have been detected only in the nucleus, except a recent report on cytoplasmic condensates formed by Arabidopsis ARF7 and ARF19[7]. Aux/IAA repressors have also been detected in the nucleus in multiple Angiosperms[8] with a few nucleocytoplasmic Aux/IAA members[9]. However, all these protein expression analyses were performed through adding an additional copy of a signaling component fused to a fluorescent protein, necessarily at a different genomic locus. Whether the endogenous copy of these proteins have same expression and stability, is an open question. Visualization of the native signaling proteins is difficult in angiosperms, as targeting the endogenous copy requires a genomic knock-in by homologous recombination. Since plant DNA repair occurs mainly via non-homologues end joining (NHEJ)[10] and the frequency of homology-based DNA repair ranges from 10^{-3} to10^{-6} [11], development of knock-in using homologous recombination and quantifying endogenous protein expression is challenging in angiosperms like Arabidopsis. High genetic redundancy of angiosperm genomes further increases the complexity (23 ARFs, 29 Aux/IAA and 6 TIR1/AFBs in Arabidopsis), restricting the analysis of individual proteins without interference from paralogous gene function.

Recent advances in genome sequencing[12], phylogenetic[13] and functional analysis[14,15] have identified a simpler NAP in the bryophyte species *Marchantia polymorpha*. The Marchantia NAP is composed of a single TIR1 auxin receptor, single Aux/IAA repressor and three ARFs representing three classes (A, B and C). Importantly, a transformation protocol for homologous recombination-based genomic knock-in has been established[16]. Despite the low efficiency of homologous recombination, millions of spores produced by Marchantia allows to scale up the transformation.

We used this method to knock-in a fluorescent tag at the C-terminus of each auxin signaling protein[16]. This allowed us to reveal the *in vivo* quantities of each auxin signaling protein and their spatial expression map in dormant gemmae. To study the colocalization patterns of the activator MpARF1 and repressor MpARF2, we created double knock-in lines of ARF1 and ARF2. Colocalization analysis at a single cell resolution uncovered differential ARF stoichiometry depending on cell types and corroborated a previously proposed transcriptional regulation model for ARFs. Overall, this chapter presents a novel, quantitative overview of the nuclear auxin signaling network in *Marchantia polymorpha.*

Results

Development of genomic knock-in lines of nuclear auxin signaling proteins

To visualize the native expression patterns of the core auxin signaling proteins, we generated genomic knock-in translational fluorescent fusion lines of *Marchantia polymorpha*. A construct carrying a fluorescent reporter coding sequence (mScarlet-I[17] or mNeonGreen[18]) and a constitutively expressed hygromycin selection marker, was flanked by cloning two genomic DNA homology arms of 3.5kb each (Figure 2.A). The upstream and downstream region from the stop codon of target gene was used as homology arms to facilitate C-terminal in-frame fusion of the fluorophore. Wildtype Marchantia spores were transformed by Agrobacterium-mediated transformation protocol[16] and knock-ins lines were selected by genotyping the transformants. A mScarlet-I fluorophore was knocked-in at the C-terminus of TIR1, Aux/IAA, the three canonical and one non-canonical ARF (ARF1, 2, 3 and ncARF). For ARF1 and 2, two additional knock-ins with mNeonGreen tag were developed.

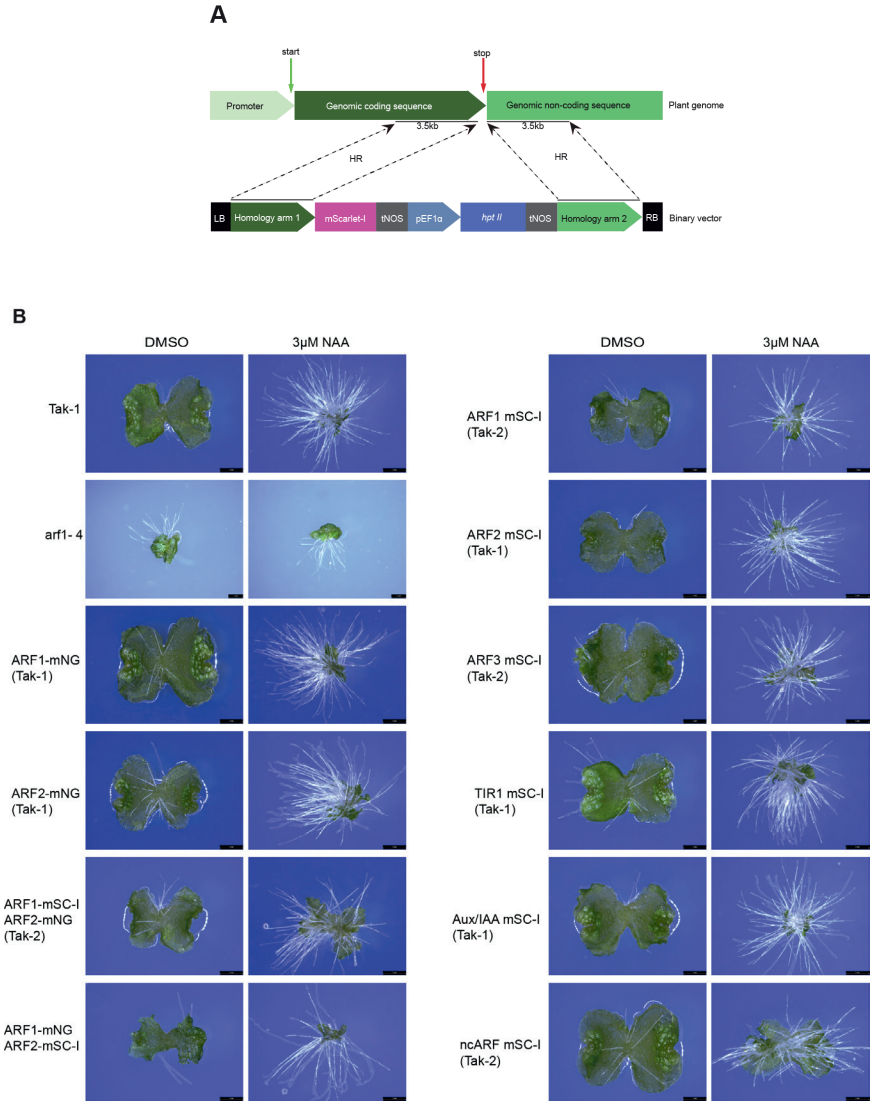

Figure 2: (A) Principle of homologous recombination based genomic knock-in of fluorescent genes at the C-terminus of endogenous gene of interest. Recombination of two homologous arms allow integration of a fluorescent reporter gene (mScarlet-I or mNeonGreen in this case) in the plant genome. (B) Physiological auxin sensitivity assay of knock-in lines. Wildtype Tak-1 strain was used as positive control. arf1-4 mutant does not respond to auxin and can be considered as a negative control. Plants were treated with 3 microMol synthetic auxin analog 1-Naphthaleneacetic acid (NAA) and imaged after one week of growth. All knock-in lines have wildtype like response of stunted thallus growth and ectopic rhizoid formation, suggesting complete functionality of the signaling proteins when fused to a fluorescent tag.

All knock-in lines showed normal development of thallus, rhizoids and gemma, unlike the severe developmental defects reported for knock-out and overexpression mutants of these proteins[13,14,19,20]. For instance, MpARF1 knock-out mutant is defective in thallus patterning, gemma development and shows auxin insensitivity[14] (Figure 2.B). Normal development of genomic knock-ins suggests normal quantity and activity of the fused proteins in these plants. To test for physiological auxin responsiveness of the knock-ins, we treated them with 3μM synthetic auxin analog 1-Naphthaleneacetic acid (NAA) and images were taken after a week. Tak-1 and Tak-2 wildtype control plants developed ectopic rhizoids on the adaxial side of the thallus, and their thallus development was strongly inhibited in response to NAA. All knock-in lines showed similar physiological auxin responses, suggesting full functionality of the tagged auxin signaling proteins (Figure 2.B).

Next, we used confocal microscopy to visualize and compare the native protein expression patterns in dormant gemmae of knock-ins. This revealed that the auxin receptor TIR1 has a wide expression pattern in dormant gemmae, while the Aux/IAA repressor showed no expression at all (Figure 3.A-B). The absence of Aux/IAA expression in dormant gemmae could be due to its rapid degradation by TIR1 in presence of high auxin concentration within the gemma cup[21]. The three Marchantia ARFs which represent 3 phylogenetic classes, showed different expression levels in dormant gemma (Figure 3.C-E). ARF1-mScarlet-I (class A) was highly expressed in the nucleus of every cell type: apical cell, rhizoids initiating cells and green cell (present between apical and rhizoid cells) of gemma, whereas ARF2-mScarlet-I (class B) showed a relatively lower expression only in the apical and green cells. It is worth noting that the rhizoid initiating cells showed high ARF1 expression, while ARF2 was not expressed in this cell type. ARF3-mScarlet-I (class C) showed a weak yet broad expression pattern at dormant stage. Unlike ARF2, ARF3-mScarlet-I was detected in all 3 cell types including rhizoid cells. The non-canonical ARF (ncARF)-mScarlet-I showed expression in almost all cell types, with relatively higher expression near the apical notch region (Figure 3.F). Together these results provide the first native expression profile of a complete nuclear auxin pathway at its endogenous protein quantities.

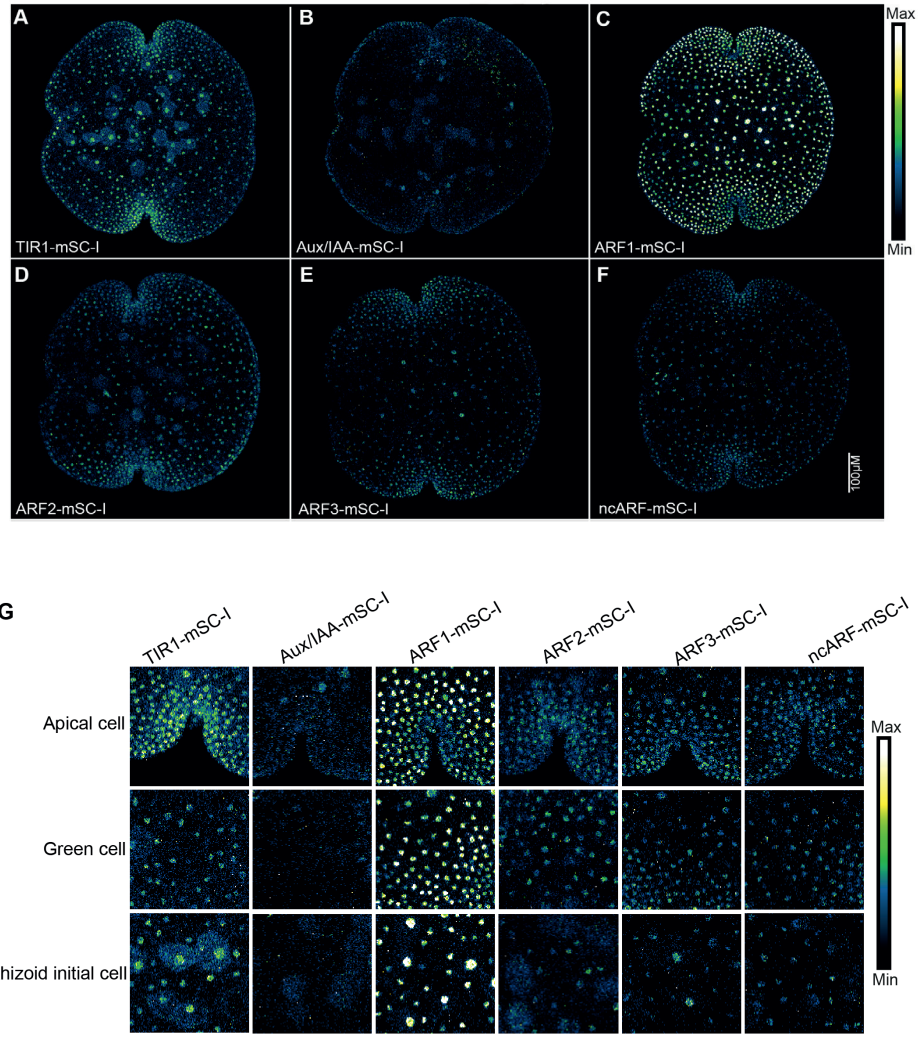

Figure 3: Overview of native and quantitative expression patterns of auxin response proteins fused to mScarlet-I (mSC-I) in dormant gemma of genomic knock-in lines. (A) TIR1-mSC-I is moderately expressed in all cell type, whereas (B) Aux/IAA-mSC-I is barely detectable. (C-E) The three classes of ARFs show clear differences in their stoichiometries. ARF1-mSC-I shows relatively high expression, whereas ARF2- and ARF3-mSC-I expression is lower. Unlike ARF1 and ARF3, ARF2 is not detectable in rhizoid initiation cells. (F) The non-canonical ARF has a weak expression in all cells. (G) Magnified images of A to F, showing protein expression in the three main cell types of gemmae. A false colour look-up table has been used to generate a quantitative map of auxin response protein expression.

Colocalization analysis revealed cell specific modes of ARF1/2 stoichiometry

Class-A and class-B ARFs were reported to compete for the same DNA binding elements[22,23] and their relative stoichiometries were proposed as a determining factor for auxin responses[19]. Such ARF competition model would work, if class-A and -B ARFs are colocalized, where differences in their relative stoichiometry would be key. Hence, we investigated the native colocalization of the ARF1 (class-A) and ARF2 (class-B) in the same tissue. To this end, we created two additional single knock-in ARF fusions with a different fluorophore mNeonGreen. Both ARF1-mNeonGreen and ARF2-mNeonGreen lines showed similar expression patterns as the mScarlet-I single knock-ins (Figure 4). We crossed the ARF1-mScarlet-I line with ARF2-mNeonGreen and ARF1-mNeonGreen line with ARF2-mScarlet-I to generate two double knock-in lines: ARF1-mScarlet-I ARF2-mNeonGreen and ARF1-mNeonGreen ARF2-mScarlet-I. Confocal imaging of the double knock-ins showed that ARF1 and ARF2 spatial expression profiles were the same irrespective of the fluorophore used (Figure 5.A-B), and similar as observed before in single ARF knock-ins.

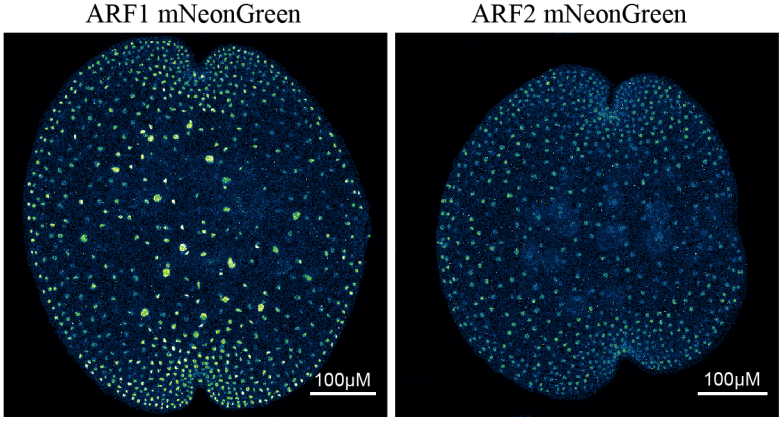

Figure 4: Overview of native expression of ARF1-mNeonGreen and ARF2-mNeonGreen in dormant gemmae. These knock-ins show the same expression patterns as observed in the mScarlet-I knock-in lines (see Figure 3.C-D).

Upon colocalization analysis of ARFs in dormant double knock-in gemmae, we noticed that ARF1 and ARF2 proteins had cell type-specific differences in their spatial expression map, similar to what we initially observed by comparing single knock-ins. In rhizoid initial cells, ARF2 showed negligible expression compared to ARF1, pointing towards a ARF1-dominated gene regulation in these cells (Figure 6.A, C). In contrast, in the meristematic apical

notch cells, ARF2 showed higher expression than ARF1 (Figure 6.A-B). This suggests a possible role of repressor ARF2 in maintaining low auxin response in the apical meristem cells despite the high auxin levels in the meristem[21]. In the green cells, present in the region between apical and rhizoid initiating cells, we observed colocalization of both ARF1 and ARF2, providing a scope of competitive ARF-DNA binding and gene regulation. These unique ARF co-localization patterns in various cell types of dormant gemmae, fulfils the requirements to fit a previously proposed ARF stoichiometry dependent gene regulation model in Marchantia[19] (Figure 7).

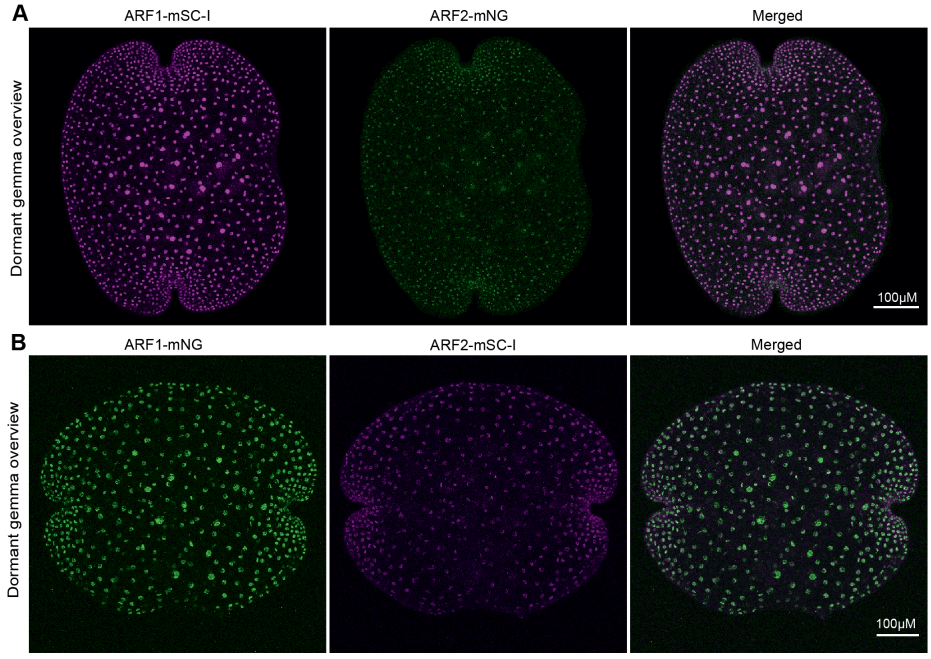

Figure 5: Overview of ARF1 and ARF2 expression in dormant gemmae of (A) ARF1-mScarlet-I (mSC-I) - ARF2-mNeonGreen (mNG) and (B) ARF1- mScarlet-I (mSC-I) - ARF2- mNeonGreen (mNG) double knock-in lines. ARF1 shows relatively higher accumulation than ARF2 and this is consistent in both double knock-ins with switched fluorophores, confirming that the expression patterns are specific to the ARFs and not influenced by mS-carlet-I or mNeonGreen.

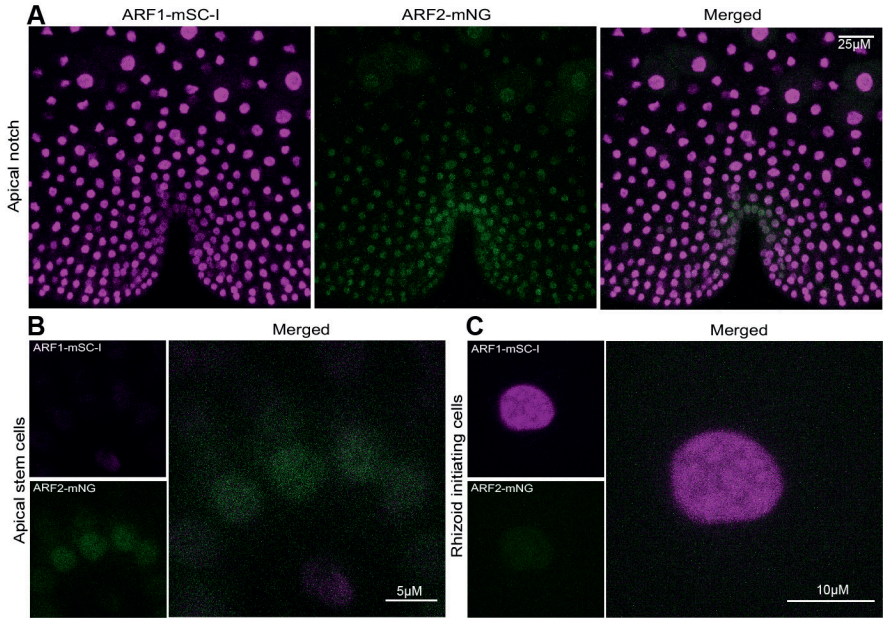

Figure 6: (A) Localization patterns of ARF1 and ARF2 near the apical notch area shows differences in the two ARF expression profile in different cell types of gemmae. The green cells comprising the region between apical notch and rhizoid cells, show co-expression of ARF1 and ARF2. (B) In apical stem cells of the notch, ARF2-mNG expression is higher than ARF1-mSC-I. (C) In the rhizoid initiating cells, a dominance of ARF1 mSC-I expression is observed. ARF2-mNG expression in rhizoid initial cells is negligible.

Discussion

The *in vivo* expression profile of a protein provides spatial context of its biological function in a cell or tissue. Although the expression of auxin signaling proteins was studied previously in angiosperms, generating tools to visualize the native protein remains challenging. Consequently, quantitative data on nuclear auxin response pathway are unavailable. Here we used *Marchantia polymorpha* as model system to develop the required tools for a quantitative survey of the auxin signaling network. Despite the low frequency of DNA homologous recombination, the availability of millions of spores from Marchantia allowed us to obtain genomic knock-in of the core NAP proteins. Fluorescently tagged native proteins were functional as manifested by their normal development and auxin sensitivity. One minor exception was the ncARF-mScarlet-I knock-in which showed partial inhibition of thallus growth on NAA treatment, compared to complete inhibition observed in other knock-ins and wildtypes. Based on the protein domain annotations, ncARF is a truncated ARF which lacks the DNA binding domain but has the middle

region and PB1 domain intact[13]. A CRISPR mutant of *MpncARF* was previously reported as less responsive to auxin treatments both physiologically and transcriptionally. Accordingly, ncARF was proposed as a positive regulator of auxin response[13]. It was suggested that ncARF PB1 domain probably interacts with AuxIAA to protect canonical ARFs from inhibition by Aux/IAA[13]. Since the C-terminal PB1 domain is the only functional domain of ncARF and we fused the mScarlet-I gene in the C-terminus of ncARF, this could have partially limited the protein function. As a result, the ncARF-mScarlet-I line showed reduced physiological response to auxin. However, the ncARF-mScarlet-I knock-in line grew normally on untreated media and developed ectopic rhizoids in response to auxin, similar to wildtype Marchantia (Figure 2.B).

Confocal microscopy on the knock-ins revealed the native expression maps of ARFs. Based on the relatively higher native expression of ARF1 in knock-in gemmae, one can anticipate the importance of this protein in gemmae development. This can be confirmed from the phenotype of the *Mparf1* knock-out mutant that forms empty gemma cups with no gemmae developed inside[14]. Both the repressor proteins, ARF2 and ARF3 showed relatively lower endogenous expression compared to the activator ARF1. One noticeable difference among the three ARF expression patterns is the presence of ARF1 and ARF3 in the rhizoid cells whereas ARF2 is not expressed in these cells. This could be due to either low activity of ARF2 promoter in the rhizoid cells or a selective regulation of ARF2 protein levels in rhizoid cells. Class A ARFs of Arabidopsis have been well documented for their regulatory function in primary and secondary root development. For example, Arabidopsis ARF5/MONOPTEROS was shown to specify root primordia via its downstream target TARGET OF MONOPTEROS7 (TMO7) in embryonic tissue[24]. Arabidopsis ARF7 and ARF19 were found to regulate lateral root development via transcriptional regulation of LATERAL ORGAN BOUNDARIES DOMAIN16 (LBD16). A double mutant of *Atarf7and Atarf19* had severe lateral root growth inhibition and reduced auxin response[25]. Higher relative concentration of MpARF1 over MpARF2 in Marchantia gemmae could allow for a broader ARF1-DNA binding landscape without any competition from ARF2 in rhizoid initial cells. This could possibly assist rhizoids cells to have a higher transcriptional response to auxin and differentiate into a rhizoid cell.
Another remarkable difference between ARF1 and ARF2 colocalization was observed in the apical cells located near the apical notch of gemmae. Apical cells are meristematic cells that divide to add new cells in developing gem-

mae. However, in dormant gemmae, apical cell division remains stalled unless the gemmae start germinating upon contact with growth medium. Presence of higher ARF2 and no ARF1 expression in dormant apical meristem cells are expected to cause a lower auxin responsiveness in these cells. Since ARF2 is a repressor of transcription[19], it could inhibit the expression of auxin response genes in apical cells that are required for initiating cell division in the meristem. Such ARF2 mediated repression of apical cell division could be a requirement for keeping gemmae dormant inside gemma cup. However, this would also mean that for gemma germination, such transcriptional repression by ARF2 must be removed by regulating ARF2 protein levels.

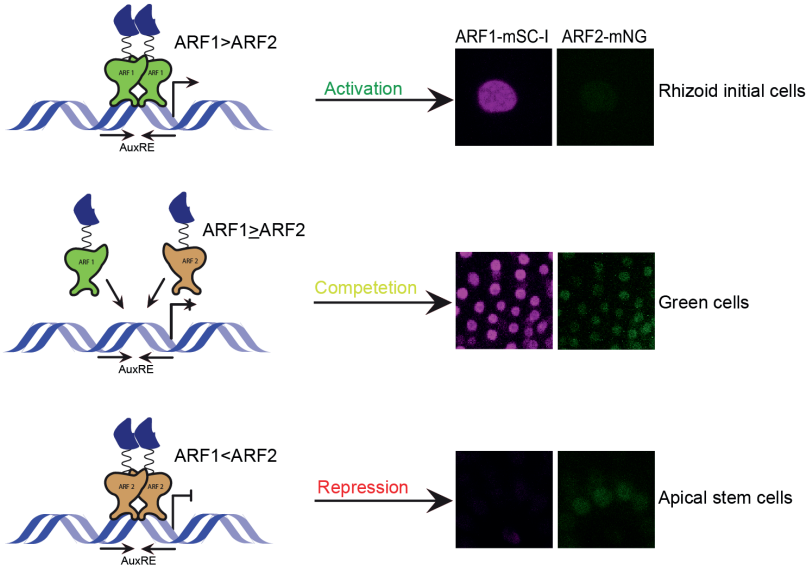

Figure 7: Three modes of gene regulation by relative stoichiometry of class A and class B ARFs, adapted from Kato et. al. 2020 (Nature Plants). In higher relative concentration of ARF1, DNA binding and gene activation is controlled by ARF1 in an auxin dependent manner (top panel). This mode might be operational in rhizoid initial cells where ARF2 expression is below detection limit and ARF1 is abundant. The second mode of gene regulation considers presence of both class A and B ARFs and competition for DNA binding and gene regulation (middle panel). Presence of both ARF1 and ARF2 in green cells could lead to such competition driven gene regulation in these cells. The third mode describes gene repression by class B ARFs, independent of cellular auxin concentrations (bottom panel). Apical meristem cells of gemmae could represent this third mode as these cells have higher ARF2 expression and no ARF1 expression.

Since both class A and class B ARFs are known to recognize the same DNA binding element in Arabidopsis[22,23], it would not be surprising if the relative concentrations of two competing ARFs would determine auxin responsiveness. The contrasting localization map of ARF1 and ARF2 in various cell types, satisfy the protein abundance requirements to support a previously proposed ARF stoichiometry dependent gene regulation model (Figure 7)[19]. The

relatively high ARF1 expression observed in rhizoid cells point towards an ARF1-dominated gene activation mode. Whereas in the apical cells we see the opposite; ARF2 abundance indicating a gene repression mode in absence of ARF1. Green cells with both ARF1 and ARF2 expression fits with competitive ARF-DNA binding mode. MpARF-DNA binding assays and transcriptome analysis at single cell resolution would help confirming these possibilities in future.

The biological function of class C ARFs has remained less explored. Recent studies on class C MpARF3 revealed their function as repressor of developmental transitions and gemma development[26,27]. Although *Mparf3* CRISPR mutants showed flat thallus growth and unaltered transcriptional response to auxin, gemma maturation inside the gemma cup was completely arrested[13]. Based on these data, ARF3 was considered as an auxin independent transcription factor involved in reproductive development. We observed a wide ARF3 expression pattern in dormant gemmae, which suggests that although ARF3 may not involve in auxin response, it could still be playing other important function. It would therefore be interesting to explore direct targets of ARF3 mediated gene repression.

In the knock-in lines we observed expression of TIR1-mScarlet-I in dormant gemmae whereas the Aux/IAA-mSCarlet-I was completely undetectable. Inside gemma cups, gemmae remain dormant in a high auxin environment[21]. Presence of TIR1 and absence of Aux/IAA in dormant gemmae could mean that gemmae perceive the high auxin environment. Consequently, Aux/IAA is degraded by the $TIR1^{SCF}$ complex. However, there is no evidence that auxin sensed at this stage can translate into a transcriptional response. Presence of repressor ARF2 in dormant gemmae could antagonize such transcriptional responses and help maintain gemmae dormancy.

Overall, we observed that all endogenous proteins of Marchantia nuclear auxin signaling network are nuclearly localized. Unlike some Arabidopsis homologs, we did not observe any cytoplasmic expression of these proteins. Thus, the recent discovery of fast auxin response pathways mediated by cytoplasmic TIR1/AFB family members might be a novel innovation in angiosperms[28,29] and absent in Marchantia. We also found that the native quantities of each signaling proteins are different based on cell type in gemmae. Importantly, the availability of these genomic knock-in lines for auxin signaling proteins, unlocks the possibilities of addressing some yet unresolved problems in auxin research. For instance, class A and B ARFs have been shown to compete for the same DNA binding sites called auxin response elements (AuxREs)[19,23]. However, the role of relative ARF stoichiometry in driving this

competitive DNA binding remains unclear due to lack of quantitative data. ARFs have been shown to homodimerize and heterodimerize *in vitro*, heterologous and overexpression systems[30,31]. These known ARF interactions have not yet been tested *in vivo* at native ARF concentrations. We hope that with this novel resource of an entire set of auxin signaling protein knock-in lines, it would be possible to answer some of these unresolved questions.

Materials and Method

Plant growth conditions

Marchantia polymorpha male Takaragaike-1 (Tak-1) and female Takaragaike-2 (Tak-2) were used as the wildtype variety. For vegetative propagation, plants were grown on ½ Gamborg B5 media plates in growth chambers with 40 µmol photons m^{-2} s^{-1} continuous white light at 22 °C. For sexual reproduction, plants were grown on 1% sucrose supplemented ½ Gamborg B5 media within hyrophonic boxes exposed to 40µmol photons m^{-2} s^{-1} continuous white fluorescent light for 1 month. Plants were then moved into 40 µmol photons m^{-2} s^{-1} continuous white light supplemented with 15µmol photons m^{-2} s^{-1} far-red light to induce antheridiophore and archegoniophore development. Plants were repeatedly crossed manually to ensure fertilization. Sporangia with mature spores were collected aseptically and used for spore transformation.

Development of genomic knock-in translational fusions

Marchantia knock-in lines were generated to study the native auxin response proteins at endogenous concentrations. A NOS terminator and a fluorescent marker gene (either mScarlet-I or mNeonGreen) were cloned sequentially at the HindIII restriction site of pJHY-TMp1 binary plasmid to create pJHY-mSC-I and pJHY-mNG vectors. After each cloning step, the HindIII site was regenerated by adding a HindIII site in the forward primer. This allowed subsequent cloning at the 5' end of the previous insert in the same plasmid. Two 3.5kb genomic DNA fragments were amplified by PCR to use as homologous arms for recombination. The first genomic DNA fragment contained the 3.5kb sequence upstream of the stop codon of the gene of interest while the second fragment was composed of the 3.5kb sequence downstream of the stop codon. The first fragment was cloned at the HindIII site and the second fragment was cloned at the AscI site of pJHY-mSC-I and pJHY-mNG. This cloning strategy was used to create homologous recombination constructs for ARF1, ARF2, ARF3, TIR1, Aux/IAA and ncARF. Wild type (Tak-1) spores were transformed by agrobacterium mediated transformation protocol described

before[16,32]. Transformants were selected on 1/2 Gamborg B5 + 100mg/litre Cefotaxime medium with hygromycin (10mg/L) selection. Genomic DNA PCR was used to isolate true knock-in lines.

Auxin sensitivity and physiological analysis of knock-ins

Knock-in lines were tested for their wildtype like growth, physiology, and auxin sensitivity. Tak-1, Tak-2 and all knock-in lines were treated with either DMSO or 1μM NAA supplemented ½ B5 media and grown for 7 days. On 8th day, plants were imaged with stereomicroscope to compare their physiological responses to auxin

Confocal Microscopy

Live Marchantia gemma imaging was done with a Leica SP8X-SMD confocal microscope equipped with a hybrid detector and a pulsed white-light laser (WLL). The mScarlet-I was excited with a 561 nm laser line (4% laser output of WLL) and mNeongreen was excited with a 506 nm laser line (4% laser output of WLL). Fluorescence emission was detected by the hybrid detector at 570 to 620 nm (for mScarlet-I) and 512nm to 560nm (for mNeongreen). All images were acquired with a water immersive 20X objective lens. Fluorescence was detected in photon counting mode and time-gated detection was used to suppress chlorophyll autofluorescence. Images were processed using ImageJ software. Maximum-intensity projections of z-stack images were used to quantify total cellular fluorescence in each nucleus analysed, normalized through background fluorescence measurements.

Author contributions

Conceptualization-S.D., D.W., J.W.B.; Experiments-S.D., I.N.; Writing and Reviewing-S.D., J.W.B., D.W.

Acknowledgements

We are thankful to Martijn de Roij for proofreading and helpful comments. S.D. is supported by The Netherlands Organization for Scientific Research (NWO) (ALWOP.402).

Supplementary table

List of primers used in this chapter

Primer Name	Primer sequence
SJD001_tNOS.FOR	gcgattaattaagcttgagctcgaatttccccgatcgttcaaacatttggcaataa
SJD002_tNOS.REV	atgcccgggcaagctagttagctcactcattaggcacccccag
SJD003_mScarlet-I.FOR	gcgattaattaagcttGGCGGCGGCAGCATGGTGAGCAAGGGCGAGG
SJD004_mScarlet-I.REV	attcgagctcaagctGTTACTTGTACAGCTCGTCCATGCC
SJD005_MpARF1geneCter.FOR	gcgattaattaagctTTGGCAGAATGAGTGTGGCCAATTCTC
SJD006_MpARF1geneCter.REV	TGCCGCCGCCaagcttGGGGCACCCCCGCTGGG
SJD007_MpARF1downstream.FOR	taaactagtggcgcgATCTCGTTTTCACACTCCACACTCCGAT
SJD008_MpARF1downstream.REV	ttatccctaggcgcgTTCCTCCCCCGCTCGAAATCAC
SJD009_MpARF2 gene C ter.FOR	gcgattaattaagctTGAGCGAGCAACACGAAGACTC
SJD010_MpARF2 gene C ter.REV	TGCCGCCGCCaagcttCATGTCGTCGCCGCGCGC
SJD011_MpARF2downstream.FOR	taaactagtggcgcgACCATATGCCTTTTTTATGTATTTAAATTCTTCATCTATTCTC
SJD012_MpARF2downstream.REV	ttatccctaggcgcgACTCCGCAATTTCGCCTCAGAGTG
SJD013_MpARF3 gene coding C ter.FOR	gcgattaattaagcttAGCATTTACCTACCGACCGACG
SJD014_MpARF3 gene coding C ter.REV	TGCCGCCGCCaagcttCCAGGCGCCTTGCGGACT
SJD015_MpARF3 downstream noncoding.FOR	taaactagtggcgcgccGAAATCGTGTTCGAATTCATCAACCTGTGTTGTATG
SJD016_MpARF3 downstream noncoding.REV	ttatccctaggcgcgAGTGGTGCCAAGTGCGGTTC
SJD017_MpTIR1 gene Cter seq.FOR	gcgattaattaagcttCAGTCTAGCCCCTCAGAGAGAAAGAG
SJD018_MpTIR1 gene Cter seq.REV	TGCCGCCGCCaagcttTTGTGCTATTTCGACAAAGTCGGG
SJD019_MpTIR1 downstream seq.FOR	taaactagtggcgcgATCTACAATTTCTTGGATCTGTTCCGACCCTGAATA
SJD020_MpTIR1 downstream seq.REV	ttatccctaggcgcgccTGTCGAGTCATGCAGCATGCCAA
SJD021_MpIAA gene seq Cter.FOR	gcgattaattaagcttGTGAGTGATTGTGCGAGGGGTG

SJD022_MpIAA gene seq Cter.REV	TGCCGCCGCCaagcttCACGTTCGGT TGAGTCGTCTTGTTTG
SJD023_MpIAA downstream noncoding.FOR	taaactagtggcgcgATGTTATTCATTCA TATACGATGTCTCTCTGTCCTCTC TTCTCT
SJD024_MpIAA downstream noncoding.REV	ttatccctaggcgcgccTTGGAAGGGAACA TGGCAGAGAAACG
SJD025_Mp ncARF coding Cter.FOR	gcgattaattaagcttACCTTTTGCGGTAC CGTCAAACAACTAATACTTTAG
SJD026_Mp ncARF coding Cter.REV	TGCCGCCGCCaagcttGTACTGTTTC AAAGTTCCAGTTCCTAAATTGTTG TAAGCA
SJD027_MpncARF downstream.FOR	taaactagtggcgcgCCTTGTTCATTACTT TTTCTATATTCATCATTTCACACA TTATTC
SJD028_MpncARF downstream.REV	ttatccctaggcgcgccATAGTCATTGGCC TCAGTTCCCTG
SJD069_ARF3 genomic.2ND.FOR	gcgattaattaagcttAGCATTTACCTACC GACCGACGCCCGCAGCATAG
SJD070_ARF3down2ND.REV	ttatccctaggcgcgAGTGGTGCCAAGTG CGGTTCGAAGTGAGG
SJD071_TIR1down2ND.REV	ttatccctaggcgcgccCTACTGTATGTAT GCGTACGAAGACTCG
SJD073 ARF3gene4K.FOR	AGCTCAAGTCTTGGACTTAGG
SJD074 ARF3gene4K.REV	TGTGTGACACCAACTGCTTCC
SJD075 ARF3down4K.FOR	TGCATATATGAGACATTGAAGG
SJD076 ARF3down4K.REV	TCAATAACCGATCAGACCAGAC
SJD077 TIR1down4K.FOR	GATGTTACATTGTGGTGTTCAC
SJD078 TIR1down4K.REV	CTCTCATCATGTGCTGAATAACTC
SJD079_mNeonGreen.FOR	gcgattaattaagcttGGCGGCGGCAGCAT GGTGAGCAAGGGCGAGGAG
SJD80_mNeonGreen.REV	attcgagctcaagctGTTACTTGTACAGCT CGTCCATGC
SJD081_ARF3genomic stitch.FOR	CAGCAGCTTCGCGCGCAATCG
SJD082_ARF3genomic stitch.REV	GAGCTCGATTGCGCGCGAAGC
SJD083-ARF3down stitch.FOR	GTGCGAAGTGAGGTCATCCACGA ATGG
SJD084-ARF3down stitch.REV	CATGATGGCCATTCGTGGATGAC CTCAC
SJD085-TIR1down stitch.FOR	CTACGGTATGCAAGTGTCTGTTGC TTCG
SJD086-TIR1down stitch.REV	ACTCGTATGCGAAGCAACAGACA CTTGC

SJD089-TIR1 down stitch.REV2	ttatccctaggcgcgccGTTCATTACACTT GCGACCGCTGCTAC
SJD091-MpARF1down.GNTYP3	CATCGGAGTGTGGAGTGTGA
SJD092-MpARF1down.GNTYP4	AAGCTGCGTGTACTATCAGC
SJD094-MpARF2down.GNTYP 3	GGCGAGACGGAAGAACAGAG
SJD095-MpARF2down.GNTYP4	GATTCGTTGCAAGTTCGTGTG
SJD097-MpARF3down.GNTYP 3	AGCATACAACACAGGTTGATG
SJD098-MpARF3down.GNTYP4	TGGTCTAACACACCATCACTC
SJD100-MpTIR1down.GNTYP 3	GAAAGGTATTCAGGGTCGGAACA G
SJD101-MpTIR1down.GNTYP4	GAACTAGTTGTCTGGAGTCTG
SJD103-MpIAAdown.GNTYP3	AGAGAGGACAGAGAGACATCG
SJD104-MpIAAdown.GNTYP4	TTGAGGAGTGGTGGTGATAG
SJD110-MpncARFgene.GNTYP2	TACCTCGTGATTCTTCTCAC
SJD111-MpncARFdown.GNTYP3	GATTGTGTACTCGGTAATGTG
SJD112-MpncARFdown.GNTYP4	CACCATGTAGGTTCATCTGAG
SJD113-MpARF1gene.GNTYP1 NEW	CGTAGACATCTTCTCACAACTG
SJD114-MpARF2gene.GNTYP1 NEW	GTGATACCATGTATGCTCAACG
SJD115-MpARF3gene.GNTYP1 NEW	CTTAGGCTGTCTTCCTGTCCTG
SJD116-MpTIR1gene.GNTYP1 NEW	CTCTCTGTACTTGCTACAATCC
SJD117-MpIAAgene.GNTYP1 NEW	GAGCCTCATTATCTTCTTCTCC
SJD119-MpncARFgene.GNTYP1 NEW	TTCTTCTATACACGTTGCATTCG

References

1. Vanneste, S. & Friml, J. Auxin: A Trigger for Change in Plant Development. *Cell* vol. 136 Preprint at https://doi.org/10.1016/j.cell.2009.03.001 (2009).
2. Weijers, D. & Wagner, D. Transcriptional Responses to the Auxin Hormone. *Annu Rev Plant Biol* **67**, 539–574 (2016).
3. Kepinski, S. & Leyser, O. The Arabidopsis F-box protein TIR1 is an auxin receptor. *Nature* **435**, 446–451 (2005).
4. Gray, W. M., Kepinski, S., Rouse, D., Leyser, O. & Estelle, M. Auxin regulates SCFTIR1-dependent degradation of AUX/IAA proteins. *Nature* **414**, 271–276 (2001).
5. Das, S., Weijers, D. & Borst, J. W. Auxin Response by the Numbers. *Trends in Plant Science* vol. 26 Preprint at https://doi.org/10.1016/j.tplants.2020.12.017 (2021).
6. Prigge, M. J. *et al.* Genetic analysis of the arabidopsis TIR1/AFB auxin receptors reveals both overlapping and specialized functions. *Elife* **9**, (2020).
7. Powers, S. K. *et al.* Nucleo-cytoplasmic Partitioning of ARF Proteins Controls Auxin Responses in Arabidopsis thaliana. *Mol Cell* **76**, 177-190.e5 (2019).
8. Hamann, T., Benkova, E., Bäurle, I., Kientz, M. & Jürgens, G. The Arabidopsis BODENLOS gene encodes an auxin response protein inhibiting MONOPTEROS-mediated embryo patterning. *Genes Dev* **16**, (2002).
9. Ludwig, Y., Berendzen, K. W., Xu, C., Piepho, H. P. & Hochholdinger, F. Diversity of stability, localization, interaction and control of downstream gene activity in the maize Aux/ IAA protein family. *PLoS One* **9**, (2014).
10. Puchta, H. The repair of double-strand breaks in plants: Mechanisms and consequences for genome evolution. *Journal of Experimental Botany* vol. 56 Preprint at https://doi.org/10.1093/jxb/eri025 (2005).
11. Offringa, R. *et al.* Extrachromosomal homologous recombination and gene targeting in plant cells after Agrobacterium mediated transformation. *EMBO Journal* **9**, (1990).
12. Bowman, J. L. *et al.* Insights into Land Plant Evolution Garnered from the Marchantia polymorpha Genome. *Cell* **171**, (2017).
13. Mutte, S. K. *et al.* Origin and evolution of the nuclear auxin response system. *Elife* **7**, 1–25 (2018).
14. Kato, H. *et al.* The roles of the sole activator-type auxin response factor in pattern formation of marchantia polymorpha. *Plant Cell Physiol* **58**, 1642–1651 (2017).
15. Flores-Sandoval, E., Eklund, D. M. & Bowman, J. L. A Simple Auxin Transcriptional Response System Regulates Multiple Morphogenetic Processes in the Liverwort Marchantia polymorpha. *PLoS Genet* **11**, 1–26 (2015).
16. Ishizaki, K., Johzuka-Hisatomi, Y., Ishida, S., Iida, S. & Kohchi, T. Homologous recombination-mediated gene targeting in the liverwort Marchantia polymorpha L. *Sci Rep* **3**, 1–6 (2013).
17. Bindels, D. S. *et al.* MScarlet: A bright monomeric red fluorescent protein for cellular imaging. *Nat Methods* **14**, (2016).
18. Shaner, N. C. *et al.* A bright monomeric green fluorescent protein derived from Branchiostoma lanceolatum. *Nat Methods* **10**, (2013).
19. Kato, H. *et al.* Design principles of a minimal auxin response system. *Nat Plants* **6**, (2020).
20. Suzuki, H., Kato, H., Iwano, M., Nishihama, R. & Kohchi, T. Nuclear auxin signaling is essential for organogenesis but not for cell survival in the liverwort Marchantia polymorpha *bioRxiv* 2022.06.21.497043 (2022)

doi:10.1101/2022.06.21.497043.
21. Eklund, D. M. *et al.* Auxin produced by the indole-3-pyruvic acid pathway regulates development and gemmae dormancy in the liverwort marchantia polymorpha. *Plant Cell* **27**, 1650–1669 (2015).
22. Freire-Rios, A. *et al.* Architecture of DNA elements mediating ARF transcription factor binding and auxin-responsive gene expression in Arabidopsis. *Proc Natl Acad Sci U S A* **117**, (2020).
23. Boer, D. R. *et al.* Structural basis for DNA binding specificity by the auxin-dependent ARF transcription factors. *Cell* **156**, 577–589 (2014).
24. Schlereth, A. *et al.* MONOPTEROS controls embryonic root initiation by regulating a mobile transcription factor. *Nature* **464**, 913–916 (2010).
25. Okushima, Y. *et al.* Functional genomic analysis of the AUXIN RESPONSE FACTOR gene family members in Arabidopsis thaliana: Unique and overlapping functions of ARF7 and ARF19. *Plant Cell* **17**, (2005).
26. Flores-Sandoval, E., Romani, F. & Bowman, J. L. Co-expression and transcriptome analysis of marchantia polymorpha transcription factors supports class c arfs as independent actors of an ancient auxin regulatory module. *Front Plant Sci* **9**, 1–21 (2018).
27. Flores-Sandoval, E. *et al.* Class C ARFs evolved before the origin of land plants and antagonize differentiation and developmental transitions in Marchantia polymorpha. *New Phytologist* **218**, 1612–1630 (2018).
28. Dubey, S. M. *et al.* The AFB1 auxin receptor controls the cytoplasmic auxin response pathway in Arabidopsis thaliana *bioRxiv* 2023.01.04.522696 (2023) doi:10.1101/2023.01.04.522696.
29. Serre, N. B. C. *et al.* AFB1 controls rapid auxin signalling through membrane depolarization in Arabidopsis thaliana root. *Nat Plants* **7**, (2021).
30. Piya, S., Shrestha, S. K., Binder, B., Neal Stewart, C. & Hewezi, T. Protein-protein interaction and gene co-expression maps of ARFs and Aux/IAAs in Arabidopsis. *Front Plant Sci* **5**, (2014).
31. Vernoux, T. *et al.* The auxin signalling network translates dynamic input into robust patterning at the shoot apex. *Mol Syst Biol* **7**, (2011).
32. Ishizaki, K., Chiyoda, S., Yamato, K. T. & Kohchi, T. Agrobacterium-mediated transformation of the haploid liverwort Marchantia polymorpha L., an emerging model for plant biology. *Plant Cell Physiol* **49**, 1084–1091 (2008).

Chapter 4

Dynamic regulation of MpARF stoichiometry is required for gemma development

Shubhajit Das[1], Martijn de Roij[1], Simon Bellows[2], Etienne Farcot[2], Dolf Weijers[1], Jan Willem Borst[1]
[1]Laboratory of Biochemistry, Wageningen University, the Netherlands
[2]School of Mathematical Sciences, University of Nottingham, United Kingdom

Part of this chapter has been published as:

Das S., Roij M., Bellows S., Kohlen W., Farcot E., Weijers D. and Borst JW (2022) Selective degradation of ARF monomers controls auxin response in Marchantia. bioRxiv.
DOI:10.1101/2022.11.04.515187

Abstract
The plant hormone auxin is a key regulator of growth and development. Auxin perception by nuclear TIR1/AFB receptors triggers proteasomal degradation of Aux/IAA repressors and releases ARF transcription factors from inhibition. ARFs can specifically bind to DNA, bringing about transcriptional changes that direct plant development. Among the three phylogenetic classes of ARFs, class-A and class-B ARFs are known to competitively bind the same DNA elements. Therefore, relative concentrations of these ARFs and their DNA binding affinities are key determinants of transcriptional auxin response. Although the *in vitro* DNA-binding affinities of ARFs were determined, the endogenous relative concentrations of ARFs are unknown. Here we used genomic fluorescent knock-in lines to track *Marchantia polymorpha* ARF protein accumulation patterns in germinating gemmae. By quantifying temporal accumulation patterns of the three MpARFs, we found that MpARF1 (class A) and MpARF2 (class B) are unstable during germination. We found that this instability is caused by proteasomal degradation, while MpARF3 (class C) lacks such regulation. Degradation during germination results in complete loss of MpARF2, whereas MpARF1 remains detectable. A consequence of different residual ARF levels is a shift in the stoichiometry of ARF1 and ARF2 in germinated gemmae. Mathematical modelling predicted this stoichiometry shift as a requirement for transcriptional activation of auxin-responsive genes. Auxin-insensitivity of gemmae overexpressing MpARF2 validated model predictions. Overall, this chapter reports a role of proteasomal ARF degradation in defining relative MpARF1/2 concentrations, essential for auxin response and gemmae development.

Introduction

Auxin influences growth of all land plant species studied. Auxin response involves transcriptional regulation of many genes, mediated by a mechanism that revolves around proteasomal degradation of Aux/IAA (Auxin/INDOLE-3-ACETIC ACID) repressors by the TIR1/AFB (TRANSPORT INHIBITOR RESPONSE/AUXIN SIGNALING F-BOX) auxin receptors[1–3]. Auxin-dependent degradation of Aux/IAAs releases DNA-binding transcription factor ARFs (AUXIN RESPONSE FACTOR) from inhibition and permits ARF-activated transcription[4,5]. Based on phylogeny and functional characterization in angiosperms, ARFs have been categorized into three classes: class A, B and C. Given that there are multiple ARF members within each class and their functions are often redundant in the angiosperm *Arabidopsis thaliana*, it is hard to derive general properties of ARF function from angiosperms. The auxin response systems in the bryophytes *Physcomitrium patens*[6] and *Marchantia polymorpha*[6–8] have a much more limited number of components, which helped to reduce complexity and derive common, core principles of ARF function[9,10]. Phylogenetic analysis showed that the nuclear auxin signaling pathway (NAP) in Marchantia consist of a single TIR1 auxin receptor, a single Aux/IAA repressor and one ARF in each of the three classes (A, B and C)[8]. Canonical ARFs are composed of three functional domains: the N-terminal DNA binding domain (DBD), the middle region (MR) and the C-terminal Phox-Bem1 (PB1) oligomerization domain. The conserved DBD allows recognition of specific DNA motifs (Auxin Response Elements) present in the upstream region of auxin-regulated genes. Single molecule FRET (Förster Resonance Energy Transfer) analysis showed that DNA binding affinities of class-A MpARF1-DBD and class-B MpARF2-DBD are within one order of magnitude, suggesting the possibility of competitive DNA binding at near-stoichiometric concentrations[9]. Together, these studies in Physcomitrium and Marchantia led to the model that auxin response is defined by an antagonistic interaction between A- and B-class ARFs, competing for the same DNA binding sites. However, this ARF antagonism model is largely built on qualitative *in vivo* data on ARF function. The true *in vivo* concentrations of ARFs, and the relative stoichiometries of antagonistic ARFs are unknown. Given that DNA binding is determined both by affinity and concentration, it is essential to quantify the relative concentrations of the A and B-class ARFs and investigate if auxin response capacity is determined by such stoichiometries.

Quantitative analysis of ARFs is challenging in the functionally redundant protein network of angiosperms. In contrast, the Marchantia NAP is much simpler with only one ARF of each class, and therefore offers a suitable system for quantitative analysis[11]. In chapter 3, using the fluorescent genomic knock-in lines, we showed that both activator (MpARF1) and repressor (MpARF2 and MpARF3) ARFs have differences in their relative expression levels in dormant gemmae. However, dynamics of ARF accumulation during growth are yet unclear. In this chapter, we used germinating Marchantia gemmae as a model to explore the temporal dynamics of the three MpARF accumulation patterns. Using both single and double ARF fluorescent knock-in lines (see Chapter 3), we found that the MpARF1 (class A) and MpARF2 (class B) protein levels are highly dynamic, and actively regulated. In contrast, MpARF3 (class C) accumulation patterns were stable throughout gemmae development. Further analysis revealed that the MpARF1 and MpARF2 levels are controlled by proteasomal degradation, impacting on MpARF1/2 stoichiometry. Mathematical model simulations, validated by experimental evidence, confirmed that regulated ARF degradation is required to change relative MpARF1/2 concentrations, essential for auxin response and gemmae development.

Results

Temporal expression maps of MpARFs during gemma development

In chapter 3, the accumulation patterns of MpARF proteins were shown in dormant gemmae. Dormant gemmae represent a stage of quiescence, while auxin activity is strongly connected to growth. We therefore explored patterns of ARF accumulation in the first 24 hours after removing gemmae from the gemmae cup, a period in which growth initiates. To this end, we used fluorescently tagged ARF knock-in lines, that we showed to have full functionality of each ARF both in the presence and absence of auxin (Chapter 3). For time-lapse imaging of live tissue, we used a microscope slide mount (Supplementary Figure 1) that allowed to grow and image the same gemmae over time. Starting with dormant gemmae at 0 hours after transfer to the mount, we checked ARF expression after 8 and 24 hours of active growth. Remarkably, while the ARF3-mScarlet-I accumulation patterns did not change in the first 24-hour time window, we found both ARF1-mScarlet-I and ARF2-mScarlet-I protein levels to progressively decline after germination (Figure 1.A-C). Given the higher starting levels of ARF1 and lower ARF2 concentrations in dormant gemmae, the former was still detectable after 24 hours, while ARF2 signal declined to undetectable levels already at 8 hours (Figure 1.A-B). Com-

parable protein accumulation dynamics were found for the ARF1-mNeonGreen and ARF2-mNeonGreen proteins (Figure 1.D), indicating that the protein level decline is independent of the fluorescent tag. Expressing unfused nuclear mScarlet-I or mNeonGreen from a constitutive promoter (pEF1α::NLS-mScarlet-I; pEF1α::NLS-mNeonGreen) led to stable expression patterns (Figure 2.F-G) showing that the protein concentration decline during gemma germination is specific to MpARF1 and MpARF2.

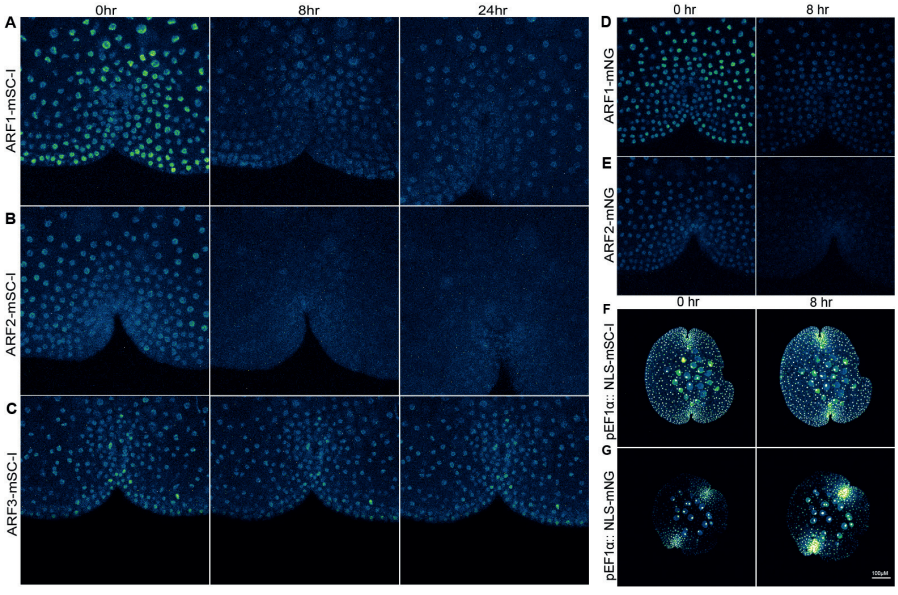

Figure 1: Comparison of temporal dynamics of ARF1, ARF2 and ARF3 fused to mScarlet-I (mSC-I) in single knock-in lines. (A-B) ARF1 and ARF2 shows fluorescence decline after gemma germination, whereas (C) ARF3 fluorescence remains unchanged in the first 24 hours. After 24 hours, ARF1 shows a low expression, whereas ARF2 is completely degraded. (D-E) ARF1-mNeonGreen and ARF2-mNeonGreen single knock-in lines show similar temporal expression patterns as observed in mScarlet-I fusion variants. (F) Non-fused fluorescent proteins are stably expressed at same developmental stages of gemmae, indicating specificity of fluorescence decline for ARF1 and ARF2.

Regulated protein degradation controls MpARF levels

Protein accumulation patterns can be actively regulated by both transcriptional and post-transcriptional mechanisms. To test whether MpARF concentration decline is transcriptionally regulated in germinating gemmae, we quantified *MpARF1* and *MpARF2* transcripts using qRT-PCR. Neither of the *ARF* transcript levels changed significantly over the first 8 hours after germination (Figure 2.A), suggesting that MpARF1 and MpARF2 protein levels are post-transcriptionally controlled. Such control could be at translational or

post-translational level. Given that there are examples of proteolytic degradation of ARF proteins in Arabidopsis[12], we asked if active protein degradation causes the decline in MpARF levels. Indeed, both proteins accumulated to much higher levels when ARF double knock-in gemmae were treated with the proteasome inhibitor MG132 (Figure 2.B-C, E). Quantification of protein accumulation patterns showed that upon MG132 treatment, ARF1 levels stabilize, whereas ARF2 concentration even slightly increased beyond the initial accumulation level. In contrast, ARF3 was unaffected by MG132 treatment (Figure 2.D-E). We validated MpARF degradation by treatment with an alternative proteasomal inhibitor Bortezomib, which also blocked degradation and caused ARF accumulation (Figure 3.A). Importantly, proteasome inhibition completely prevented the decline of ARF1 and ARF2 fluorescence signals (Figure 2.B-C, E). These results imply that both ARF1 and ARF2, but not ARF3, are proteasomally degraded.

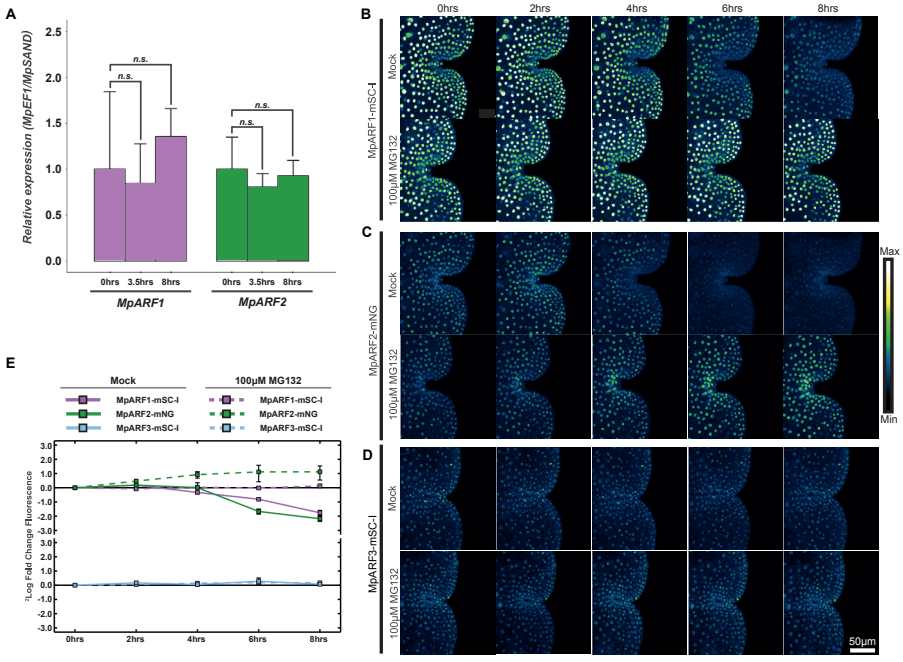

Figure 2: (A) qRT-PCR of MpARF1 and MpARF2 shows stable gene transcription during gemma germination. (B-D) Time-course imaging of MpARF1, MpARF2 and MpARF3 in germinating gemmae. Both MpARF1 and MpARF2 fluorescence signal starts to decline after germination. ARF2-mNG fluorescence is undetectable after 6 hours, whereas ARF1-mSC-I expression is maintained at 8 hours. Upon treatment with proteasome inhibitor 100μM MG132, the signal decline of ARF1-mSC-I and ARF2-mNG is blocked, implying proteasomal regulation of ARF1 and ARF2. Contrarily, ARF3-mSC-I expression remains stable in both mock and 100μM MG132 treated samples, suggesting that ARF3 lacks proteasomal regulation, unlike ARF1 and ARF2. (E) Quantification of ARF1, ARF2, and ARF3 protein expression fold changes in mock and 100μM MG132 treated samples.

To investigate which biological signal might trigger MpARF degradation during germination, we exogenously treated double knock-in gemmae with common plant hormones and their inhibitors. Hormones including auxin, abscisic acid, gibberellic acid, and jasmonic acid were ineffective in preventing degradation. Similarly, auxin transport or biosynthesis inhibitor were also ineffective, suggesting ARF degradation is not controlled by auxin or other tested hormones.

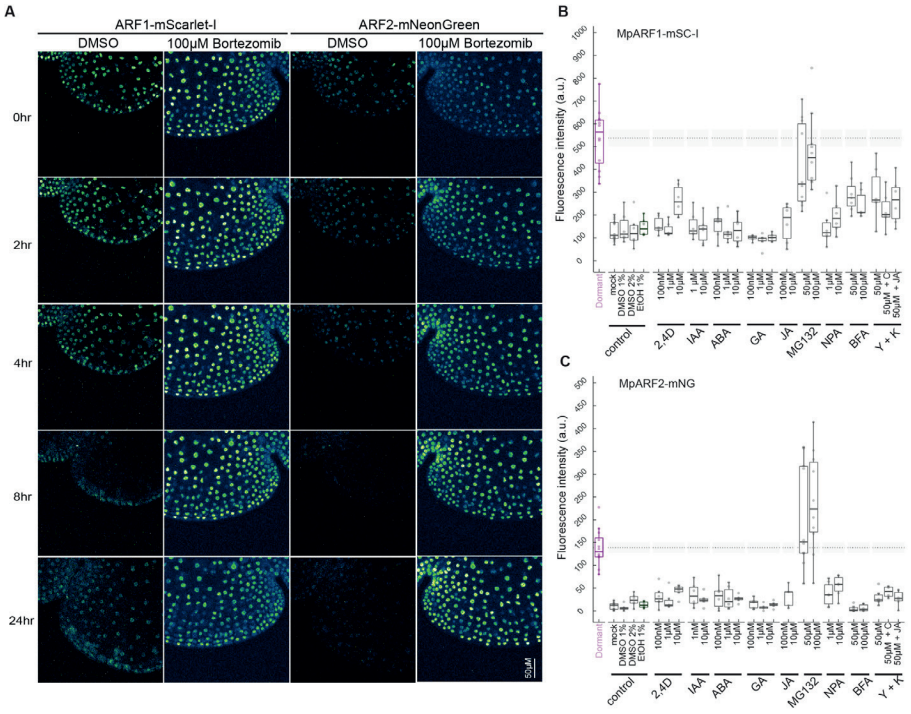

Figure 3: (A) Treatment with an alternative proteasomal degradation inhibitor Bortezomib also blocks the degradation of ARF1-mScarlet-I (mSC-I) and ARF2-mNeonGreen (mNG). (B-C) Treatment with common plant hormones including auxin (2,4-D and IAA), abscisic acid (ABA), gibberellic acid (GA), jasmonic acid (JA) do not have any effect on MpARF degradation. Auxin transport NPA or endocytosis inhibitor Brefeldin-A (BFA) also has no effect. Co-treatment of auxin biosynthesis inhibitor Yucasin (Y) and Kynurenine (K) alone or in combination with cold treatment and JA treatment also fails to stabilize MpARFs. Only proteasomal inhibitor MG132 can block ARF degradation.

Proteasomal degradation leads to higher ARF1/2 stoichiometry

A key question is what function this regulated ARF degradation serves. Given that it was previously proposed that auxin responsiveness in Marchantia is determined by the stoichiometry of ARF1 and ARF2[9], one possibility is that this stoichiometry is actively regulated by ARF degradation. In chapter 3, we found that ARF1 and ARF2 are present in different stoichiometries in differ-

ent cell types. We asked whether ARF1/2 stoichiometries in dormant gemmae change following germination. Therefore, we quantified the ARF1 and ARF2 levels in germinating gemmae and calculated the ARF1:ARF2 ratio over the first 8 hours (Figure 4.A). For comparable fluorophore brightness, we used mNeonGreen single knock-in lines in this experiment. Quantified ARF ratios suggested that the different ARF degradation profiles result in an increase of the ratio of ARF1:ARF2 after germination. The ratio increased from approximately 3.8 at dormant stage to up to 8 in the 6-8 hours grown gemmae. This increase in ARF1/2 stoichiometry caused a positive shift in relative MpARF1 levels in the cell and provides a scope for ARF1-dependent gene activation.

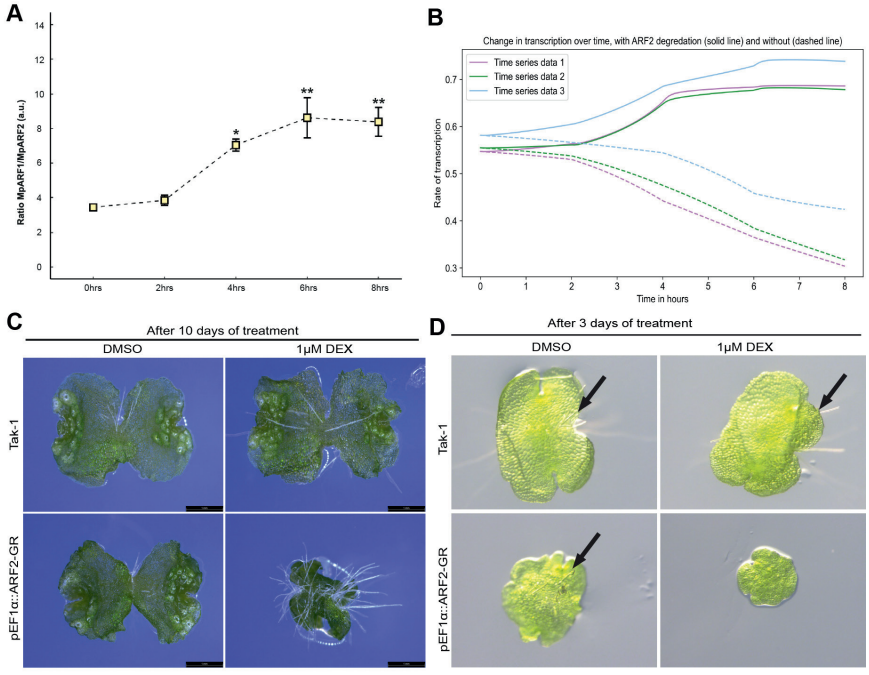

Figure 4: (A) Quantification of ARF1:ARF2 stoichiometry during gemmae germination in ARF1-mNG and ARF2-mNG single knock-in lines. (B) Mathematical model predicted transcription pattern of an auxin inducible gene during gemmae germination. Solid lines indicate transcription rate in normal condition, whereas dashed lines indicate transcription rate in absence of proteasomal degradation of ARF2. (C) Inducible ARF2 overexpression leads to retarded growth. pEF1::ARF2-GR lines were treated with 1μM dexamethasone and plant growth was compared with wild-type. After 3 days of DMSO treatment, both wild-type Tak-1and pEF1::ARF2-GR lines grew similarly. However, on dexamethasone treatment, induced ARF2-GR overexpression lines growth was affected negatively in comparison to wild-type. (D) Inducible ARF2 overexpression leads to delayed gemmae germination. pEF1::ARF2-GR lines were treated with 1μM dexamethasone and plants were checked for rhizoid formation as a sign for germination. After 3 days of DMSO treatment, both wild-type Tak-1and pEF1::ARF2-GR lines developed rhizoids. However, only Tak-1 developed rhizoids on dexamethasone treatment. No rhizoid was formed in induced ARF2-GR overexpression lines.

ARF1/2 stoichiometry increase is necessary for germination and growth

We next asked what the impact of this change in ARF1:ARF2 stoichiometry may be, and first developed a mathematical model of the minimal Marchantia NAP and its known interactions (see Text box 1). Using a piecewise polynomial function, we fitted quantified ARF1 and ARF2 temporal expression profiles into the mathematical model, where the effect of changing ARF1 and ARF2 levels on the outcome of auxin response was modelled as the transcription of a hypothetical ARF-regulated gene. Model simulations predicted that the ARF1:ARF2 ratio increase would enhance transcriptional response output (Figure 4.B). Conversely, simulated loss of ARF2 degradation predicted an opposite effect on response output (Figure 4.B). Thus, ARF2 degradation may be required to switch from an inactive to an active transcriptional state of auxin-regulated genes.

Text Box 1: Description of mathematical model for auxin signaling in Marchantia

Our initial goal was to create an auxin signaling model for Marchantia to test out hypotheses. To do so we have altered an established auxin signaling model, the Farcot model[13], to better represent Marchantia specifically.
The model we present is specific to modeling transcription rates relative to MpARF1 and MpARF2 concentrations within a gemma in the first 8 hours after dormancy. Time dependent simulations were run via Python3.8 utilizing primarily SciPy and NumPy packages, specifically using the ODE solver scipy.intergrate.odeint.

The model takes the form of the following equations:

$$\frac{dA_1}{dt} = \pi_{A_1} - 2\alpha_{A_1A_1}A_1A_1 + 2\theta_{D_{A_1A_1}}D_{A_1A_1} - \alpha_{A_1A_2}A_1A_2 + \theta_{A_1A_2}D_{A_1A_2} - \alpha_{GA_1}GA_1 + \theta_{GA_1}G_{A_1} \quad -\alpha_{A_1GA_1}A_1G_{A_1}\theta_{A_1GA_1}G_{A_1A_1} - \alpha_{A_1GA_2}A_1G_{A_2} + \theta_{A_1GA_2}G_{A_1A_2}$$

$$\frac{dA_2}{dt} = \pi_{A_2} - \alpha_{A_1A_2}A_1A_2 + \theta_{A_1A_2}D_{A_1A_2} - 2\alpha_{A_2A_2}A_2A_2 + 2\theta_{A_2A_2}D_{A_2A_2} - \alpha_{A_2GA_1}A_2G_{A_1} + \theta_{A_2GA_1}G_{A_1A_2} \quad -\alpha_{GA_2}GA_2 + \theta_{GA_2}G_{A_2} - \alpha_{A_2GA_2}G_{A_2}A_2 + \theta_{A_2GA_2}G_{A_2A_2}$$

$$\frac{dD_{A_1A_1}}{dt} = -\mu_{A_1A_1}D_{A_1A_1} + \alpha_{A_1A_1}A_1A_1 - \theta_{D_{A_1A_1}}D_{A_1A_1} - \alpha_{A_1A_1G}D_{A_1A_1}G + \theta_{A_1A_1G}G_{A_1A_1}$$

$$\frac{dD_{A_1A_2}}{dt} = -\mu_{A_1A_2}D_{A_1A_2} + \alpha_{A_1A_2}A_1A_2 - \theta_{A_1A_2}D_{A_1A_2} - \alpha_{A_1A_2G}D_{A_1A_2}G + \theta_{A_1A_2G}G_{A_1A_2}$$

$$\frac{dD_{A_2A_2}}{dt} = -\mu_{A_2A_2}D_{A_2A_2} + \alpha_{A_2A_2}A_2A_2 - \theta_{A_2A_2}D_{A_2A_2} + \theta_{A_2A_2G}G_{A_2A_2} - \alpha_{A_2A_2G}D_{A_2A_2}G$$

$$\frac{dG}{dt} = -\alpha_{GA_1}GA_1 + \theta_{GA_1}G_{A_1} - \alpha_{GA_2}GA_2 + \theta_{GA_2}G_{A_2} - \alpha_{A_1A_1G}D_{A_1A_1}G + \theta_{A_1A_1G}G_{A_1A_1} - \alpha_{A_1A_2G}D_{A_1A_2}G + \theta_{A_1A_2G}G_{A_1A_2} - \alpha_{A_2A_2G}D_{A_2A_2}G + \theta_{A_2A_2G}G_{A_2A_2}$$

$$\frac{dG_{A_1}}{dt} = \alpha_{GA_1}GA_1 - \theta_{GA_1}G_{A_1} - \alpha_{A_1GA_1}A_1G_{A_1} + \theta_{A_1GA_1}G_{A_1A_1} - \alpha_{A_2GA_1}A_2G_{A_1} + \theta_{A_2GA_1}G_{A_1A_2}$$

$$\frac{dG_{A_2}}{dt} = \alpha_{GA_2} GA_2 - \theta_{GA_2} G_{A_2} - \alpha_{A_1GA_2} A_1 G_{A_2} + \theta_{A_1GA_2} G_{A_1A_2} - \alpha_{A_2GA_2} G_{A_2} A_2 + \theta_{A_2GA_2} G_{A_2A_2}$$

$$\frac{dG_{A_1A_1}}{dt} = \alpha_{A_1GA_1} A_1 G_{A_1} - \theta_{A_1GA_1} G_{A_1A_1} + \alpha_{A_1A_1G} D_{A_1A_1} G - \theta_{A_1A_1G} G_{A_1A_1}$$

$$\frac{dG_{A_1A_2}}{dt} = \alpha_{A_2GA_1} A_2 G_{A_1} - \theta_{A_2GA_1} G_{A_1A_2} + \alpha_{A_1GA_2} A_1 G_{A_2} - \theta_{A_1GA_2} G_{A_1A_2} + \alpha_{A_1A_2G} D_{A_1A_2} G - \theta_{A_1A_2G} G_{A_1A_2} \frac{dG_{A_2A_2}}{dt} = \alpha_{A_2A_2G} D_{A_2A_2} G - \theta_{A_2A_2G} G_{A_2A_2} + \alpha_{A_2GA_2} G_{A_2} A_2 - \theta_{A_2GA_2} G_{A_2A_2}$$

$$\frac{dh}{dt} = l_1 G_{A_1} + l_2 G_{A_1A_1}$$

Where,
A_1 denotes the concentration of MpARF1,
A_2 denotes the concentration of MpARF2,
D_{XY}, $X, Y \in \{A_1, A_2\}$ denotes the concentration of an X:Y dimer,
G , G_{A_1}, G_{A_2}, $G_{A_1A_1}$, $G_{A_1A_2}$, $G_{A_2A_2}$ denote the proportion or the probabilities the promoter is free, bound with MpARF1, MpARF2, MpARF1:MpARF1 dimer, MpARF1:MpARF2 dimer or MpARF2:MpARF2 dimer respectively,
h denotes the concentration of mRNA being produced.

The parameter values used are in the table below

Variable	Value	Description
$\alpha_{A_1A_1}$	1	Rate of association of ARF1 with itself
$\alpha_{A_1A_2}$	1	Rate of association of ARF1 with ARF2
$\alpha_{A_2A_2}$	1	Rate of association of ARF2 with itself
α_{A_1G}	K_{on1}	Rate of association of an ARF1 and the promoter
α_{A_2G}	K_{on2}	Rate of association of an ARF2 and the promoter
$\alpha_{A_1A_1G}$	$2K_{on1}$	Rate of association of an ARF1:ARF1 dimer and the promoter

$\alpha_{A_1A_2G}$	$K_{on1} + K_{on2}$	Rate of association of an ARF1:ARF2dimer and the promoter
$\alpha_{A_2A_2G}$	$2K_{on2}$	Rate of association of an ARF2:ARF2 dimer and the promoter
$\theta_{A_1A_1}$	1	Rate of disassociation of ARF1 with itself
$\theta_{A_1A_2}$	1	Rate of disassociation of ARF1 with ARF2
$\theta_{A_2A_2}$	1	Rate of disassociation of ARF2 with itself
θ_{A_1G}	K_{off1}	Rate of disassociation of an ARF1 and the promoter
θ_{A_2G}	K_{off2}	Rate of disassociation of an ARF2 and the promoter
$\theta_{A_1A_1G}$	$\frac{1}{2}K_{off1}$	Rate of disassociation of an ARF1:ARF1 dimer and the promoter
$\theta_{A_1A_2G}$	$\left(K_{off1}^{-1} + K_{off2}^{-1}\right)^{-1}$	Rate of disassociation of an ARF1:ARF2dimer and the promoter
$\theta_{A_2A_2G}$	$\frac{1}{2}K_{off2}$	Rate of disassociation of an ARF2:ARF2 dimer and the promoter
$\mu_{A_1A_1}$, $\mu_{A_1A_2}$ or $\mu_{A_2A_2}$	0.05	Rate of decay of ARF oligomers
l_1	1	Rate of transcription caused by an ARF1 monomer
l_2	10	Rate of transcription caused by an ARF1:ARF1 dimer
$\pi_{A_1}(t)$	$\frac{dTotalARF1}{dt}(t) + \mu_{A_1A_2} + 2\mu_{A_1A_1}$	Term that keeps total MpARF1 concentration matching experimental data
$\pi_{A_2}(t)$	$\frac{dTotalARF2}{dt}(t) + \mu_{A_1A_2} + 2\mu_{A_2A_2}$	Term that keeps total MpARF2 concentration matching experimental data

Model assumptions:

In the model, decrease in total concentration of ARFs is assumed to be via the removal of ARF monomers. This is achieved via the and terms and is inspired by our understanding that the area of an ARF targeted for destruction is the DNA binding domain. We assume in this model that there is no effect on the rate of transcription caused by MpAux/IAA due to its degradation in the early hours gemmae growth.

With respect to parameterization, we assume that the association and disassociation rate between ARFs is 1 for simplicity, and in absence of any quantitative experimental estimates. We assume ARF1 dimers are more effective in promoting transcription than ARF1 monomers and we assume ARF1 monomers and dimers containing ARF2 do not promote transcription. With respect to the association and disassociation of ARF molecules and the promoter we assume that dimers bind the ARF at a rate that is the summation of the rates of the constituent monomers. Furthermore, we assume that the rate of disassociation of dimers is the inverse of the sum of the inverses of the rates of dissociation of the constituent monomers. This in effect makes the rate of disassociation of dimers lower than that of either constituent monomer whilst considering how well either binds the promoter.

Time series simulations:

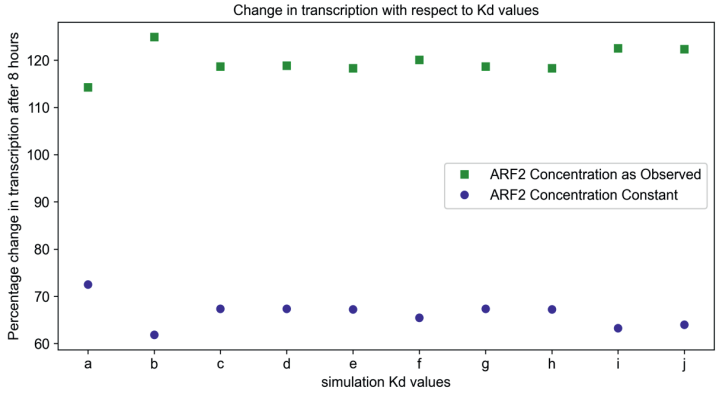

To produce time series simulations using the model for each individual time series dataset we set and equal to a piecewise linear interpolation of the time series data and used the parameters above. To compare the effect the differing Kds of MpARF1 and MpARF2 had on the system we varied in 10 differ-

ent combinations to represent either ARF having a greater Kd than the other whilst also altering the association and disassociation rates.

Kd schemes for the x axis of the graph
a-ARF1Kd/ARF2Kd = 4, ARF1:Kon = 1 Koff = 1 ARF2:Kon = 1 Koff = 4
b-ARF1Kd /ARF2Kd = 4, ARF1:Kon = 1 Koff = 1 ARF2:Kon = 1/4 Koff = 1
c - ARF1Kd / ARF2Kd = 4, ARF1:Kon = 1 Koff = 1 ARF2:Kon =1/2 Koff = 2
d - ARF1Kd / ARF2Kd = 4, ARF1:Kon =1/2 Koff = 2 ARF2:Kon =1/4 Koff = 4
e - ARF1Kd / ARF2Kd = 4, ARF1:Kon = 2 Koff = 1/2 ARF2:Kon = 1/2 Koff = 2
f - ARF1Kd / ARF2Kd = 1, ARF1:Kon = 1 Koff = 1 ARF2:Kon = 1 Koff = 1
g - ARF1Kd / ARF2Kd = 4, ARF1:Kon = 1 Koff = 1 ARF2:Kon = 2 Koff = 1/2
h - ARF1Kd / ARF2Kd = 4, ARF1:Kon = 1/2 Koff = 2 ARF2:Kon = 1 Koff = 1
i - ARF1Kd / ARF2Kd = 1/4, ARF1:Kon = 1 Koff = 1 ARF2:Kon = 1/2 Koff = 2
j - ARF1Kd / ARF2Kd = 1/4, ARF1:Kon = 2 Koff = 1/2 ARF2:Kon = 1 Koff = 1

To test the model prediction that regulated, low ARF2 levels are needed for activating auxin response in gemmae, we overexpressed ARF2 constitutively (pEF1α::ARF2 and pEF1α::ARF2-Citrine) and in a Dexamethasone inducible (pEF1α::ARF2-GR) manner in wild-type background. Inducing ARF2-GR activity with Dexamethasone prevented thallus growth (Figure 4.C) and caused delayed formation of rhizoids (Figure 4.D), a reliable marker for auxin response output. Likewise, 2-week-old stable overexpression lines (pEF1α::ARF2 and pEF1α::ARF2-Citrine) had multiple apical notches, were strongly defective in their growth, lacked gemmae cups and were insensitive to auxin treatment (1-Napthaleneacetic acid; 1-NAA; Figure 5.A). The high fluorescence signal detected in stable overexpression lines of ARF2 (pEF1α::ARF2-Citrine) further confirmed that the auxin insensitivity is indeed caused by high ARF2 concentrations (Figure 5.B). These results support the model prediction that elevated levels of ARF2 inhibit auxin response. Therefore, targeted removal of ARF2 by proteasomal degradation is required to initiate germination and gemmae growth.

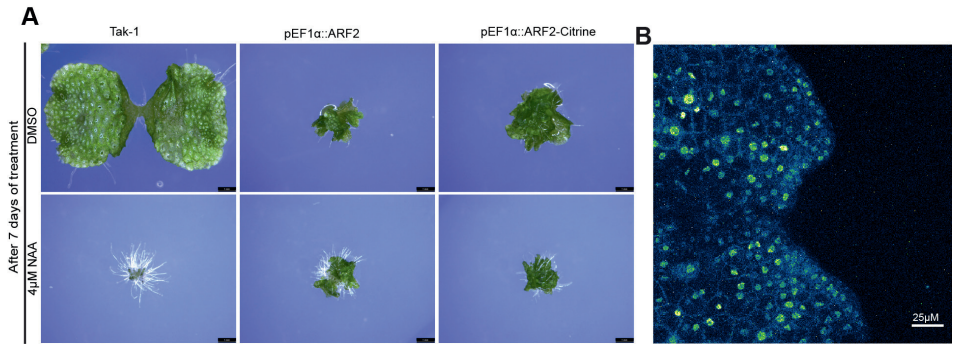

Figure 5: (A) Constitutive overexpression of ARF2 in pEF1α::ARF2 and pEF1α::ARF2-Citrine line leads to auxin resistance. (B) High expression of ARF2-Citrine in pEF1α::ARF2-Citrine line confirms that the auxin resistance phenotype is indeed due to the high expression of ARF2.

Discussion

Biological systems are ever dynamic. Depending on environmental conditions and developmental stages, cellular signaling networks are continuously adapted. Many of these adaptations require active regulation of protein stability and function. In chapter 3, using fluorescent ARF knock-in lines, we showed that all three Marchantia ARFs are expressed in dormant gemmae. However, these ARF expression maps described protein accumulation at dormant stage, without any information on temporal expression patterns in actively growing tissue. To track the temporal dimension of ARF expression, here we used quantitative imaging on growing gemmae of single and double knock-in lines. Upon tracking the protein levels of the three ARFs, we observed one consistent pattern. The class A activator ARF1 and class B repressor ARF2 accumulation patterns both declined within a few hours following dormancy release. After 8 hours, ARF2 levels dropped to undetectable levels while ARF1 maintained a low expression even after 24 hours. The class C repressor ARF3 levels, however, remained constant in the first 24 hours. Similar temporal dynamics confirmed in knock-in lines with ARFs fused to different fluorophores, eliminated any possibility of the fluorescent tag causing protein instability. Since our microscope set up allowed tracking ARF expression in the same gemma, we in fact were able to image the same nuclei for 24 hours. Using this experimental setup, we generated a unique ARF temporal expression map, devoid of any variation among gemmae samples.

We found the *MpARF* transcript quantities did not significantly change over the same time window, suggesting that control of either translation, protein stability or both cause the decline in levels. Indeed, both ARF1 and ARF2 levels were proteasomally regulated, as confirmed by individual treatment

with two different proteasome inhibitors. Upon treatment with these inhibitors, we noticed an interesting difference in the accumulation patterns of non-degraded ARF1 and ARF2. While the ARF1 concentration remained constant, ARF2 levels appeared to accumulate beyond its concentration at dormant stage. Quantification of relative fold-changes in ARF concentration, confirmed this observation. It is possible that this difference is caused by a higher turnover rate for ARF2 than for ARF1, but it is also possible that the ARF1 gene is feedback regulated by accumulation of either ARF1 or ARF2 following proteasome inhibition. We have not tested translational control of ARF1 and ARF2. There are examples of regulation of ARF translational efficiency[14], and we cannot exclude that such regulation contributes to the observed dynamics. However, we can positively identify ARF degradation as a mechanism that controls accumulation.

ARF2 degradation resulted in a complete loss of the fluorescence signal while ARF1 still showed low expression even after 24 hours. This apparently favours ARF1 function by eliminating competition from ARF2. Quantifying the ratio of ARF1/2 concentrations in mNeonGreen single knock-in lines, we found that ARF1/2 stoichiometry rises gradually after dormancy release. Within 6 hours, the ratio almost doubles, favouring ARF1. As anticipated, mathematical simulations predicted an upregulation of transcription rate correlated with ARF1/2 stoichiometry increase. However, the predicted amplitude of transcriptional upregulation in the model was modest. In angiosperms, and even the fern *Ceratopteris richardii*, auxin-responsive genes show large differences in expression level between untreated and auxin-treated conditions, leading to high amplitudes of up to 100-fold[15]. In contrast, Marchantia auxin-regulated genes do not show more than 2 to 3-fold upregulation upon auxin induction[16]. This probably has to do with the simpler NAP in Marchantia. The large amplitudes in Ceratopteris were caused by lower expression in the absence of auxin, rather than higher levels in its presence[15,16]. Thus, more effective repression in the absence of auxin – conditioned by Aux/IAA repressors – likely explains the capacity for large response amplitudes in vascular plants. Likewise, the single Aux/IAA in Marchantia may be limiting such effective repression. Model simulations in absence of a proteasomal regulation on ARF2 resulted in an opposite output with clear transcriptional downregulation. This suggests that ARF2 degradation is probably a necessity to release the dormancy and to switch from an inactive to active transcriptional state of auxin regulated genes. We could validate the prediction from our mathematical model that ARF2 degradation is a requirement for switching to

active auxin response. Overexpression of ARF2 led to phenotypes such as delay in gemma germination, lack of gemma cup formation, and strong auxin resistance. The high fluorescence levels detected for pEF1α::ARF2-Citrine, confirmed high ARF2 accumulation in these lines and validates that growth defects are correlated with ARF2 accumulation (Figure 5.B). Furthermore, the ARF2 overexpression lines developed very few rhizoids, which we can attribute to the high ARF2 levels in rhizoid cells (Figure 5.B), antagonizing rhizoid development by ARF1.

Overall, we could connect ARF degradation with an active control of A/B ARF stoichiometry. Even in the absence of any treatment, and in static observation, gemmae represent a rich landscape of ARF1:ARF2 stoichiometries (see also chapter 3). From first principles, and supported by mathematical modeling, these sites of varying stoichiometries should translate to areas with different auxin response outputs. Indeed, we observed that the cells with the most "activating" stoichiometry are rhizoid initial cells, that are known to be highly sensitive to externally applied auxin. Thus, the endogenous ARF expression patterns will likely translate to a corresponding map of auxin sensitivities. Unfortunately, these are hard to map at present due to the absence of a cellular-resolution reporter for mapping auxin response output. Given that manipulating the stoichiometry does prevent normal auxin response and development, we do expect that the maps – both in the gemmae studied here and beyond – will be an exciting starting point to map sites of auxin action.

A key question is how changes in ARF stoichiometry are brought about. In principle, any gene/protein regulatory process can contribute to protein accumulation, and this stoichiometry therefore offers a central pivot point in controlling auxin output. While it remains to be seen what transcriptional inputs contribute to diverse ARF gene expression patterns, we do see that – given unequal starting levels – a relatively generic degradation rate can create large changes in ARF1:ARF2 stoichiometry. Identification of components in the degradation mechanism, as well as in (post)transcriptional control will help resolve the tuning mechanisms.

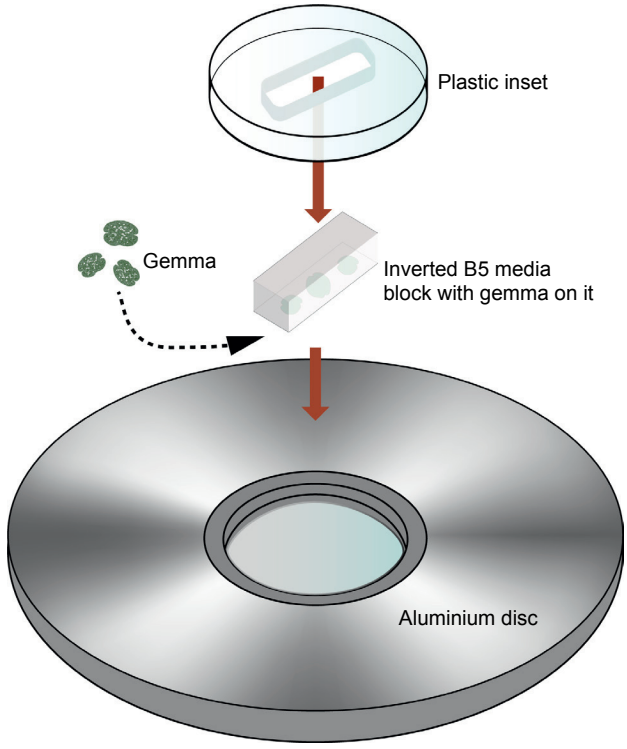

Supplementary Figure 1: Basic design of the microscope slide mount, used for time lapse imaging experiments. B5 media is poured and allowed to solidify inside the plastic inset. The media is supplemented with desired treatment or mock before casting in the inset. When media solidifies, gemmae are carefully placed on top of the media and covered with a round coverslip. The plastic inset containing the gemmae on the media block, is inverted and placed on the aluminium disc and tightened with a screw to prevent movement. Evaporation of water from the reverse side of media block is prevented by sealing with parafilm.

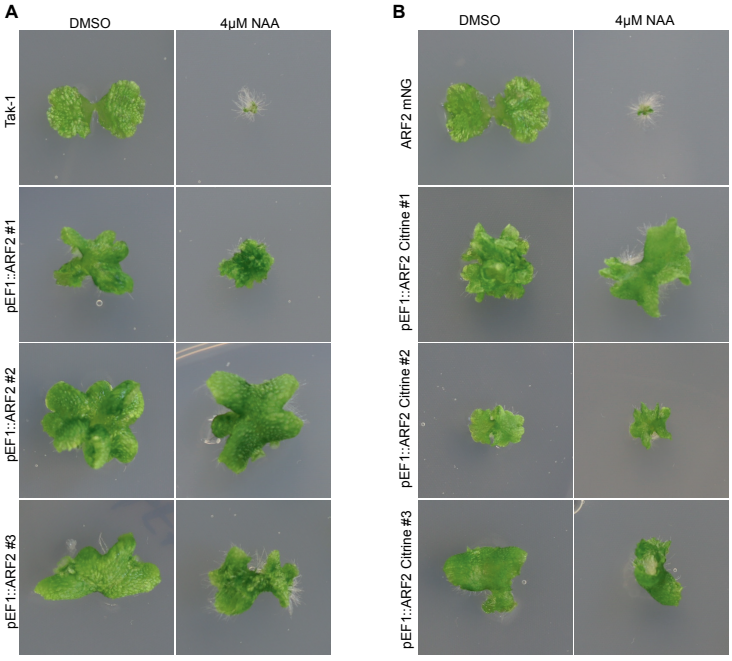

Supplementary Figure 2: Constitutive overexpression of ARF2 or ARF2-Citrine leads to auxin insensitivity. (A) Three independent pEF1::ARF2 lines showing auxin resistance in comparison with Tak-1 control. (B) Three independent pEF1::ARF2-Citrine lines showing auxin insensitivity in comparison to ARF2-mNG knock-in.

Materials and method

Plant growth conditions

Marchantia polymorpha male Takaragaike-1 and female Takaragaike-2 plants were used as the wild-type variety. For vegetative propagation, plants were grown on ½ Gamborg B5 media plates in growth chambers with 40 µmol photons m^{-2} s^{-1} continuous white light at 22 °C. For sexual reproduction, plants were grown on 1% sucrose supplemented ½ Gamborg B5 media within hyrophonic boxes exposed to 40µmol photons m^{-2} s^{-1} continuous white fluorescent light for 1 month. Plants were then moved into 40µmol photons m^{-2} s^{-1} continuous white light supplemented with 15µmol photons m^{-2} s^{-1} far-red light to induce antheridiophore and archegoniophore development. Plants were repeatedly crossed to ensure fertilization. Sporangia with mature spores were collected aseptically and used in spore transformation.

Microscope slide mount setup for time lapse imaging

A microscope slide mount was set up for live imaging of gemmae to precisely track a selected set of cells for temporal protein expression analysis. The mount consisted of a circular aluminium disc with a plastic inset fitted at the centre of the disc (Supplementary Figure 2). Melted ½ B5 media with or without desired treatments were poured into the cavity of the plastic inset and allowed to solidify. Gemmae were carefully placed on top of the solidified media and covered with a round coverslip. The bottom of the mount was sealed with parafilm to prevent any evaporation and media drying during time series imaging. Between two imaging time points in a time series experiment, the mounts were placed inverted in the growth chambers to keep the gemmae exposed to light and allow normal growth.

Confocal live cell imaging

All live cell imaging was done on a Leica SP8X-SMD confocal microscope equipped with hybrid detectors and a pulsed (40MHz) white-light laser (WLL). mNeonGeen and mScarlet-I were excited with the 506 nm and 561 nm laser lines, respectively. The laser powers were set at 4% output to avoid bleaching of the fluorophores. Fluorescence was detected between 512-560nm (mNeonGreen) and 570 to 620nm (mScarlet-I) using hybrid detectors in photon counting mode. Z-stack images of 1.5µm were acquired using a 20X water immersion objective lens and time-gated detection to suppress autofluorescence. Images were processed using ImageJ software. Maximum-intensity projections of z-stack images were used to quantify total cellular fluorescence in each nucleus analysed, corrected for background fluorescence.

RNA extraction, cDNA synthesis and qPCR

Total RNA was extracted from gemmae collected from gemma cups of 4-week-old Tak-1 and knock-in plants and subsequently incubated in liquid ½B5 medium for 0, 3.5, and 8 hours, before freezing in liquid nitrogen. RNA was extracted from ground tissue using the TRIzol reagent and Qiagen Plant mini kit. On-column RNase-free DNase (Qiagen) treatment was performed before final elution. cDNA was synthesized from 1 µg total RNA using the iScript Reverse Transcriptase kit (Biorad). qPCR reactions were carried out with 2x IQ SYBR green (Biorad) on a CFX384 Touch Real-Time PCR detection system (Bio-Rad). Data analysis was performed as described by Taylor et. al.[17]. Housekeeping genes *MpEF1a* and *MpSAND* were used for transcript level normalization.

Inducible ARF2 overexpression

For inducible ARF2 overexpression, the pEF1::ARF2-GR lines were used[9]. Plants (n=10 per genotype) were treated with either DMSO or 1µM dexamethasone in B5 media and imaged after 3 days to look for rhizoid formation as an indicator of gemma germination.

Author contributions

Conceptualization-S.D., S.B., E.F., D.W., J.W.B.; Experiments-S.D., M.R.; Mathematical modeling-S.B., E.F.; Writing and Reviewing-S.D., J.W.B., D.W.

Acknowledgements

We are thankful to Netherlands Organization for Scientific Research (NWO) (ALWOP.402) for funding this project.

Supplementary table

List of primers used in this chapter

Primer name	Sequence
SJD154-MpEF1a promoter.FOR	gtagcgattaattaagctcaaatgagtcacacacattgttgagagaca
SJD155-MpEF1a promoter.REV	GCTGCCGCCGCCaagGACCTTTCTCTTCTTCTTTGGAGCC ATcaacctttctgcaggcac
SJD185 EF1promoter.SEQ.FOR	ttggttccgtgcttctatgg
SJD186-ARF1.qFOR	CCATCTGAGTTCGTAATCCC
SJD187-ARF1.qREV	CATGTATCTTCGCACACCT
SJD188-ARF2.qFOR	CTACACGAAGATTCACAAGC
SJD189-ARF2.qREV	ACTTCTTGTCGAACAGCTC
SJD198-mNG internal.REV	CAAAGATGTGTAACTCATGTGTCG
SJD249 ARF2CDS_TOPO.FOR	**CACC**ATGTCAGAAGCATCTTCCATCAC
SJD251 ARF2_FL_CDS.REV	CATGTCGTCGCCGCGCG

References

1. Dharmasiri, N., Dharmasiri, S. & Estelle, M. The F-box protein TIR1 is an auxin receptor. *Nature* **435**, 441–445 (2005).
2. Kepinski, S. & Leyser, O. The Arabidopsis F-box protein TIR1 is an auxin receptor. *Nature* **435**, 446–451 (2005).
3. Gray, W. M., Kepinski, S., Rouse, D., Leyser, O. & Estelle, M. Auxin regulates SCFTIR1-dependent degradation of AUX/IAA proteins. *Nature* **414**, 271–276 (2001).
4. Ulmasov, T., Hagen, G. & Guilfoyle, T. J. ARF1, a transcription factor that binds to auxin response elements. *Science (1979)* **276**, 1865–1868 (1997).
5. Ulmasov, T., Hagen, G. & Guilfoyle, T. J. Dimerization and DNA binding of auxin response factors. *Plant Journal* **19**, (1999).
6. Prigge, M. J., Lavy, M., Ashton, N. W. & Estelle, M. Physcomitrella patens auxin-resistant mutants affect conserved elements of an auxin-signaling pathway. *Current Biology* **20**, (2010).
7. Bowman, J. L. *et al.* Insights into Land Plant Evolution Garnered from the Marchantia polymorpha Genome. *Cell* **171**, (2017).
8. Flores-Sandoval, E., Eklund, D. M. & Bowman, J. L. A Simple Auxin Transcriptional Response System Regulates Multiple Morphogenetic Processes in the Liverwort Marchantia polymorpha. *PLoS Genet* **11**, 1–26 (2015).
9. Kato, H. *et al.* Design principles of a minimal auxin response system. *Nat Plants* **6**, (2020).
10. Lavy, M. *et al.* Constitutive auxin response in Physcomitrella reveals complex interactions between Aux/IAA and ARF proteins. *Elife* **5**, (2016).
11. Das, S., Weijers, D. & Borst, J. W. Auxin Response by the Numbers. *Trends in Plant Science* vol. 26 Preprint at https://doi.org/10.1016/j.tplants.2020.12.017 (2021).
12. Salmon, J., Ramos, J. & Callis, J. Degradation of the auxin response factor ARF1. *Plant Journal* **54**, 118–128 (2008).
13. Farcot, E., Lavedrine, C. & Vernoux, T. A modular analysis of the auxin signalling network. *PLoS One* **10**, 1–26 (2015).
14. Rosado, A., Li, R., van de Ven, W., Hsu, E. & Raikhel, N. v. Arabidopsis ribosomal proteins control developmental programs through translational regulation of auxin response factors. *Proc Natl Acad Sci U S A* **109**, (2012).
15. Yu, J. *et al.* Molecular Evolution of Auxin-Mediated Root Initiation in Plants. *Mol Biol Evol* **37**, (2020).
16. Mutte, S. K. *et al.* Origin and evolution of the nuclear auxin response system. *Elife* **7**, 1–25 (2018).
17. Taylor, S. C. *et al.* The Ultimate qPCR Experiment: Producing Publication Quality, Reproducible Data the First Time. *Trends in Biotechnology* vol. 37 Preprint at https://doi.org/10.1016/j.tibtech.2018.12.002 (2019).

Chapter 5

Selective degradation of ARF2 monomers controls auxin response in Marchantia

Shubhajit Das, Martijn de Roij, Dolf Weijers, Jan Willem Borst
Laboratory of Biochemistry, Wageningen University, the Netherlands

Part of this chapter has been published as:

Das S., Roij M., Bellows S., Kohlen W., Farcot E., Weijers D. and Borst JW (2022) Selective degradation of ARF monomers controls auxin response in Marchantia. bioRxiv.
DOI:10.1101/2022.11.04.515187

Abstract
Selective protein degradation is a common regulatory mechanism in many eukaryotic signaling pathways. In plants, auxin signaling is highly regulated by ubiquitin-dependent targeted proteolysis. Auxin binding to TIR1/AFB F-box receptors enhance their interaction with Aux/IAA repressors that leads to Aux/IAA degradation, permitting auxin response by ARF transcription factors. Previous studies in Arabidopsis and our data on Marchantia ARFs showed that the expression levels of ARFs are also under the control of proteasomal pathway. However, neither the ARF degradation mechanism nor its biological function has yet been identified. Here we dissected the *Marchantia polymorpha* ARF2 protein domains and identified a degron in MpARF2-DBD. Mapping the degron in the MpARF2-DBD dimer structure revealed that the degron is positioned at the interface of the dimerization domain 2 (DD2) of ARF2-DBD. Thus, dimerization would make the degron inaccessible to the degradation system and stabilize MpARF2. Exposing the degron by disrupting ARF2 DBD dimerization leads to accelerated protein degradation, suggesting ARF2-DBD dimerization and degradation are indeed mutually exclusive events. Combined mutations of the ARF2 degron motif and DBD dimerization led to strongly retarded plant growth, suggesting that active removal of monomers is required for normal plant development.

Introduction

Selective degradation of proteins is an important regulatory mechanism in eukaryotic development[1]. Majority of selective protein degradation occurs via the ubiquitin-dependent proteasomal pathway which functions as three-step enzymatic reaction to dispatch a target protein into the 26S proteasomal complex[2]. Selectivity of protein degradation in this system is generated by interactions of ubiquitin ligase enzymes with short sequence motifs in their substrates[3]. These motifs are called "degrons" and are usually sufficient for degradation. Degrons are generally unique, short stretches of hydrophobic amino acids that either remain buried inside the protein structure or shielded by interacting protein partners[4]. Exposure of a degron due to misfolding or loss of interaction, induces degron recognition and protein degradation[5].

Ubiquitin-dependent active protein degradation regulates multiple hormone signaling pathways in plants[1]. A very well characterized example is the auxin dependent proteasomal degradation of Aux/IAA (AUXIN/INDOLE-3-ACETIC ACID) repressors in nuclear auxin signaling pathway (NAP)[6]. Perception of auxin by TIR1/AFB (TRANSPORT INHIBITOR RESPONSE/AUXIN SIGNALING F-BOX) receptors and formation of TIR1/AFB-auxin-Aux/IAA complex triggers this proteolysis[7]. Aux/IAA degradation allows ARFs (AUXIN RESPONSE FACTORS)[6,8] to bind specific DNA motifs and regulate expression of auxin responsive genes[9]. However, regulatory protein degradation in NAP is not limited to only Aux/IAAs. Besides Aux/IAA, the TIR1 auxin receptor which itself is the F-box member of the SCF (SKP1-CULLIN-F-box) proteasomal complex, also undergoes autocatalytic proteolysis in the absence of Aux/IAA substrates[10,11]. Decoupling TIR1 from the SCF complex prevents its auto-degradation, causing growth defects and auxin resistance[11]. Furthermore, ARF transcription factors have also been reported to undergo proteolysis in Arabidopsis (AtARF1, 6, 7, 17, and 19)[12–14]. However, unlike Aux/IAA and TIR1, the underlying mechanisms and biological importance of ARF degradation has remained unexplored.

Based on transactivation assays in Arabidopsis protoplast[15] and phylogenetic analysis[16], ARFs have been divided as class A (transcription activators), B and C (transcription repressors). DNA binding assays and DNA-ARF co-crystal structures suggested that A- and B-class ARFs can bind the same TGTC(TC/GG) auxin response element (AuxRE) and are therefore proposed to engage in a competition for binding sites at near-stoichiometric concentrations[17,18]. Given their competitive interaction and reports of both class A activator (At-

ARF 6, 7, 19)[13,14] and class B repressor (AtARF1) degradation[12], a plausible outcome of ARF degradation is a change in the relative ARF-A/B stoichiometry that defines auxin response. Despite the potential importance, the reported examples of ARF degradation could not be associated with any biological process, delaying investigation of the ARF degradation mechanism. In chapter 4, we found that *Marchantia polymorpha* ARF1 (Class A) and ARF2 (Class B) are proteasomally degraded, leading to a shift in ARF1/2 stoichiometry that favours MpARF1. We found a clear association of MpARF degradation with gemma germination and auxin sensitivity. Therefore, ARF degradation in germinating gemmae provides a great starting point to investigate the degradation mechanism and its biological importance.

In this chapter, we aimed to identify the degron responsible for MpARF2 degradation. Canonical ARFs have three conserved domains: an N-terminal DNA binding domain (DBD), C-terminal Phox and Bem1 (PB1) domain and an intrinsically disordered middle region (MR). To understand which of the three domains is required for ARF2 degradation, we performed domain deletion experiments and identified a short degron motif in DBD. The degron sits at the interface of dimerization domain 2 (DD2) in MpARF2-DBD dimer structure, which possibly makes dimerization and degradation mutually exclusive. We confirm this hypothesis by mutational analysis and show that monomeric MpARF2 are prone to degradation and stabilization of MpARF2 monomers are detrimental to plant growth.

Results

Identification of a degron driving MpARF2 degradation

In chapter 4, we found that MpARF1 and MpARF2 are proteasomally degraded upon gemma germination. As an initial step in dissecting the mechanisms underlying regulated ARF degradation, we focused on identifying requirements for MpARF2 degradation. To identify the ARF2 domain that mediates degradation, we first expressed each of the three conserved MpARF2 domains (DBD, MR and PB1) and the full-length (FL) as mNeonGreen protein fusion, driven by a 2kb MpARF2 promoter fragment, and explored accumulation before and after germination. A nuclear localization signal (SV40 NLS) was added in-frame to ensure nuclear entry of the fused ARF domains. We performed time-lapse confocal imaging on dormant (0 hour) and germinated gemmae (8 hours) to check for stability of the fused proteins. Full-length MpARF2-mNeonGreen was expressed at dormant stage but degraded after germination (Figure 1.A), as observed before for the ARF2 knock-in lines

(Chapter 3). Both the MR and PB1-mNeonGreen fusion proteins strongly accumulated at 0 hours and 8 hours after germination, suggesting that these domains do not carry the degradation signal. In contrast, the DBD-mNeonGreen fusion protein showed hardly any expression, neither at dormant stage nor after 8 hours (Figure 1.A). However, treatment with the proteasomal inhibitor MG132 caused hyper-accumulation of both DBD-mNeonGreen and FL-mNeonGreen (Figure 1.B), confirming that the DBD carries the signal that is sufficient for MpARF2 degradation. Interestingly, the DBD alone was much less stable at dormant stage than full-length protein (Figure 1.A), suggesting that a structural feature within full-length MpARF2 might be protecting it from degradation at dormant stage.

To identify a minimal degron motif within MpARF2-DBD, we tiled the DBD into 8 short fragments of 75 amino acids, with each carrying 25 overlapping residues with neighbouring fragments (Figure 1.C). Each fragment was expressed as mNeonGreen fusion in Marchantia, as we did before for the three MpARF2 domains. All DBD fragments, except fragments 5, 6 and 7 showed strong and stable nuclear accumulation (Figure 1.C) in both dormant and germinated gemmae. Fragments 5, 6 and 7 did not show expression, but treatment with MG132 caused protein accumulation (Figure 1.D). This identifies the region encompassed by these three fragments as a degron sufficient for MpARF2 degradation.

These experiments demonstrate sufficiency of these regions for degradation, but do not tell if the degron is required in the context of the larger domain. We therefore divided the 25 amino acid overlapping region between fragment 6 and 7 into 3 smaller overlapping motifs of 12 amino acids each and swapped each motif with the equivalent sequences from the non-degradable MpARF3 protein in the context of full-length MpARF2-DBD-mNeonGreen. Among these, only the first motif swap led to stable accumulation of ARF2-DBD, while the other two were degraded (Figure 1.E-F). Thus, this delineation identifies a minimal 12 amino acid region in the MpARF2 DBD that is both necessary and sufficient for regulated degradation.

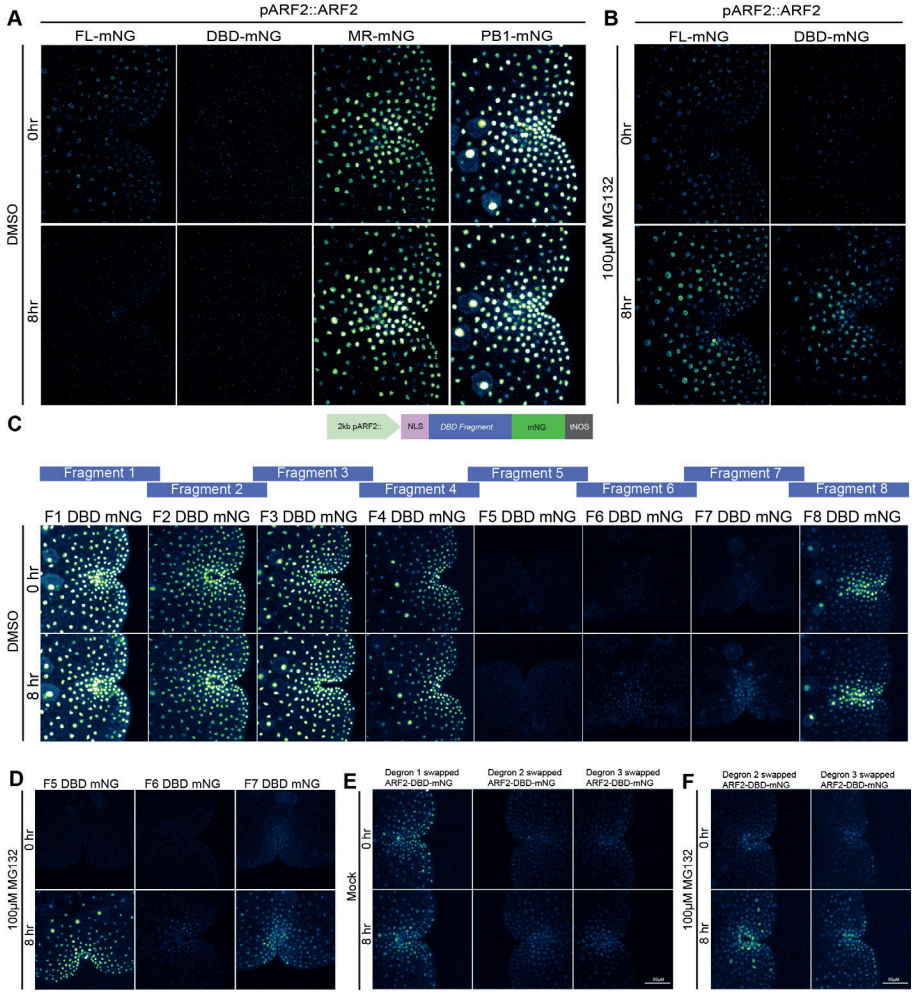

Figure 1: (A) ARF2 domain split analysis. Each domain of ARF2 fused to mNeonGreen (mNG) was expressed separately to determine the location of the degradation signal in the protein. Both the MR and the PB1 domain show high stability at 0 and 8 hours. The full-length ARF2 is stable at dormant stage, but it is degraded after germination. The DBD is degraded already at dormant stage. (B) 100μM MG132 treatment can inhibit degradation of both full-length and ARF2-DBD. (C) ARF2-DBD fragment analysis to narrow down the location of the degron. ARF2-DBD was divided into 8 overlapping fragments and fused to mNG. Expression of each fragment in plants shows that fragments 5,6 and 7 are instable in dormant stage, whereas all other fragments are stable after 8 hours. (D) 8 hours of 100μM MG132 treatment on fragments 5,6 and 7 is sufficient to block degradation of these fragments. (E) ARF2 DBD degron swap experiment. The 25 amino acid overlapping region between ARF2-DBD fragment 6 and 7 were divided into three small motifs. Each small motif was named as degron 1, 2 and 3. We swapped these small motifs in ARF2-DBD with homologous sequences from ARF3-DBD, which lacks proteasomal regulation. Swapping degron 2 and degron 3 with ARF3 sequence is not sufficient to stop ARF2-DBD degradation. Only when the degron 1 (the first 12 amino acids in the overlap between fragment 6 and 7) is replaced, ARF2-DBD becomes stable both at dormant stage and after 8 hours of growth. (F) MG132 treatment blocks the degradation of degron 2 and degron 3 swapped ARF2-DBD, confirming their proteasomal degradation.

Mutations in conserved degron of class B ARFs leads to auxin insensitivity

Besides our systematic search for the ARF2 degron in Marchantia, a simultaneous but independent forward genetic screen was conducted in Prof. Mark Estelle's laboratory to identify auxin-resistant mutants of the moss *Physcomitrium patens*. Through personal communications we learned that using UV mutagenesis, two auxin-resistant mutants were identified, both of which contained point mutations in the ARFb2-DBD of Physcomitrium (PpARFb2^{E266K} and PpARFb2^{R269Q}). Importantly, both mutations caused increased PpARF2 stability. Due to the high similarity in the regulation of class B ARF stability in two bryophyte species Physcomitrium and Marchantia, we wondered whether this is a conserved degradation mechanism. Therefore, we aligned the PpARFb2 and MpARF2 protein sequences and identified the homologous amino acids (E297 and R300) in MpARF2. Coincidentally, these residues were located at the C-terminal end of ARF2-DBD fragment 5, immediately adjacent to the overlapping region between fragment 5 and 6, suggesting parallels between MpARF2 and PpARFb2 degradation. Using site directed mutagenesis, we generated a pARF2::MpARF2^{E297K}-mNG line to test MpARF2 stability. A first striking feature observed in pARF2:: MpARF2^{E297K}-mNG gemmae was the presence of multiple apical notches, unlike the usual two oppositely positioned notches in wild-type gemmae (Figure 2.A). Upon checking for protein stability using confocal imaging, we indeed found the ARF2^{E297K} mutation to render higher stability of the protein in dormant gemmae (Figure 2.B). To our surprise, there was still considerable degradation of MpARF2^{E297K} after gemma germination and a lower (relative to its expression at dormant stage) level of mutant ARF2 accumulation was sustained. Nevertheless, the low yet detectable levels of ARF2^{E297K} in germinated gemmae, was sufficient to cause gemma germination inside gemma cup and insensitivity to externally applied auxin (Figure 2.D-E). These results confirm that the identified degron represents a conserved signal for class B ARF degradation in bryophytes. However, this analysis also shows that there are multiple mechanisms that control MpARF2 stability in dormant gemmae and following germination.

Figure 2: Multiple sequence alignment showing conservation between *Physcomitrium patens* ARFb2, *Marchantia polymorpha* ARF1 and ARF2. Degron residues identified by mutagenesis in PpARFb2 are indicated by black triangle. MpARF2-DBD fragments 5,6 and 7 identified as responsible for MpARF2 degradation are underlined.

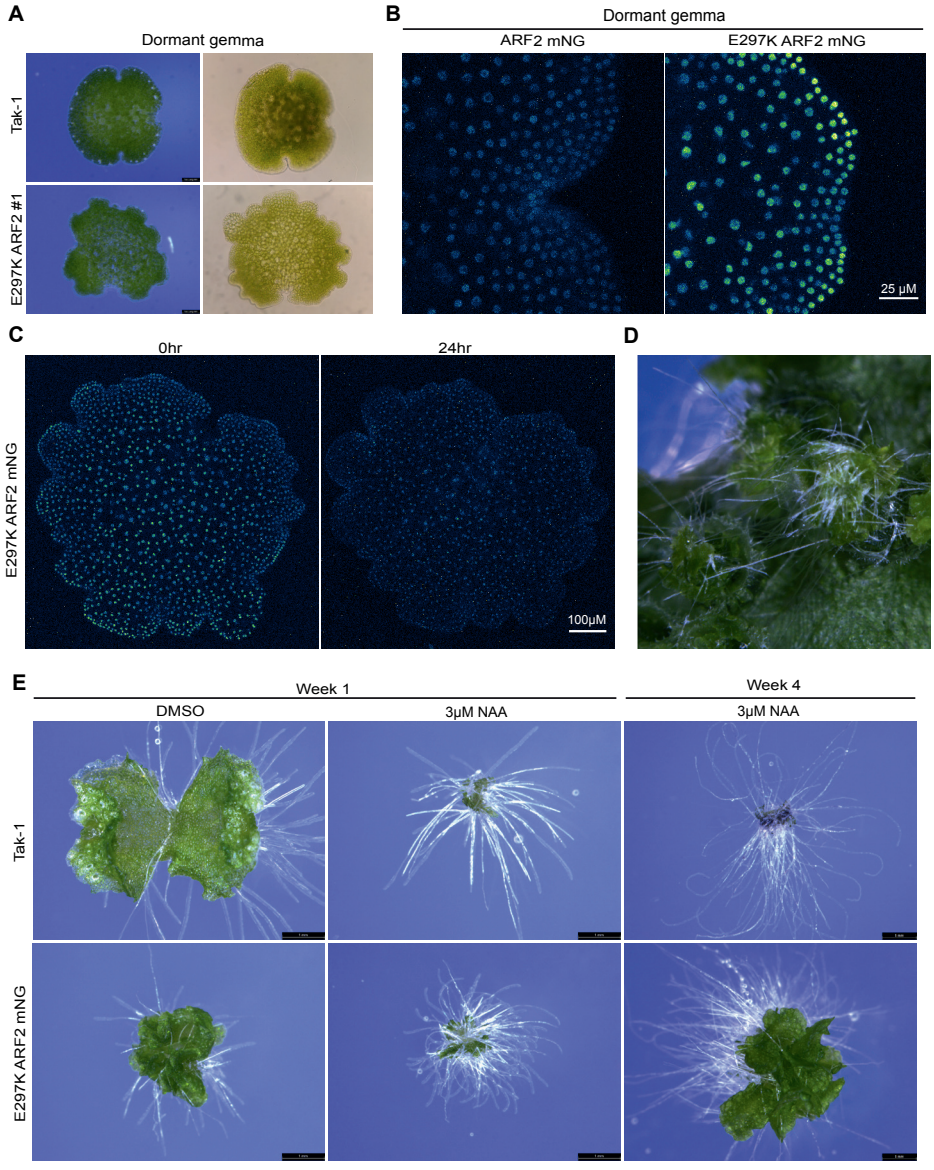

Figure 3: (A) pARF2::MpARF2^{E297K}-mNG gemmae contain multiple apical notches. (B) pARF2::MpARF2^{E297K}-mNG has higher stability compared to wild type ARF2-mNG. (C) Despite higher stability in dormant stage, there is considerable degradation of pARF2::MpARF2^{E297K}-mNG after germination. However, there is still detectable amount of protein left after 24 hours. (D) The pARF2::MpARF2^{E297K}-mNG mutant gemmae start germinating inside the gemma cup and (E) are auxin insensitive.

Selective degradation of ARF2 monomers is required for normal development

Previously, a crystal structure of the MpARF2 DBD bound to a synthetic auxin responsive element (inverted repeat 7) was published[18]. We used this protein structure to map the location of the minimal degron fragments that can drive MpARF2 degradation. All three fragments (5,6 and 7) of MpARF2-DBD could be mapped onto the homodimerization interface (Figure 4.A). ARF-DBD dimerization is required for high-affinity DNA binding in Arabidopsis[17,19]. Arabidopsis ARF5/MP protein that cannot dimerize through their DBD fail to complement the *arf5/mp* mutant[17]. The location of the degron at this interface prompts the hypothesis that MpARF2 degradation selectively targets monomers, since the degron would be occluded in the dimer. To test this hypothesis, we engineered a dimerization mutation into the MpARF2-DBD ($ARF2^{G286I}$) and assessed its stability. As predicted, this mutant is highly unstable, and causes loss of protein accumulation even in dormant gemmae (Figure 4.B).

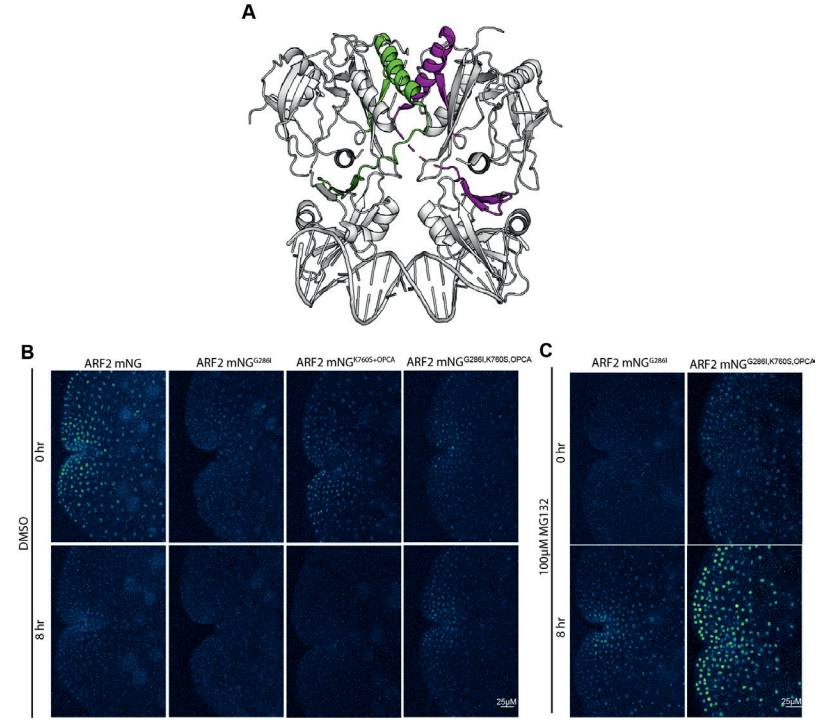

Figure 4: (A) Mapping fragments 5,6 and 7 on the crystal structure of ARF2-DBD shows that the degron is located at the DBD dimer interface. (B) Time-lapse imaging of ARF2 dimerization mutants. Disruption of DBD dimerization ($ARF2^{G286I}$), PB1 dimerization ($ARF2^{K760S+OPCA}$) and double dimerization ($ARF2^{G286I+K760S+OPCA}$) in ARF2 causes degradation of the full-length proteins in dormant stage. (C) Treatment with proteasomal degradation inhibitor results in accumulation of both the DBD dimerization mutant and the DBD PB1 double dimerization mutant.

In addition to the DBD, most ARFs have a C-terminal PB1 domain that can also serve as homotypic dimerization domain[20,21]. These two dimerization domains likely act cooperatively, with each favouring dimerization at the other domain[17,22]. Given that the DBD alone is less stable than the full-length MpARF2, we explored if dimerization through the PB1 domain indirectly stabilizes MpARF2. We therefore engineered a PB1 dimerization mutant ($ARF2^{K760S,\ OPCA}$), and found this to render MpARF2 highly unstable (Figure 4.B)[21]. Likewise, combining the $ARF2^{G286I}$ and $ARF2^{K760S,\ OPCA}$ mutations led to similar instability compared to each single mutant (Figure 4.B). MG132 treatment allowed mutant proteins to accumulate, confirming their degradation due to mutations (Figure 4.C). These results are consistent with the idea of cooperative dimerization preventing degradation of MpARF2.

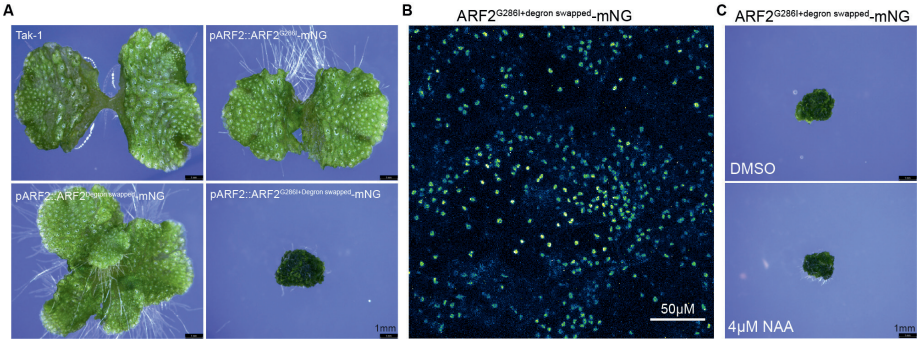

Figure 5: (A) Severe growth defects in Marchantia expressing ARF2 with the DBD dimer mutation and degron mutation ($ARF2^{G286I+F6F7\ swapped}$) compared to plants expressing ARF2 mutated in either the DBD dimerization or degron swapped. The double mutant does not have any differentiation of tissue and grows as a mass of undifferentiated callus. This shows the negative effect of a stable ARF2 monomer in plants and highlights the importance of ARF2 degradation by proteasome. (B) Stable expression of pARF2::$ARF2^{G286I+Degron\ swapped}$-mNG in the undifferentiated tissue, confirming stability of the monomeric protein due to degron swap with ARF3 sequence. (C) The double mutant $ARF2^{G286I+Degron\ swapped}$-mNG line shows reduced sensitivity to auxin. Growth of green tissue is not inhibited, although there is slight increase in rhizoid formation.

If the MpARF2 dimerization interface occludes the degron, and allows for selective degradation of monomeric MpARF2, a key question is what function this serves. We therefore engineered a version of MpARF2 in which both DBD dimerization and degradation are prevented without affecting any other property of the protein and expressed it from an ARF2 promoter fragment. To prevent DBD dimerization, we used the G286I mutation, and the swap of sub-degron motif 1 (region shared between DBD fragment 6 and 7 in Figure1.C) from MpARF3 was used to prevent degradation. This should lead to the stable accumulation of monomeric MpARF2 that cannot dimerize via DBD. This MpARF2 double mutant showed a striking phenotype, lacking a flat thallus, rhizoids, gemmae or gemma cups, whereas the individual DBD

dimerization mutant or degron motif 1 swap alone showed mild effects on growth (Figure 5.A). The double mutant grew as a mass of undifferentiated cells and this strong phenotype was observed in all (n=10) independent transformants, suggesting accumulation of monomeric MpARF2 strongly interferes with normal development. Accumulation of nondegradable ARF2 in the callus-like tissue of the double mutant was confirmed by detection of fluorescence signal (Figure 5.B). On treatment with exogeneous auxin, the double mutant growth was unaffected, showing that auxin-induced thallus growth inhibition can be antagonized by higher MpARF2 stability (Figure 5.C). Together, these findings suggest that biological functions of MpARF2 degradation are twofold; (1) it changes MpARF1:MpARF2 stoichiometry to favour ARF1-mediated transcriptional activation (see Chapter 4) and (2) selective degradation prevents the accumulation of MpARF2 monomers that negatively affects tissue differentiation and plant growth.

Discussion

In this chapter, our goal was to identify the degradation signal in MpARF2 protein structure and to uncover the biological role of ARF2 degradation. By mapping the degron motif in MpARF2, we made a surprising discovery: the region both necessary and sufficient for degradation is located at the interface between both DBD monomers in the protein dimer. While the possibility of degron occlusion is based on our observation in the protein dimer structure, we cannot be certain that dimerization blocks the degron. However, it is extremely unlikely that in the full-length protein dimer, this DBD interface will be accessible for interaction with the proteolysis adaptor protein. Thus, our finding suggests a regulatory mechanism where degradation selectively targets MpARF2 monomers. We observed that mutations that interfere with dimerization render proteins unstable, and this includes mutations in the N-terminal DBD and C-terminal PB1 domain of MpARF2. This suggests that cooperative dimerization protects the protein from degradation and, also helps to rationalise the earlier findings that the MpARF1 PB1 domain is essential for *in vivo* function, yet can be replaced by an entirely unrelated dimerization domain[18]. This also aligns with the recent smFRET (single-molecule Förster resonance energy transfer) data showing that PB1 domain is required for stronger dimerization and DNA binding of ARFs[22]. A mutant version of MpARF2 that can neither dimerize nor be degraded leads to extremely strong growth and developmental phenotypes, suggesting that indeed, monomers are detrimental to normal development. A key question is why this is the case. A plausible explanation is that the limited specificity

of an ARF monomer for 4 conserved nucleotides (TGTC) allows binding of monomers across the genome (one in every 256 bases), while an inverted repeat of the same element would lead to a specificity that is orders of magnitude higher (one in every 65,536 bases). As such, a monomer could be a loose cannon in auxin-dependent gene regulation (Figure 7). While this interpretation is plausible, and to some degree testable, it is a mystery why this problem was not solved by evolving higher homotypic ARF dimerization affinity. Is the dynamic regulation of the monomer-dimer equilibrium important for auxin response, perhaps under environmental influences, or are there structural and functional constraints that we are yet to identify?

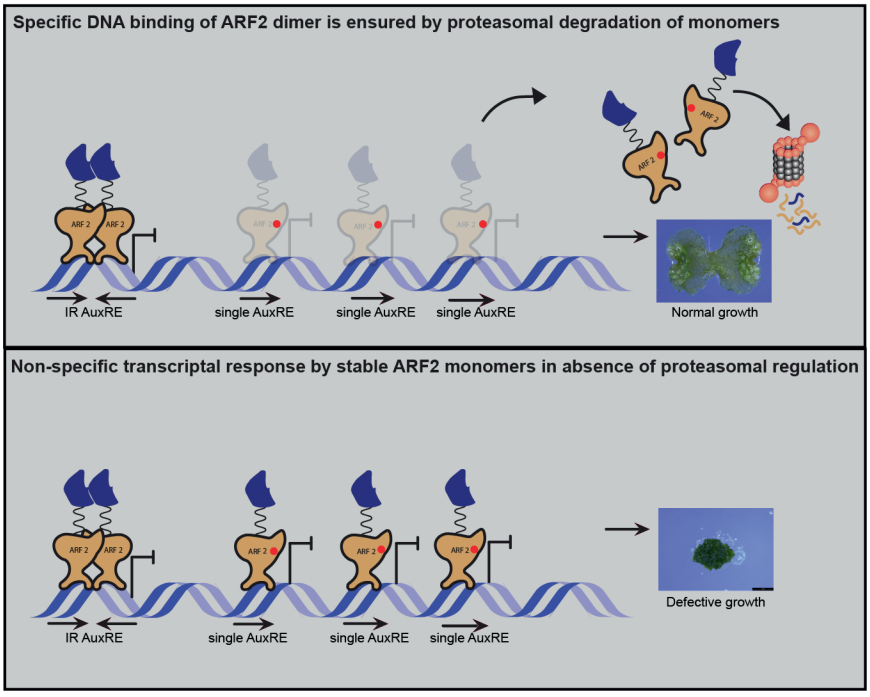

Figure 7: Proposed model showing the necessity of a monomer specific degradation mechanism for specific auxin response. In presence of proteasomal regulation, ARF2 monomers are selectively removed (upper panel), allowing only ARF2 dimers to bind DNA with specificity. In absence of this regulation (lower panel), monomers repress genes by non-specific DNA interaction and cause growth defects.

ARFs can bind to inverted (IR), everted (ER) and direct (DR) repeats of their binding site, with defined spacing[17,19,23,24]. The MpARF2 degron maps to the dimerization interface that is generated in unbound, or IR motif bound ARF's. This conformation creates an ARF dimer where each monomer is a mirror image of the other. However, cooperative binding to DR or ER elements would likely require a different conformation, in which the degron is exposed. Therefore, selective MpARF2 monomer degradation may additionally act as

a mechanism to favour class B ARF binding to IR motifs only, whereas binding to DR or ER elements would be prevented by proteasomal degradation. This offers a testable hypothesis that a competitive ARF DNA binding model could be valid only for IR-type auxin responsive elements (AuxRE), and DR or ER-type AuxREs containing genes could be exclusively regulated by class A MpARF1.

Now that we have identified the degron motif for MpARF2, it will be interesting to see if the mechanisms underlying MpARF1 degradation work similarly. The region spanning the degron is highly conserved between MpARF1 and MpARF2, which makes it likely that the same binding partner mediates degradation of both proteins. If so, this would directly mean that the control of A/B ARF stoichiometry and monomer/dimer equilibrium are mechanistically connected. However, an alternate hypothesis is that distinct proteasomal adapters exist for class A and B ARFs, leaving scope for diversification in their regulation and function. A similar degradation mechanism would limit any possibility of exclusive stability/accumulation of a class of ARF in a specific tissue in a specific time. Therefore, identification of ARF binding partners, such as E3 ubiquitin ligase subunits may help to address this question.

MpARF1 and MpARF2 are the sole representatives of the A-class and B-class ARFs in Marchantia, and both share ancestry with proto-A/B-ARFs in algal ancestors[25]. It is thus plausible that DBD-mediated degradation is a property inherited from the algal ancestor. This urges the question of how widespread this type of regulation is. Several of the 23 Arabidopsis ARFs (AtARF1, AtARF6, AtARF7, AtARF17 and AtARF19) have been reported to be proteasomally degraded[12,14,26]. Neither the degron nor the biological relevance of these degradation is known, but there is clearly a potential for this degradation mechanism to be intimately connected to auxin response. Therefore, it would be important to find conservation of degron and E3 ligases for ARF degradation beyond bryophytes.

Finally, with identifying ARF proteolysis, it now seems that all components in the NAP are subject to selective degradation. Aux/IAAs are degraded in an auxin-dependent manner[6]. Intriguingly, when not engaged in binding Aux/IAA proteins, Arabidopsis TIR1 protein is targeted from degradation[27]. Thus, auxin response is marked by profound proteasomal degradation, which may be a requirement for the system to rapidly adapt to changing internal and external conditions.

Materials and method

Plant growth conditions

Marchantia polymorpha male Takaragaike-1 (Tak-1) and female Takaragaike-2 (Tak-2) plants were used as the wild-type variety. For vegetative propagation, plants were grown on ½ Gamborg B5 media plates in growth chambers with 40 µmol photons m^{-2} s^{-1} continuous white light at 22 °C. For sexual reproduction, plants were grown on 1% sucrose supplemented ½ Gamborg B5 media within boxes exposed to 40µmol photons m^{-2} s^{-1} continuous white fluorescent light for 1 month. Plants were then moved into 40 µmol photons m^{-2} s^{-1} continuous white light supplemented with 15µmol photons m^{-2} s^{-1} far-red light to induce antheridiophore and archegoniophore development. Plants were repeatedly crossed manually to ensure fertilization. Sporangia with mature spores were collected aseptically and used in spore transformation.

Confocal live cell imaging

All live cell imaging was done on a Leica SP8X-SMD confocal microscope equipped with hybrid detectors and a pulsed (40MHz) white-light laser (WLL). mNeonGeen and mScarlet-I were excited with the 506 nm and 561 nm laser lines, respectively. The laser powers were set at 4% output to avoid bleaching of the fluorophores. Fluorescence was detected between 512-560nm (mNeonGreen) and 570 to 620nm (mScarlet-I) using hybrid detectors in photon counting mode. Z-stack images of 1.5µm were acquired using a 20X water immersion objective lens and time-gated detection to suppress autofluorescence. Images were processed using ImageJ software. Maximum-intensity projections of z-stack images were used to quantify total cellular fluorescence in each nucleus analysed, corrected for background fluorescence.

ARF2 domain split analysis

To locate the degron within ARF2 protein structure, each domain of ARF2 was expressed separately in plants. In pJHY-TMp1 vector backbone, a ~1.1kb promoter of ARF2 was cloned with respective DBD or MR or PB1 domains or full length ARF CDS fused to an mNeonGreen fluorescent marker. Each CDS was fused to an N-terminal SV40 NLS sequence to ensure nuclear localization of the protein. All primers were designed with appropriate overlapping overhangs and HiFi DNA assembly master mix (NEB) was used for cloning. Constructs were transformed in wild-type spores and transformants were selected on hygromycin selection plates.

ARF2 DBD fragment analysis
To narrow down the core degron region within ARF2 DBD, the DBD was divided into 8 fragments of 75aa each. Each fragment had a 25aa overlap with its preceding and succeeding fragments. All 8 fragments, fused to an N-terminal SV40NLS sequence, were cloned at the HindIII site of pJHY-mNeonGreen plasmid. A ~2kb ARF2 promoter was cloned upstream of each fragment. These constructs were used to generate 8 transgenic lines expressing different parts of the ARF2 protein fused with mNeonGreen marker.

ARF2 dimerization mutant analysis
ARF2 dimerization mutant lines were created to test the stability of monomeric ARF2. Overlapping primers with mutated nucleotides were used to amplify ARF2 CDS and cloned at HindIII site of pJHY- mNeonGreen plasmid, using NEB HiFi cloning master mix. G286I (DBD dimerization mutation), K760S+OPCA (PB1 dimerization mutation), and G286I+K760S+OPCA double dimerization mutant ARF2 CDS were cloned in frame with mNeonGreen tag and under the pARF2 promoter. Each construct was transformed in WT spores to generate 3 different dimerization mutant variants. Gemmae of these plants were used to visualize mutant ARF2 expression and stability during dormancy and growth.

ARF2 DBD degron swap with ARF3 DBD sequence
The 25aa overlapping region between fragment 6 and fragment 7 of ARF2 DBD were divided into 3 fragments of 12aa each. These 12aa fragments from ARF2 DBD were swapped with the aligned sequences from ARF3 DBD. Overlapping primers with ARF3 sequence at 5' end, were used to amplify the ARF2 CDS and fragments were cloned into pJHY- mNeonGreen using NEB HiFi cloning master mix.

Author contributions
Conceptualization-S.D., D.W., J.W.B.; Experiments-S.D., M.R.; Writing and Reviewing-S.D., J.W.B., D.W.

Acknowledgements
We thank Prof. Mark Estelle and Dr. Michael Prigge for providing us the details of PpARFb2 mutants, Juriaan Rienstra for his help with mapping the degron regions in MpARF2 structure using PyMol software. S.D. is supported by The Netherlands Organization for Scientific Research (NWO) (ALWOP.402).

Supplementary Table 1
List of primers used in this chapter

Pimer name	sequence
SJD205-pARF2.FOR	tagcgattaattaagctGCATTCTCGCTCACCTGCCTGA
SJD206-pARF2.REV	ATGCTGCCGCCGCCaagcttGGTCGGAACTTCTGTCTAAAATGC
SJD207-NLS-ARF2DBD.FOR	GTTCCGACCaagctTATGGCTCCAAAGAAGAAGAGAAAGGTCATGTCAGAAGCATCTTCC
SJD208-NLS-ARF2DBD.REV	TGCCGCCGCCaagctGGAAGGGCTCCACTTCCCAT
SJD209-NLS-ARF2MR.FOR	GTTCCGACCaagctTATGGCTCCAAAGAAGAAGAGAAAGGTCTCTCCCTCCACGACCATC
SJD210-NLS-ARF2MR.REV	TGCCGCCGCCaagctGATTGGATCTCTGGGGACCCTTATCCT
SJD211-NLS-ARF2PB1.FOR	GTTCCGACCaagctTATGGCTCCAAAGAAGAAGAGAAAGGTCAAGACGTCGCAAAATTTC
SJD212-NLS-ARF2PB1.REV	TGCCGCCGCCaagctGCATGTCGTCGCCGCGCG
SJD213	tagcgattaattaagctAAAAGCCTGTAATCACACGACG
SJD214	tagcgattaattaagctAAGGCAGCCAAAATACAGCCTCCTAATA
SJD215	tagcgattaattaagctCACCAGCCCCTCCCTCTGTA
SJD216	AATACTAGACGCGCTCCACT
SJD217	AAATGCTAGACTACGCAGCT
MdR1	AGTCTAGCATTTTAGACAGAAGTT
MdR2	TCTCAGGGGTGAGAATGGCCA
MdR3	gtagcgattaattaagctACTCTCTGATGTTGTGAAGGACG
MdR4	gaaattcgagctcaagcttGGTCGGAACTTCTGTCTAAAATGCTAGAC
MdR5	AGAAGTTCCGACCAAGCTTATGGCTCCAAAGAAGAAGAGAAAGGTCATGGTGAGCA
MdR6	GAAATTCGAGCTCAAGCTTTACTTGTACAGCTCGTCC
MdR7	CACATTCTGAGTCAGTGAACAGG
SJD219.pARF2.PacI.FOR	GATTAATTAAAAAAGCCTGTAATCACACGACG
SJD220.pARF2.PacI.REV	tcttaattaaGGTCGGAACTTCTGTCTAAAATGC
SJD221.NLSARF2DBD.FOR	GACCTTAATtaagctATGGCTCCAAAGAAGAAGAGAAAGGTCATGTCAGAAGCATCTTCC
SJD222.NLSARF2MR.FOR	GACCTTAATtaagctATGGCTCCAAAGAAGAAGAGAAAGGTCTCTCCCTCCACGACCATC

SJD223.NLSARF2PB1.FOR	GACCTTAATtaagctATGGCTCCAAAGAAGAAGAGAAAGGTCAAGACGTCGCAAAATTTC
SJD235 F1-ARF2DBD.REV	TGCCGCCGCCaagctG**TGCCTTCTGAGGACCAG**
SJD236 F2-ARF2DBD.FOR	GTTCCGACCaagctTATGGCTCCAAAGAAGAAGAGAAAGGTC**TCCAACGTCTCCGTAGCA**
SJD237 F2-ARF2DBD.REV	TGCCGCCGCCaagctG**GCTGAGTTGTATGTCGTTG**
SJD238 F3-ARF2DBD.FOR	GTTCCGACCaagctTATGGCTCCAAAGAAGAAGAGAAAGGTC**GAACTCGACGCCCAAATT**
SJD239 F3-ARF2DBD.REV	TGCCGCCGCCaagctG**GGTATCAGAGACAGTGAG**
SJD240 F4-ARF2DBD.FOR	GTTCCGACCaagctTATGGCTCCAAAGAAGAAGAGAAAGGTC**GACTGCGCCGAGCCCCCG**
SJD241 F4-ARF2DBD.REV	TGCCGCCGCCaagctG**TTGACCTCGAAATATGTGAC**
SJD242 F5-ARF2DBD.FOR	GTTCCGACCaagctTATGGCTCCAAAGAAGAAGAGAAAGGTC**CCTCCAAATCAGGAATTA**
SJD243 F5-ARF2DBD.REV	TGCCGCCGCCaagctG**GGGTTGCAGTTGTTGCTGG**
SJD244 F6-ARF2DBD.FOR	GTTCCGACCaagctTATGGCTCCAAAGAAGAAGAGAAAGGTC**CTGTTTCTCAGGGGTGAG**
SJD245 F6-ARF2DBD.REV	TGCCGCCGCCaagctG**CACAGCCTTGAGGTACTTAG**
SJD246 F7-ARF2DBD.FOR	GTTCCGACCaagctTATGGCTCCAAAGAAGAAGAGAAAGGTC**TTCTCTCTAATTTACAAC**
SJD247 F7-ARF2DBD.REV	TGCCGCCGCCaagctG**ATTAACCTGGAGGGATCTC**
SJD248 F8-ARF2DBD.FOR	GTTCCGACCaagctTATGGCTCCAAAGAAGAAGAGAAAGGTC**GGAACTATCACCGGAATT**
SJD254 K760S.mARF2.FOR	gtagctacacgaGCattcacaagcagggatcg
SJD255 K760S.mARF2.REV	cgatccctgcttgtgaatGCtcgtgtagctac
SJD256 OPCA.mARF2.FOR	gtgtacacagCAcacgaagacgCAgtcctcctcgtgg
SJD257 OPCA.mARF2.REV	ccacgaggaggacTGcgtcttcgtgTGctgtgtacac
SJD258 ARF2.SEQ.FOR	agctgattctgaaacgtcaagc
SJD259 ARF2.FLCDS.FOR	CCGACCTTAATtaagctATGTCAGAAGCATCTTCC
SJD260 G286I.mARF2.FOR	ccaacgatgcacatcATCgttctcgcggccgc
SJD261 G286I.mARF2.REV	gcggccgcgagaacGATgatgtgcatcgttgg

SJD280 DEG1.SWAP.FOR	TTCGAGGTCGTCTACTACCCTCGCGCCAGCACGGCC GAGTTCGTTATTCCGTACTCTAAG
SJD281 DEG1.SWAP.REV	GGCCGTGCTGGCGCGAGGGTAGTAGACGACCTCGA ATCGAGATTTCTCCGTTGCCGCATG
SJD282 DEG2.SWAP.FOR	GCGCCAGCACGGCCGAGTTCTGCGTCAAAGCGCAG GCCTACCTCAAGGCTGTGAAAAGCA
SJD283 DEG2.SWAP.REV	GGCCTGCGCTTTGACGCAGAACTCGGCCGTGCTGGC GCGAGGGTTGTAAATTAGAGAGAA
SJD284 DEG3.SWAP.FOR	TTCTGCGTCAAAGCGCAGGCCGTCAAGGCGGCCCTC AAAAGCAACTTCAACGTTGGC
SJD285 DEG3.SWAP.REV	GAGGGCCGCCTTGACGGCCTGCGCTTTGACGCAGAA CTCCGAAGGGCAAGATCGAGG
SJD289 pARF2.SEQ.FOR	TAATCAGCTGCGTAGTCTAGC
SJD292 ARF2DBD.DEGSW AP.HiFi.FOR	TAGCATTTTAGACAGAAGTTCCGACCaagctTATGGCT CC
SJD293 ARF2DBD.DEGSW AP.HiFi.REV	GCTCACCATGCTGCCGCCGCCaagctGG
SJD303 F6F7.FOR	CACCGTGTTGACGTCTCCAACG
SJD304 F6F7.REV	GAAGTTGCTTTTCACAGCCTTG
SJD305 E297K.mARF2.FO R	ccatgcggcaacgAAGaaatctcgattctctctaatttacaacc
SJD306 E297K.mARF2.RE V	atcgagatttCTTcgttgccgcatgggcagc
SJD307 A2DBDF7.NLS.FO R	CAGAAGTTCCGACCaagctTATGTTCTCTCTAATTTACA ACCCTCG
SJD308 A2DBDF7.NLS.RE V	CTGCCGCCGCCaagctGGACCTTTCTCTTCTTCTTTGGA GCATTAACCTGGAGGGATCTC

References

1. Hellmann, H. & Estelle, M. Plant development: Regulation by protein degradation. *Science* vol. 297 Preprint at https://doi.org/10.1126/science.1072831 (2002).
2. Collins, G. A. & Goldberg, A. L. The Logic of the 26S Proteasome. *Cell* vol. 169 Preprint at https://doi.org/10.1016/j.cell.2017.04.023 (2017).
3. Kleiger, G. & Mayor, T. Perilous journey: A tour of the ubiquitin-proteasome system. *Trends in Cell Biology* vol. 24 Preprint at https://doi.org/10.1016/j.tcb.2013.12.003 (2014).
4. Timms, R. T. & Koren, I. Tying up loose ends: The N-degron and C-degron pathways of protein degradation. *Biochemical Society Transactions* vol. 48 Preprint at https://doi.org/10.1042/BST20191094 (2020).
5. Varshavsky, A. N-degron and C-degron pathways of protein degradation. *Proceedings of the National Academy of Sciences of the United States of America* vol. 116 Preprint at https://doi.org/10.1073/pnas.1816596116 (2019).
6. Gray, W. M., Kepinski, S., Rouse, D., Leyser, O. & Estelle, M. Auxin regulates SCFTIR1-dependent degradation of AUX/IAA proteins. *Nature* **414**, 271–276 (2001).
7. Tan, X. *et al.* Mechanism of auxin perception by the TIR1 ubiquitin ligase. *Nature* **446**, 640–645 (2007).
8. Zenser, N., Ellsmore, A., Leasure, C. & Callis, J. Auxin modulates the degradation rate of Aux/IAA proteins. *Proc Natl Acad Sci U S A* **98**, 11795–11800 (2001).
9. Weijers, D. & Wagner, D. Transcriptional Responses to the Auxin Hormone. *Annu Rev Plant Biol* **67**, 539–574 (2016).
10. Stuttmann, J., Parker, J. E. & Noël, L. D. Novel aspects of COP9 signalosome functions revealed through analysis of hypomorphic csn mutants. *Plant Signal Behav* **4**, (2009).
11. Yu, H. *et al.* Untethering the TIR1 auxin receptor from the SCF complex increases its stability and inhibits auxin response. *Nat Plants* **1**, (2015).
12. Salmon, J., Ramos, J. & Callis, J. Degradation of the auxin response factor ARF1. *Plant Journal* **54**, 118–128 (2008).
13. Powers, S. K. *et al.* Nucleo-cytoplasmic Partitioning of ARF Proteins Controls Auxin Responses in Arabidopsis thaliana. *Mol Cell* **76**, 177-190.e5 (2019).
14. Jing, H. *et al.* Regulation of AUXIN RESPONSE FACTOR condensation and nucleo-cytoplasmic partitioning. *Nat Commun* **13**, 4015 (2022).
15. Ulmasov, T., Hagen, G. & Guilfoyle, T. J. Activation and repression of transcription by auxin-response factors. *Proc Natl Acad Sci U S A* **96**, (1999).
16. Finet, C., Berne-Dedieu, A., Scutt, C. P. & Marlétaz, F. Evolution of the ARF gene family in land plants: Old domains, new tricks. *Mol Biol Evol* **30**, (2013).
17. Boer, D. R. *et al.* Structural basis for DNA binding specificity by the auxin-dependent ARF transcription factors. *Cell* **156**, 577–589 (2014).
18. Kato, H. *et al.* Design principles of a minimal auxin response system. *Nat Plants* **6**, (2020).
19. Freire-Rios, A. *et al.* Architecture of DNA elements mediating ARF transcription factor binding and auxin-responsive gene expression in Arabidopsis. *Proc Natl Acad Sci U S A* **117**, (2020).
20. Guilfoyle, T. J. The PB1 domain in auxin response factor and aux/IAA proteins: A versatile protein interaction module in the auxin response. *Plant Cell* **27**, 33–43 (2015).
21. Nanao, M. H. *et al.* Structural basis for oligomerization of auxin transcriptional

regulators. *Nat Commun* **5**, 3617 (2014).
22. Fontana, M. *et al.* Cooperative action of separate interaction domains promotes high-affinity DNA binding of Arabidopsis thaliana ARF transcription factors. *bioRxiv* 2022.11.16.516730 (2022) doi:10.1101/2022.11.16.516730.
23. Galli, M. *et al.* The DNA binding landscape of the maize AUXIN RESPONSE FACTOR family. *Nat Commun* **9**, (2018).
24. Stigliani, A. *et al.* Capturing Auxin Response Factors Syntax Using DNA Binding Models. *Mol Plant* **12**, 822–832 (2019).
25. Mutte, S. K. *et al.* Origin and evolution of the nuclear auxin response system. *Elife* **7**, 1–25 (2018).
26. Lakehal, A. *et al.* A Molecular Framework for the Control of Adventitious Rooting by TIR1/AFB2-Aux/IAA-Dependent Auxin Signaling in Arabidopsis. *Mol Plant* **12**, (2019).
27. Yu, H. *et al.* Untethering the TIR1 auxin receptor from the SCF complex increases its stability and inhibits auxin response. *Nat Plants* **1**, (2015).

Chapter 6

Dynamics of input and output of the auxin response system in early gemma development

Shubhajit Das[1], Martijn de Roij[1], Sumanth Mutte[1], Wouter Kohlen[2], Dolf Weijers[1], Jan Willem Borst[1]
[1]Laboratory of Biochemistry, Wageningen University, the Netherlands
[2]Laboratory of Molecular Biology Wageningen University, the Netherlands

Part of this chapter has been published as:

Das S., Roij M., Bellows S., Kohlen W., Farcot E., Weijers D. and Borst JW (2022) Selective degradation of ARF monomers controls auxin response in Marchantia. bioRxiv. DOI:10.1101/2022.11.04.515187

Abstract

Auxin is a small signaling molecule essential for the highly adaptive plant life. The nuclear auxin signaling pathway acts as an input/output system where the auxin signal is fed into the network by a TIR1-Aux/IAA coreceptor complex. At the core of this network, the ARF transcription factors process the auxin input signal and return an output in the form of transcriptional change. Since plant development is a continuous process, auxin signaling is required to adapt dynamically to program plant growth. In previous chapters, we explored the dynamics of the auxin signaling core by following ARF levels in Marchantia gemmae transitioning from a dormant state to active germinated stage. To have an integrative view of the pathway, here we have investigated the dynamics of auxin input, the single MpTIR1 receptor and the single MpAux/IAA repressor. We found an inversely correlated concentration dynamics of free auxin (Indole-3-acetic acid) and MpTIR1 receptor levels. In addition, Aux/IAA repressor stability analysis showed high sensitivity towards auxin, suggesting fast relay of signal to ARFs. Finally, we quantified the system output by analysing the transcriptional changes correlated with auxin receptor-repressor dynamics and observed major reprogramming in active gemmae. Furthermore, we show that the auxin responses in gemmae are unique at different stages after germination. Overall, this chapter presents the dynamics of auxin input signal leading to a differential transcriptional response during gemmae germination.

Introduction

Auxins are a group of small organic molecules that control a multitude of developmental processes in plants[1–3]. The major natural form of auxin is Indole-3-Acetic Acid (IAA; referred to as auxin)[4]. Auxin is perceived by a nuclear F-box containing receptor protein family TIR1/AFBs (TRANSPORT INHIBITOR RESPONSE/AUXIN SIGNALING F-BOX)[5,6]. Auxin-bound TIR1/AFB receptors selectively ubiquitinate Aux/IAA (Auxin/INDOLE-3-ACETIC ACID) repressors in an auxin concentration dependent manner, leading to their proteasomal degradation[7]. Degradation of Aux/IAA acts as an activating switch as it releases ARFs (AUXIN RESPONSE FACTORs) from inhibition. Following Aux/IAA degradation, the auxin input signal is processed by ARFs, resulting in a transcriptional output[8,9]. Studies in both angiosperms and bryophytes revealed that ARFs are a conserved family of DNA binding proteins and are divided into three phylogenetic classes-A, B, and C[8,10–12]. Reported ARF-DNA interaction analysis showed that auxin-dependent class-A and auxin-independent class-B ARFs have similar DNA binding preferences, leading to a mechanism where the transcriptional output is determined by relative abundance of two competing ARF classes[13–16]. Using this relatively simple nuclear signaling pathway, auxin regulates processes such as germination[17], embryogenesis[17,18], meristem maintenance[19], root development[20], defence[20], and stress response[21]. Therefore, nuclear auxin signaling pathway (NAP) operates as an input/output device where auxin acts as the input signal that is received by the TIR1/AFB-Aux/IAA co-receptor complex. The received signal is processed by the competitive function of class-A and B ARFs and finally the output is returned in the form of transcriptional reprogramming that controls plant growth.

Plant development is a continuous and adaptive process. Since auxin is wired intricately with development, it is expected that the nuclear auxin signaling could also be dynamically regulated. Despite the immense progress in genetic and biochemical characterization of NAP components in angiosperms, the dynamics of the native signaling proteins are largely unknown. This is partially caused by the staggering number of potential protein interactions in angiosperm NAP systems that impede a dynamic view of the complete network. During evolution, the relatively simple ancestral auxin signaling circuit has expanded its complexity by gene duplications, whereas the basic blueprint has been retained in the liverwort species *Marchantia polymorpha*. Therefore, an integrative analysis of NAP dynamics is probably possible only in a simpler protein network as the Marchantia NAP. In previous chapters, we

investigated the expression of ARFs, the central processing units of NAP and their dynamic regulation. What remains unknown is how the dynamics of the TIR1-Aux/IAA auxin perception module and the auxin input signal itself feed into the pathway and control transcriptional output[22].

Dynamic signaling is mostly associated with changes in developmental stages or adaptation to a new environment. Marchantia gemma germination is a key developmental transition step where dormant tissue initiates active growth[23], and therefore provides an excellent window to explore auxin input and output changes. In this chapter, we first focused on the dynamics of auxin and its receptor MpTIR1 during gemma germination. We found an inversely correlated concentration dynamics of free auxin (Indole-3-acetic acid) and MpTIR1 receptor levels. In addition, we investigated auxin-dependent degradation of MpAux/IAA and found that this conserved mechanism leads to instability of MpAux/IAA in dormant gemmae. To estimate auxin response kinetics, we quantified auxin-dependent degradation rate of MpAux/IAA repressor. We explored the natural transcriptional landscape and auxin response capacity of gemmae during transition from dormancy to germination, as an outcome of the dynamic signal input and processing.

Results

Receptor-Ligand dynamics in the Marchantia NAP

High auxin concentration is known to maintain gemmae dormancy in gemma cups[23,24], indicating that germination and growth must involve a readjustment in auxin levels. Therefore, we quantified the temporal dynamics of free auxin concentration in developing gemmae. In Marchantia, a major form of auxin is Indole-3-acetic acid (IAA) produced by the IPA (Indole pyruvic acid) pathway[24]. Using LC-MS, we quantified total free IAA concentrations at different stages of gemma development. An auxin concentration of over 4 picomole/gram fresh weight was determined at both 0 hour (dormant) and after 3.5 hours of growth (Figure1.A). However, auxin levels dropped to less than1 picomole/gram fresh weight after 8 and 24 hours of germination, showing a clear decline which correlates with gemmae growth. This is in agreement with a transition from potentially inhibitory higher, to permissive lower concentrations during gemmae growth[23,25].

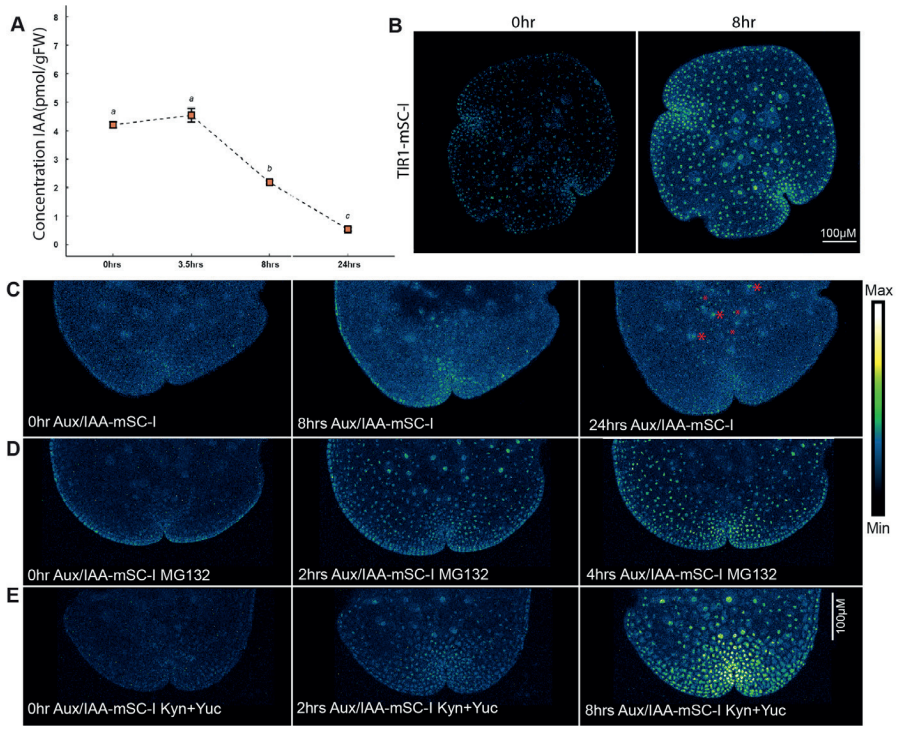

Figure 1: Dynamics of auxin, TIR1 and Aux/IAA during early gemma development. (A) Auxin concentration dynamics of free IAA in germinating gemmae. LC-MS quantification shows total IAA levels drop with gemmae germination. (B) Time-lapse imaging of TIR1-mSC-I shows that the expression levels gradually increase after gemma germination. (C) Time -lapse imaging of mock treated Aux/IAA-mSC-I shows no signal up to 8 hours of growth. A low expression of Aux/IAA is detected at 24 hours (highlighted with red asterisks), suggesting increased stability of the protein after germination. (D) Treatment with 100mM MG132 caused accumulation of Aux/IAA within 2 hours (E) Inhibition of auxin biosynthesis by 50mM Kynurenine and 50mM Yucasin, lowers auxin concentration and stablizes Aux/IAA, confirming conserved auxin dependency of the repressor degradation.

In chapter 3, we showed that MpTIR1 has low expression at dormant stage. Since auxin concentration declined during gemma germination, we wondered whether receptor levels are also tuned accordingly. To this end, we performed time-lapse confocal microscopy on MpTIR1-mScarlet-I knock-in line. We found that MpTIR1 levels sharply increased in the first 8-hours of gemmae germination (Figure1.B). The overall pattern of accumulation, both in terms of subcellular localization and expression in multiple cell types, did not change over time. This suggests that TIR1 levels globally increase after germination. It cannot be concluded from visualizing only protein accumulation whether this increase in levels is cause by transcriptional, post-transcriptional, translational, or post-translational control, or a combination of these.

MpAux/IAA is proteasomally degraded in auxin-rich dormant gemmae

A direct effect of TIR1-dependent auxin perception is the proteasomal degradation of Aux/IAA repressor proteins[7,26]. We showed that MpTIR1-mScarlet-I is expressed in dormant gemmae (Figure 1B), whereas MpAux/IAA-mScarlet-I was undetectable (Chapter 3). This suggests either that Aux/IAA is not expressed in dormant gemmae, or that the high auxin levels in dormant gemmae constitutively trigger instability of MpAux/IAA. Since we found that auxin levels declined after germination (Figure1.A), it is possible that MpAux/IAA is also stabilized post germination. We therefore followed MpAux/IAA expression in the first 24 hours of germination. We did not observe any MpAux/IAA-mScarlet-I fluorescence signal in the first 8 hours but detected a weak nuclear signal in rhizoid initial cells after 24 hours (Figure 1.C). This finding is consistent with Aux/IAA patterns being driven by auxin-dependent degradation at earlier stages, followed by accumulation due to decreased degradation at later stages. To test this hypothesis directly and exclude that Aux/IAA accumulation patterns are conditioned by transcriptional control, we treated gemmae with the proteasome inhibitor MG132. This led to clear nuclear protein accumulation within 2 hours (Figure 1.D) and suggests that IAA dynamics determine endogenous Aux/IAA accumulation patterns in early gemmae development.

To test if indeed MpAux/IAA patterns are a result of auxin dynamics, we depleted IAA accumulation by applying inhibitors of the two enzymes involved in its biosynthesis. TRYPTOPHAN AMINOTRANSFERASE OF ARABIDOPSIS (TAA1) and YUCCA (YUC) can be inhibited L-Kynurenine and Yucasin inhibitors, respectively[27,28]. To effectively deplete IAA, we combined the two inhibitors and visualized MpAux/IAA accumulation. Nuclear MpAux/IAA-mScarlet-I accumulation was detected across gemma within 2 hours of inhibitor treatment (Figure 1.E). This clearly demonstrated that MpTIR1 is active throughout gemma development in mediating IAA-triggered MpAux/IAA degradation. These findings suggest that TIR1-Aux/IAA permissive signal is required in both dormant and active stage, but an increased auxin sensitivity and ARF1/2 stoichiometry (see Chapter 4) are probably required for dormancy release and organogenesis.

Determination of the MpAux/IAA protein half-life

The pace of auxin input signal relay from TIR1/AFBs to ARFs depends on degradation rate of Aux/IAA repressors. A quick transcriptional response to auxin therefore relies on rapid degradation of Aux/IAAs[29]. Arabidopsis has

multiple Aux/IAAs previously shown to have a wide range of degradation rates from 10 minutes to 1.3 hours and this diversity in AtAux/IAA stability was proposed determine the kinetics of auxin response during lateral root development[30]. However, Marchantia has only a single Aux/IAA repressor[31] and its rate of degradation is unknown. Since a quantitative model of NAP would be incomplete without Aux/IAA turnover rate[32], we determined the half-life of the native protein *in vivo*.

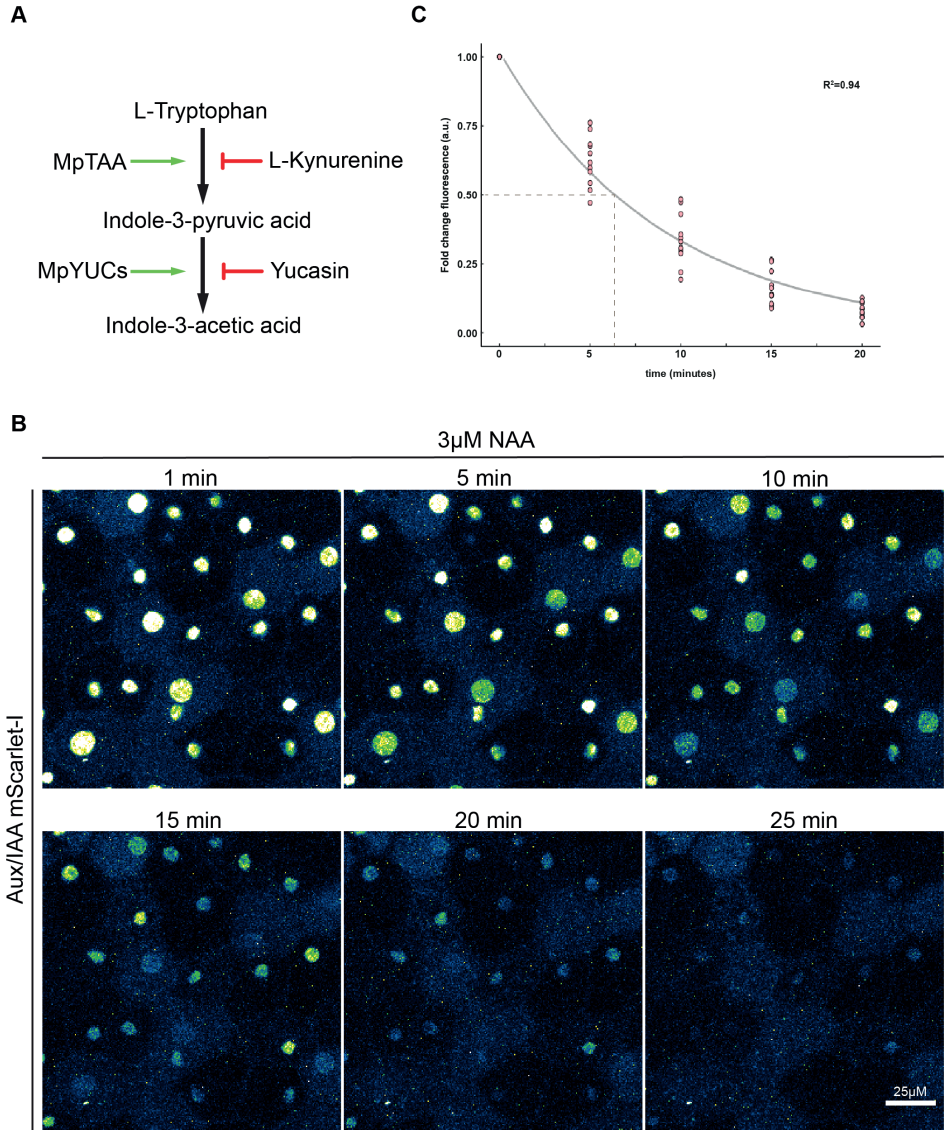

Figure 2: (A) Auxin biosynthesis via Indole pyruvic acid pathway is catalyzed by two key enzymes TRYPTOPHAN AMINOTRANSFERASE OF ARABIDOPSIS (TAA1) and YUC-

CA (YUC). To lower auxin levels in tissue, both enzymes can be chemically inhibited by L-Kynurenine and Yucasin respectively. (B) Time-lapse imaging on MpAux/IAA-mScarlet-I gemmae pre-treated with L-Kynurenine and Yucasin. Upon auxin treatment, fluorescence rapidly declines due to MpAux/IAA-mScarlet-I degradation. (C) Fitting quantified fluorescence data on an exponential decay curve determines MpAux/IAA half-life as 6.5 minutes.

Given that MpAux/IAA is undetectable in dormant gemmae and levels are very low even after 24 hours (Figure 1.C), it is impossible to determine protein half-life. However, as auxin depletion stabilizes the protein, we should be able to follow its decline upon re-supply of IAA after its initial depletion. We therefore first reduced endogenous auxin levels in dormant gemmae by pre-treatment with L-Kynurenine and Yucasin (Figure 2.A). After overnight inhibitor pre-treatment, high accumulation levels of Aux/IAA in nucleus was observed, which allowed us to determine auxin dependent degradation rate of MpAux/IAA. Gemmae with high Aux/IAA accumulation were treated with 3 μM NAA (1-Napthaleneacetic acid) and protein stability was followed by time-lapse confocal microscopy (Figure 2.B). By fluorescence signal quantification and data fitting of the obtained exponential decay curve (Figure 2.C), we determined MpAux/IAA half-life as 6.5 minutes. This suggests an Aux/IAA degradation rate that can be considered fast compared to known degradation rates in Arabidopsis that range from 10 minutes for AtAux/IAA1 to 80 minutes for AtAux/IAA 28[29,33]. This also suggests that the ancestral condition of the NAP includes fast Aux/IAA turnover, and that slower degradation rates found in Arabidopsis are a derived property.

MpTOPLESS co-repressor expression is stable in actively growing gemmae

In Arabidopsis, Aux/IAA-mediated transcriptional repression is mediated by the co-repressor protein TOPLESS (TPL)[34]. TPL interacts with the EAR motif in Aux/IAAs[35], and loss of this motif, of TPL, or of the Aux/IAA-TPL interaction causes loss of the repression brought about by Aux/IAAs[36]. TPL therefore represents the main mechanism for inhibition of gene expression in the absence of auxin. Interestingly, TPL can also interact with class-B and -C ARFs directly[35] to repress gene expression. To address if the capacity for gene repression through TPL is dynamic during gemmae development, we generated a pTPL::TPL-mNG line and performed time-lapse imaging in germinating gemmae. In both dormant and germinated gemmae, we found MpTPL stably expressed in every cell type. This suggests that dynamics of MpTPL accumulation may not strongly regulate auxin-dependent gene expression.

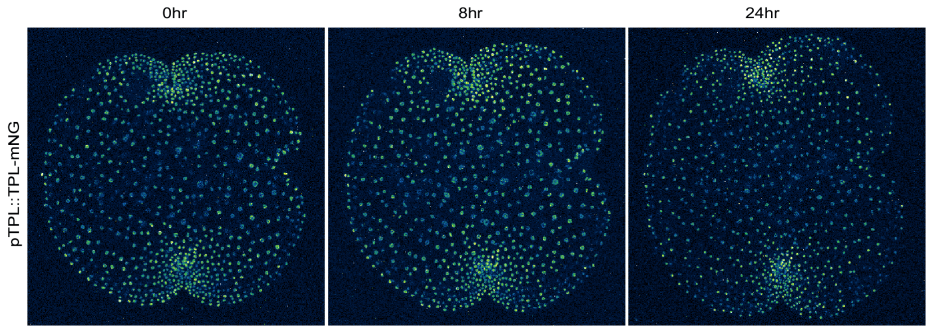

Figure 3: Spatiotemporal expression pattern of pTPL::TPL-mNeonGreen gemmae. The protein is expressed in all cell types and detected throughout development from dormant to 24 hours after germination.

Transcriptional reprogramming in germinating gemmae

Dormant gemmae represents a metabolically inactive stage with minimal signs of growth[23]. Upon germination, it starts to grow, establish dorsiventral polarity and develop rhizoids[23]. We showed that in the same time frame, endogenous auxin levels and its receptor concentration also changes. The dynamics of the NAP components and the accompanying growth processes must require transcriptional changes and high metabolic activity, which are minimal in dormant gemmae. To capture the early transcriptional changes during germination and the effect of dynamic auxin concentration in NAP response, we performed an RNA sequencing experiment on gemmae collected from 0 hour (dormant), 3.5 hours and 8 hours of growth. Principal component analysis resulted in a strong clustering within biological replicates and a high variance between different time points, suggesting major differences in the transcriptomes at different developmental stages (Figure 4.A). After 3.5 hours of gemmae growth, we found hundreds of differentially regulated genes which was even more prominent after 8 hours (Figure 4.B). While a major overlap of the genes differentially regulated at 3.5 and 8 hours indicates a sustained progression of transcriptional changes, genes uniquely regulated at these time points were also detected (Figure 4.C). Among the nuclear auxin signaling components, *MpARF1* and *MpARF2* expression levels were comparable among the three time points (Figure 4.D), corroborating our previous qRT-PCR data in Chapter 4. For *MpARF3*, however, we observed transcriptional downregulation. This is in contrast with the stable expression of MpARF3-mScarlet-I protein (chapter 4).

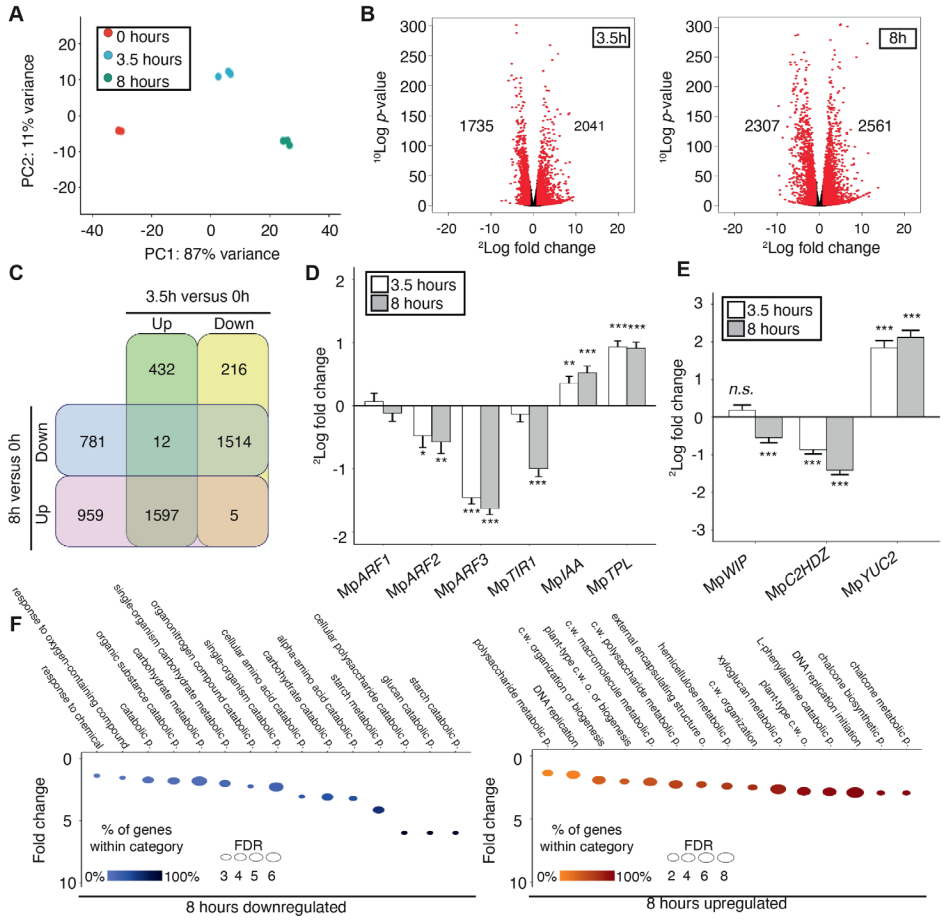

Figure 4: PCA plot of RNA-seq transcriptomes of gemmae cultured in B5 medium for 3.5 and 8 hours as well as dormant gemmae. **b.** Volcano plot showing the number of significantly (p_{adj}<0.05, in red) differentially expressed genes (DEGs) after 3.5h and 8h of growth compared to the dormant state. Non-DEGs are represented by black dots. **c.** Venn diagram illustrating overlap of DEGs in 3.5h and 8h gemmae. **d.** Expression levels of key components of the NAP (left) and MpPIN proteins (right) after 3.5h and 8h of growth on a ^{2}Log scale. Asterisks indicate * p_{adj}<0.05; ** p_{adj}<0.01; *** p_{adj}<0.001. **e.** Gene Ontology analysis showing the 15 most enriched GO terms for biological process (based on the lowest *p*-values) after 8 hours in the down -and upregulated gene pools. Color scale corresponds to the percentage of genes found within the given category and dot size showcases the False Discovery Rate. y-axis depicts the fold change, i.e. observed count/expected count. Abbreviations in GO terms are: p. = process; c.w. = cell wall; o. = organization.

Interestingly, both *MpAux/IAA* repressor and *MpTPL* co-repressor transcripts were upregulated after germination, while at the protein level, MpTPL remains stably expressed and MpAux/IAA expression does increase slightly. Therefore, both transcriptional upregulation and reduced auxin concentration may contribute to increase in MpAux/IAA accumulation. In our transcriptome data, *MpTIR1* is downregulated after gemma germination, contrary to the clear increase of protein expression observed in the knock-ins (Figure 1.E). This discordance could be due to factors such as longer protein half-life or delayed translation due to mRNA secondary structures and highlights the importance of quantitative analysis at protein level.

To investigate auxin response changes during early stages of germination, we initially checked the expression of the most commonly studied auxin regulated genes in Marchantia (Figure 4.E). Previously, *MpWIP* and *MpC2HDZ* genes have been shown to be positively regulated by auxin whereas *MpYUC2* transcription was downregulated upon auxin treatment[13,37]. In our transcriptome data, we found both *MpWIP* and *MpC2HDZ* transcripts downregulated and *MpYUC2* upregulated, indicating lower auxin levels at later time points (Figure 4.E). This is in line with our total IAA quantification data that shows reduction in auxin levels after germination (Figure 1.D). Based on expression of *MpWIP, MpC2HDZ and MpYUC2,* there seems to be lower auxin response after germination. However, expression of this limited number of genes may give a biased view and not reflect the general pattern of response. Based on our MpARF1/2 ratio data in chapter 4 an increased auxin response can be expected after germination. Gene ontology analysis indicated that among upregulated genes at 8 hours, there are genes related to DNA replication, cell wall organisation and secondary metabolism, all of which are associated with growth. Therefore, to understand the general output pattern in entire auxin dependent transcriptome, we extracted a list of about a hundred auxin-regulated genes from available transcriptome data of auxin-treated wild-type plants[38]. By comparing expression of all these genes in our transcriptome data, we obtained a more global, unbiased view of auxin output after germination (Figure 5). Transcript levels of the majority of auxin-upregulated genes were higher after germination and likewise, transcript counts of most auxin-downregulated genes were lower in germinated gemmae. Thus, at a global scale, transcriptional auxin response is elevated after dormancy release. Among the auxin-upregulated genes, a specific cluster showed peak expression at 3.5 hours, correlated with the sharp increase in ARF1/2 ratio (see chapter 4) at this time point. A smaller cluster of genes among both up- and downregulated

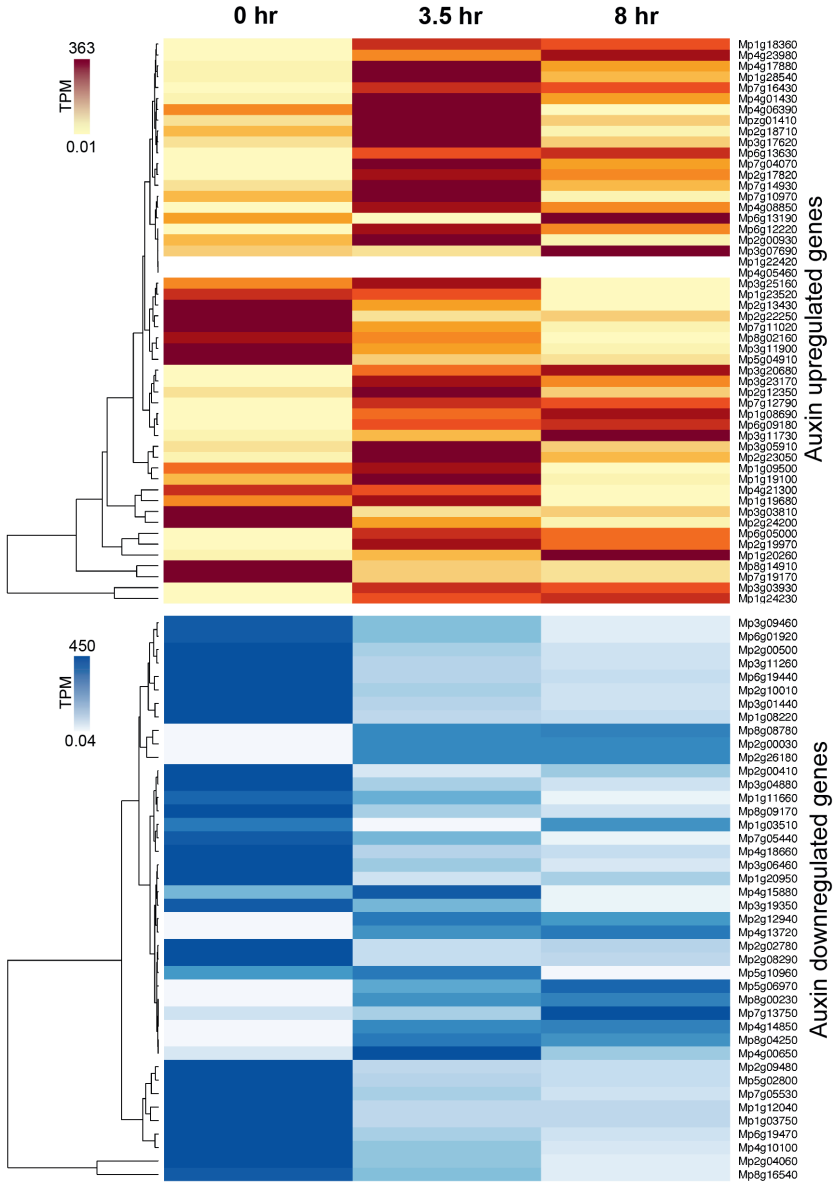

Figure 5: Transcriptional dynamics of auxin responsive genes during gemmae germination. A list of auxin responsive genes was extracted from available transcriptome data38 and transcripts per million (TPM) values of those genes in the three time points during germination were plotted in a heatmap. Most of the genes, including both up and downregulated ones, suggest an increased auxin dependent transcription. This is particularly prominent in the pattern of down regulated set of genes which are downregulated after germination, indicating increased auxin response output. Likewise, most of auxin upregulated set of genes are upregulated after germination, and many of them are at a peak at 3.5hrs when ARF1/2 ratio was shown to rise (chapter 4).

sets, showed an opposite regulation. For instance, transcript levels of a set of known auxin-upregulated genes were lower after germination. Similarly, a few auxin-downregulated genes had increased transcript levels after germination. These expression patterns correlate more with declining auxin levels, than ARF1/2 ratio. Therefore, the majority of transcriptional responses are likely regulated by an increased ARF1/2 ratio while expression of a smaller set of genes is synchronized to auxin and regulated by individual ARF levels.

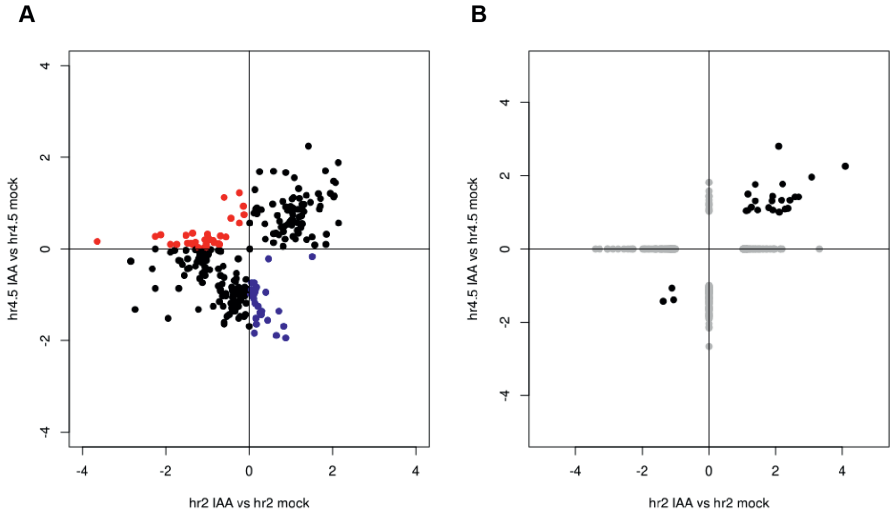

Figure 6: Plot of $\log_2$(Fold change) differentially regulated genes between 2 hour and 4.5-hour old gemmae treated with mock or auxin. (A) Plot of fold changes in average transcript per million (TPM) counts of all differentially regulated genes in the two time points. Commonly regulates genes are marked as black. Genes with opposite regulation at 2 hour and 4.5 hours are indicated with blue and red colours respectively. (B) Plot of only the significantly regulated genes that are common (in black) and unique (in grey) in the two time points.

Dynamics in the auxin input module and the ARF ratio increase cause a major reorganization of NAP in germinated gemmae. We wondered whether this reorganization leads to a shift in the capacity to respond to auxin. To compare this capacity to external auxin before and after germination, we treated gemmae that had been grown (outside of the cup) for 1 hour or and 3.5 hours, with 1μM IAA or mock for 1 hour. Thus, we collected the auxin-treated samples as 2-hour and 4.5-hour-old gemmae. We compared gemmae transcriptomes of the two time points and found hundreds of genes that are differentially regulated between the two stages of development (Figure 6.A), suggesting that capacity for auxin response changes following germination. In total, 289 genes (152 genes at 2 hours and 137 genes at 4.5 hours) were differentially regulated by auxin in the two time points, of which only 26 genes were com-

mon between the time points (Figure 6.A). Thus, the remaining 263 genes represent a set of genes that are uniquely auxin-regulated in either time point. It is worth noting that, despite having a large gene set showing opposite regulation between two time points (Figure 6.A; red and blue dots), no genes were commonly regulated with opposite patterns with statistical significance (Figure 6.B).

Discussion

Vegetative reproduction of Marchantia begins with the germination of dormant gemmae, a step highly interconnected with dynamic auxin signaling[23]. By following the levels of MpTIR1 receptor, MpAux/IAA repressor, and auxin (IAA) itself we captured the early dynamics in the input signals of NAP. We showed that gemmae progresses from a dormant state with high auxin, low receptor, and low Aux/IAA to an active growth state with low auxin, high receptor, and higher Aux/IAA. Therefore, as auxin levels decline, auxin sensitivity goes up and the capacity for Aux/IAA-dependent auxin response dynamically changes during development. Gemma cups provide a high-auxin environment[23,24], that effectively causes degradation of Aux/IAA proteins at dormant state, whereas reduced auxin levels after germination partially stabilizes Aux/IAA. Thus, the entire input module of NAP is readjusted during germination. A main activation switch in this auxin input module is the Aux/IAA degradation that activates class-A MpARF1 mediated gene regulation. In angiosperms, a diverse range of Aux/IAA half-lives among multiple family members set differential auxin sensitivity across tissue[30]. Since the kinetics of transcriptional auxin response depends on degradation rate of the Aux/IAA repressor, we quantified MpAux/IAA half-life using genomic knock-in lines. A 6.5-minute half-life of the native MpAux/IAA protein suggests that the ancestral copy of Aux/IAA is highly sensitive to auxin, whereas the relatively less sensitivity of Arabidopsis homologs is an evolutionary derivative[29]. This quantitative data on MpAux/IAA turnover will be useful in building a predictive quantitative model for Marchantia NAP.

Transcriptional gene repression by NAP has two routes: an auxin-dependent repression by MpAux/IAA[26,39,40] and an auxin-independent repression by MpARF2[13]. A common player in both routes is the MpTPL co-repressor. Previous studies in Marchantia have confirmed functional conservation of MpTPL in gene repression in association with Aux/IAA and interaction with MpARF2[13,31]. While investigating a co-regulation of Aux/IAA-TPL repressor and co-repressor pair, we found that MpTPL-mNeonGreen levels remain

stable throughout gemma germination. Therefore, MpTPL function in auxin response dynamics during germination might be required, but not as a limiting step. Noticeably, MpTPL-mNeonGreen was expressed in every cell type of both dormant and germinated gemmae. Thus, instead of cell specific functions, MpTPL might be required as a general co-repressor, as earlier studies confirmed TPL function in meristem maintenance, circadian clock regulation, gibberellic acid signaling, strigolactone signaling and jasmonic acid signaling[41].

To capture the changes in NAP output, we analyzed transcriptomes of gemmae in the same growth stages when auxin inputs are dynamic. While analyzing the transcript levels of auxin signaling genes, we noticed ARF1 and ARF2 levels were stable, as observed in chapter 4. Surprisingly, for ARF3 a clear downregulation at transcript level was noticed, whereas protein levels did not change in our data in chapter 4. A similar discrepancy between transcript and protein levels were noticed for TPL, where protein levels did not change despite increasing transcription. The most severe inconsistency was observed for MpTIR1 mRNA and protein levels. While transcriptome data showed downregulated MpTIR1 transcript levels after 8 hours of germination, we observed an increased accumulation of the protein. These mRNA-protein paradoxes are not uncommon in eukaryotes and can be attributed to multiple intermediate regulatory mechanisms. For example, high stability of mRNA could be an explanation for the differences observed in MpTPL mRNA and protein levels. If the mRNAs are unstable due to high AU rich sequences in the 3'UTR[42] or if the mRNA is under the control of small RNAs, increased transcription may not translate into protein expression. While these uncorrelations can be counterintuitive, they also highlight the importance of studying signaling pathways at the level of proteins, rather than solely relying on the transcriptomes.

Previously, it was shown that TIR1/AFBs in Arabidopsis can be regulated post transcriptionally. For instance, *AtTIR1/AFB* mRNA levels are negatively regulated by microRNA393[43]. However, a miRNA-based regulation of MpTIR1 depends on the conservation of miRNA393 homologs in Marchantia. In absence of Aux/IAA substrate AtTIR1 can also undergo auto-degradation. As we observed that in dormant stage there is no MpAux/IAA available for degradation, it is possible that MpTIR1 degrades itself[44]. This auto-degradation is inhibited in stabilization and availability of MpAux/IAA substrate in low auxin environment of germinated gemmae.

Thousands of genes including many auxin-responsive genes were found to be differentially regulated after gemmae germination. On initial examination of the most commonly used auxin responsive gene expression, we found down-regulation of *MpWIP* and *MpC2HDZ* and upregulation of *MpYUC2*, an opposite regulation pattern compared to reported expression of these genes in auxin treated tissue. Thus, based on the expression these three genes, auxin response in germinated gemmae is lower, correlated with the declining free auxin (IAA) levels. However, in chapter 4, we found that during gemmae germination MpARFs (class-A and B) degrade, and MpARF1/2 stoichiometry increases. A conceivable outcome of ARF degradation is lowered transcription of genes that are solely regulated by either MpARF1 or MpARF2. However, for the genes controlled by both ARFs, an increase in ARF1/2 stoichiometry in favour of ARF1 should induce gene transcription, as predicted by model simulations. In addition, about one hundred genes are mis-regulated in published transcriptome of *Mparf1-4* knock-out mutant. Thus, there are many genes besides WIP, C2HDZ, YUC2 that represent the complete auxin dependent transcriptome. Comparison of this larger set of auxin-responsive genes, we found a view that is more general and different from the pattern observed initially with three candidate genes. Expression of most auxin-dependent genes suggests an overall increase in auxin output after germination. These larger clusters of genes follow the trend of MpARF1/2 ratio dynamics. A smaller set of auxin-regulated genes followed the decline pattern of individual ARFs and auxin itself. Therefore, not all auxin-regulated genes are necessarily upregulated upon germination and an increase of the ARF1/2 stoichiometry. Genes regulated by ARF competition are upregulated whereas genes regulated by only ARF1 may become down regulated due to reduced protein levels. Additionally, genes can also be upregulated due to removal of ARF2 repression.

Considering the major shifts in MpTIR1 and MpARF protein levels, we looked for any influence on auxin response before and after this shift. Comparison of gemmae transcriptomes after auxin treatment indeed identified hundreds of genes that are specific to the stage of gemmae development. Thus, at different time points during germination, the NAP dynamics generates different combinations of auxin and signaling proteins that results in unique auxin-dependent transcription. In this analysis, we used gemmae that were grown for 1 hour and 3.5 hours on normal growth media before treating them with auxin for another hour. The initial growth on normal media allowed to provide a

more uniform condition before treating the samples with auxin. Since the accumulation of most NAP proteins does not change in the first hour, we grew the dormant batch of gemmae equally as the set used for 3.5-hour treatment. In retrospect, this pre-treatment does not seem necessary. Although the first hour of gemmae may not have detectable NAP dynamics, this period is probably sufficient to start transcriptional changes required for germination. Since 0-hour dormant gemmae and 8-hour hour germinated gemmae have the most dramatic differences in auxin and NAP protein accumulation, treatment with auxin at this two time points would have resulted in more significant differences and identification of a larger set of uniquely regulated genes.

An active developmental transition to germination involves initiation of multiple signaling pathways that might contribute to the global reprogramming of transcriptome. In our comparative transcriptome analysis, we observed differential regulation of a wide variety of genes, some even unrelated to auxin signaling. This could partly be caused by the dynamics of multiple other growth factors in gemmae. Furthermore, we compared the transcript levels in whole gemmae, which has different levels of auxin and ARFs based on cell type. Thus, our data may have considerable amount of background dynamics and lacks spatial information. A systematic analysis of cell type specific transcriptome analysis would be more informative in future.

In conclusion, our analysis of NAP input and output dynamics complemented with ARF dynamics in previous chapters, provides a unique integrative view of auxin signaling in transition. We were able to show that dormancy is associated with high auxin, low receptor, and high ARF1/2 stoichiometry, whereas growth requires lower auxin, higher receptor, and higher ARF1/2 stoichiometry. Thus, the capacity to respond to auxin depends on both the TIR1-Aux/IAA “permissive” machinery and the relative function of ARF transcription factors.

Materials and method

Plant growth conditions

Marchantia polymorpha male Takaragaike-1 (Tak-1) and female Takaragaike-2 (Tak-2) were used as the wildtype variety. For vegetative propagation, plants were grown on ½ Gamborg B5 media plates in growth chambers with 40 µmol photons m^{-2} s^{-1} continuous white light at 22 °C. For sexual reproduction, plants were grown on 1% sucrose supplemented ½ Gamborg B5 media within hyrophonic boxes exposed to 40µmol photons m^{-2} s^{-1} continuous white fluorescent light for 1 month. Plants were then moved into 40 µmol photons m^{-2} s^{-1} continuous white light supplemented with 15µmol photons m^{-2} s^{-1} far-red light to induce antheridiophore and archegoniophore development. Plants were repeatedly crossed manually to ensure fertilization. Sporangia with mature spores were collected aseptically and used in spore transformation.

Microscope slide mount setup for time course imaging

A microscope slide mount was set up for live imaging of gemma to precisely track a selected set of cells for temporal protein expression analysis. The mount consisted of a circular aluminium disc with a plastic inset fitted at the centre of the disc (Supplementary Figure 2). Melted ½ B5 media with or without desired treatments were poured into the cavity of the plastic inset and allowed to solidify. Gemma was carefully placed on top of the solidified media and covered with a round coverslip. The bottom of the mount was sealed with parafilm to prevent any evaporation and media drying during time series imaging. Between two imaging time points in a time series experiment, the mounts were placed inverted in the growth chambers to keep the gemmae exposed to light and allow normal growth of gemmae.

Confocal live cell imaging

All live cell imaging was done with a Leica SP8X-SMD confocal microscope equipped with a hybrid detector and a pulsed white-light laser (WLL). The mScarlet-I was excited with a 561 nm laser line (4% laser output of WLL) and mNeongreen was excited with a 506nm laser line (4% laser output of WLL). Fluorescence emission was detected by the hybrid detector at 570 to 620 nm (for mScarlet-I) and 512nm to 560nm (for mNeongreen). All images were acquired in photon counting mode at on a 20X objective lens and time-gated detection mode was used to suppress autofluorescence. Images were processed using ImageJ software. Maximum-intensity projections of z-stack images were used to quantify total cellular fluorescence in each nucleus analysed, normalized through background fluorescence measurements.

Total Indole-3 -acetic acid (IAA) and oxidized IAA quantification

Total IAA was quantified to estimate the total cellular auxin levels during gemma growth. Gemmae were collected from 4-week-old Tak-1 plants. Tak-1 gemmae were grown on liquid ½ B5 media and samples were collected after 0, 3.5, 8 and 24 hrs of growth. Samples were snap frozen in liquid Nitrogen and ground into fine power and weighed. For the extraction of indole-3-acetic acid (IAA) ~150 mg of snap-frozen plant material was used per sample. Tissue was ground to a fine powder at -80˚C using 3-mm stainless steel beads at 50 Hz for 2*30 seconds in a TissueLyser LT (Qiagen, Germantown, USA). Ground samples were extracted with 1 mL of cold methanol containing [phenyl 13C6]-IAA (0.1 nmol/mL) as an internal standard in a 2-mL eppendorf tube as previously described[45]. Samples were filtered through a 0.45 µm Minisart SRP4 filter (Sartorius, Goettingen, Germany) and measured on the same day. IAA was analyzed on a Waters Xevo TQs tandem quadruple mass spectrometer.

RNA extraction and sequencing

Marchantia gemma were were collected from gemma cups of 4-week-old wild type Tak-1 plants. Gemmae were filtered and snap frozen after 0 (dormant), 3.5 and 8 hours of growth on liquid B5 media. RNA was extracted from ground tissue using the TRIzol reagent and Qiagen Plant mini kit. An on-column RNase-free DNase (Qiagen) treatment was performed before final elution. RNA quality and integrity were checked in bioanalyzer (Agilent Bioanalyzer 2100 Nano). RNA samples were sequenced by Illumina NovaSeq6000 at BGI. The quality of the raw fastq reads were analyzed in FastQC. Reads were then mapped onto the *M. polymorpha* genome (MpTak1v5.1, accessed through MarpolBase; https://marchantia.info/download/tak1v5.1/), which was performed using HISAT2 v2.2.1[65], with -dta and -trim5 10 specified. SAM and BAM files were handled using SAMTOOLS v1.11[66]. The raw reads were then counted using FeatureCounts v2.0.1 [67], parameters were as follows: -t exon; -g gene_id; -Q 30; -p; -primary. The results from FeatureCounts were imported into R v3.6.1 and raw count normalization as well as the identification of differentially expressed genes ($p_{adj} < 0.05$) was performed using DESeq2[68]. Genes with a total read count below 45 were excluded from the analysis while genes with an absolute ^{2}Log fold change of > 1 and p_{adj} of < 0.05 were deemed differentially expressed.

For auxin treatment, wild type gemmae were grown on liquid B5 media in two batches. One batch was grown for 1 hour and another one for 3.5 hours.

After this both batches were treated with either 1μM IAA or DMSO (mock) for 1 hour. All samples were collected, frozen and later used for RNA extraction and sequencing.

Gene Ontology analysis

Gene IDs of differentially expressed genes for the respective timepoints were used as input for the PlantRegMap server (http://plantregmap.gao-lab.org/)[69]. The *M. polymorpha* genome was used as the background with a *p*-value cut-off of $p<0.05$ to distinguish enriched GO terms.

Author contributions

Conceptualization-S.D., D.W., J.W.B.; Experiments-S.D., M.R., S.M., W.K; Writing and Reviewing-S.D., J.W.B., D.W.

Acknowledgements

We thank Juriaan Rienstra for helpful comments on this chapter. S.D. is supported by The Netherlands Organization for Scientific Research (NWO) (ALWOP.402).

Supplementary table 1

List of 26 commonly regulate genes after auxin treatment (Figure 6.A)

	Log2(foldchange)	
GeneID	**hr2.IAA**	**hr4.5.IAA**
Mp5g03090	2.09	2.8
Mp7g10960	1.89	1.31
Mp6g07050	4.09	2.26
Mp3g22470	2.43	1.33
Mp3g16900	1.27	1.14
Mp2g23050	2.21	1.77
Mp7g09020	-1.06	-1.39
Mp3g11900	1.12	1.04
Mp3g16930	2.58	1.42
Mp7g01430	2.28	1.09
Mp3g11090	2.37	1.11
Mp7g16430	2.69	1.42
Mp7g10970	1.39	1.31
Mp4g23980	1.79	1.13
Mp8g02160	1.17	1.5
Mp3g01570	1.91	1.44
Mp7g16420	1.16	1.05
Mp2g24200	2.1	1.01
Mp8g06300	1.39	1.76
Mp1g20260	2.18	1.33
Mp2g25340	1.92	1.06
Mp1g02980	1.46	1.06
Mp1g07890	-1.11	-1.07
Mp5g19050	2.11	1
Mp4g01840	-1.37	-1.43
Mp6g03670	3.08	1.96

Supplementary table 2
List of primers used in this chapter

Pimer name	Sequence
SJD160 TPLgenomic.FOR	gtagcgattaattaagctTGTGCCATGGAGATCTGCGAC
SJD161 TPLgenomic.REV	GCTGCCGCCGCCaagctcTCTCGGAGCTTGATCAGAATTTTGAATG
SJD162 TPLdownstream.FOR	gtttaaactagtggcgcgCCGACTAGTGGATAGAGAAATTAG
SJD163 TPLdownstream.REV	ctgttatccctaggcgcgACTAATTCGTAGATTGAGCTG
SJD164-TPLup.SEQ.REV	CTACTTTATAGTTCATTGCAACG
SJD165-TPLdown.SEQ.REV	CACGACACAGACAGATAACATC
SJD268 pTPL.FOR	GATTAATTAAGATTTGAACGTCCGAGGTGGTG
SJD269 pTPL.REV	tcttaattaaTGTACGCTGTTCCTATCGC
SJD270 TPL CDS.FOR	GTACAttaattaagctATGTCATCGTTAAGCAGGGAGCTCG
SJD271 TPL CDS.REV	TGCCGCCGCCaagctGTCTCGGAGCTTGATCAGAATTTTGAATGGAGG
SJD276 pTPL internal.FOR	CTCCTCCTCCTCGGTTTCAG
SJD277 TPL.CDS internal.FOR	GAACGCATTCGTTATTGGGTACC
SJD290 TPLCDS.HiFi.FOR	GGAACAGCGTACAttaattaATGTCATCGTTAAGCAGGGA
SJD291 TPLCDS.HiFi.REV	TCACCATGCTGCCGCCGCCTCTCGGAGCTTGATCAGA
SJD330.pTPL.FOR	TtgtaaaacgacggccagtgccaGATTTGAACGTCCGAGGTGGTG

References

1. Benjamins, R. & Scheres, B. Auxin: The Looping Star in Plant Development. *Annu Rev Plant Biol* **59**, 443–465 (2008).
2. Vanneste, S. & Friml, J. Auxin: A Trigger for Change in Plant Development. *Cell* vol. 136 Preprint at https://doi.org/10.1016/j.cell.2009.03.001 (2009).
3. Kepinski, S. & Leyser, O. Plant development: Auxin in loops. *Current Biology* vol. 15 Preprint at https://doi.org/10.1016/j.cub.2005.03.012 (2005).
4. Mashiguchi, K. *et al.* The main auxin biosynthesis pathway in Arabidopsis. *Proc Natl Acad Sci U S A* **108**, (2011).
5. Kepinski, S. & Leyser, O. The Arabidopsis F-box protein TIR1 is an auxin receptor. *Nature* **435**, 446–451 (2005).
6. Dharmasiri, N., Dharmasiri, S. & Estelle, M. The F-box protein TIR1 is an auxin receptor. *Nature* **435**, 441–445 (2005).
7. Gray, W. M., Kepinski, S., Rouse, D., Leyser, O. & Estelle, M. Auxin regulates SCFTIR1-dependent degradation of AUX/IAA proteins. *Nature* **414**, 271–276 (2001).
8. Roosjen, M., Paque, S. & Weijers, D. Auxin Response Factors: Output control in auxin biology. *J Exp Bot* **69**, 179–188 (2018).
9. Weijers, D. & Wagner, D. Transcriptional Responses to the Auxin Hormone. *Annu Rev Plant Biol* **67**, 539–574 (2016).
10. Chandler, J. W. Auxin response factors. *Plant Cell Environ* **39**, 1014–1028 (2016).
11. Guilfoyle, T. J. & Hagen, G. Auxin response factors. *Curr Opin Plant Biol* **10**, 453–460 (2007).
12. Li, S. B., Xie, Z. Z., Hu, C. G. & Zhang, J. Z. A review of auxin response factors (ARFs) in plants. *Front Plant Sci* **7**, 1–7 (2016).
13. Kato, H. *et al.* Design principles of a minimal auxin response system. *Nat Plants* **6**, (2020).
14. Boer, D. R. *et al.* Structural basis for DNA binding specificity by the auxin-dependent ARF transcription factors. *Cell* **156**, 577–589 (2014).
15. Galli, M. *et al.* The DNA binding landscape of the maize AUXIN RESPONSE FACTOR family. *Nat Commun* **9**, (2018).
16. Stigliani, A. *et al.* Capturing Auxin Response Factors Syntax Using DNA Binding Models. *Mol Plant* **12**, 822–832 (2019).
17. Liu, X. *et al.* Auxin controls seed dormancy through stimulation of abscisic acid signaling by inducing ARF-mediated ABI3 activation in Arabidopsis. *Proc Natl Acad Sci U S A* **110**, (2013).
18. Verma, S., Attuluri, V. P. S. & Robert, H. S. An Essential Function for Auxin in Embryo Development. *Cold Spring Harbor perspectives in biology* vol. 13 Preprint at https://doi.org/10.1101/cshperspect.a039966 (2021).
19. Vernoux, T., Besnard, F. & Traas, J. Auxin at the shoot apical meristem. *Cold Spring Harbor perspectives in biology* vol. 2 Preprint at https://doi.org/10.1101/cshperspect.a001487 (2010).
20. Kazan, K. & Manners, J. M. Linking development to defense: auxin in plant-pathogen interactions. *Trends in Plant Science* vol. 14 Preprint at https://doi.org/10.1016/j.tplants.2009.04.005 (2009).

21. Korver, R. A., Koevoets, I. T. & Testerink, C. Out of Shape During Stress: A Key Role for Auxin. *Trends in Plant Science* vol. 23 Preprint at https://doi.org/10.1016/j.tplants.2018.05.011 (2018).
22. Farcot, E., Lavedrine, C. & Vernoux, T. A modular analysis of the auxin signalling network. *PLoS One* **10**, 1–26 (2015).
23. Kato, H., Yasui, Y. & Ishizaki, K. Gemma cup and gemma development in Marchantia polymorpha. *New Phytologist* vol. 228 Preprint at https://doi.org/10.1111/nph.16655 (2020).
24. Eklund, D. M. *et al.* Auxin produced by the indole-3-pyruvic acid pathway regulates development and gemmae dormancy in the liverwort marchantia polymorpha. *Plant Cell* **27**, 1650–1669 (2015).
25. Eklund, D. M. *et al.* Auxin produced by the indole-3-pyruvic acid pathway regulates development and gemmae dormancy in the liverwort marchantia polymorpha. *Plant Cell* **27**, 1650–1669 (2015).
26. Worley, C. K. *et al.* Degradation of Aux/IAA proteins is essential for normal auxin signalling. *Plant Journal* **21**, 553–562 (2000).
27. Nishimura, T. *et al.* Yucasin is a potent inhibitor of YUCCA, a key enzyme in auxin biosynthesis. *Plant Journal* **77**, (2014).
28. He, W. *et al.* A small-molecule screen identifies L-Kynurenine as a competitive inhibitor of TAA1/TAR activity in Ethylene-Directed Auxin Biosynthesis and root growth in Arabidopsis. *Plant Cell* **23**, (2011).
29. Dreher, K. A., Brown, J., Saw, R. E. & Callis, J. The Arabidopsis Aux/IAA protein family has diversified in degradation and auxin responsiveness. *Plant Cell* **18**, 699–714 (2006).
30. Guseman, J. M. *et al.* Auxin-induced degradation dynamics set the pace for lateral root development. *Development (Cambridge)* **142**, (2015).
31. Flores-Sandoval, E., Eklund, D. M. & Bowman, J. L. A Simple Auxin Transcriptional Response System Regulates Multiple Morphogenetic Processes in the Liverwort Marchantia polymorpha. *PLoS Genet* **11**, 1–26 (2015).
32. Das, S., Weijers, D. & Borst, J. W. Auxin Response by the Numbers. *Trends in Plant Science* vol. 26 Preprint at https://doi.org/10.1016/j.tplants.2020.12.017 (2021).
33. Zenser, N., Ellsmore, A., Leasure, C. & Callis, J. Auxin modulates the degradation rate of Aux/IAA proteins. *Proc Natl Acad Sci U S A* **98**, 11795–11800 (2001).
34. Szemenyei, H., Hannon, M. & Long, J. A. TOPLESS mediates auxin-dependent transcriptional repression during Arabidopsis embryogenesis. *Science (1979)* **319**, (2008).
35. Choi, H. S., Seo, M. & Cho, H. T. Two TPL-binding motifs of ARF2 are involved in repression of auxin responses. *Front Plant Sci* **9**, (2018).
36. Szemenyei, H., Hannon, M. & Long, J. A. TOPLESS mediates auxin-dependent transcriptional repression during Arabidopsis embryogenesis. *Science (1979)* **319**, (2008).
37. Honkanen, S. *et al.* The Mechanism Forming the Cell Surface of Tip-Growing Rooting Cells Is Conserved among Land Plants. *Current Biology* **26**, 3238–3244 (2016).
38. Mutte, S. K. *et al.* Origin and evolution of the nuclear auxin response system. *Elife* **7**, 1–25 (2018).

39. Luo, J., Zhou, J. J. & Zhang, J. Z. Aux/IAA gene family in plants: Molecular structure, regulation, and function. *International Journal of Molecular Sciences* vol. 19 Preprint at https://doi.org/10.3390/ijms19010259 (2018).
40. Ulmasov, T., Murfett, J., Hagen, G. & Guilfoyle, T. J. Aux/IAA proteins repress expression of reporter genes containing natural and highly active synthetic auxin response elements. *Plant Cell* **9**, (1997).
41. Plant, A. R., Larrieu, A. & Causier, B. Repressor for hire! The vital roles of TOPLESS-mediated transcriptional repression in plants. *New Phytologist* vol. 231 Preprint at https://doi.org/10.1111/nph.17428 (2021).
42. Hao, S. & Baltimore, D. The stability of mRNA influences the temporal order of the induction of genes encoding inflammatory molecules. *Nat Immunol* **10**, (2009).
43. Bian, H. *et al.* Distinctive expression patterns and roles of the miRNA393/TIR1 homolog module in regulating flag leaf inclination and primary and crown root growth in rice (Oryza sativa). *New Phytologist* **196**, (2012).
44. Yu, H. *et al.* Untethering the TIR1 auxin receptor from the SCF complex increases its stability and inhibits auxin response. *Nat Plants* **1**, (2015).
45. Ruyter-Spira, C. *et al.* Physiological effects of the synthetic strigolactone analog GR24 on root system architecture in arabidopsis: Another belowground role for strigolactones? *Plant Physiol* **155**, (2011).

Chapter 7

General Discussion

Auxin is almost synonymous with plant development[1,2]. The fact that auxin is directly or indirectly wired in every branch of plant life, makes auxin both fascinating and enigmatic subject at the same time. Qualitative analysis of the nuclear auxin signaling pathway (NAP) in angiosperms have revealed a remarkable complexity of genetic and biochemical interactions[3,4]. Disentangling this complex wiring and understanding NAP at its core is a formidable challenge. Fortunately, recent research advances in early diverging land plant species with simpler, ancestral NAP has helped unfolding these core principles[5,6]. *Marchantia polymorpha* is one such exciting bryophyte model species[7]. While the common ancestral position of Marchantia in land plant phylogeny has fascinated evolutionary biologists, the simpler genetic architecture of the NAP has drawn attention of plant developmental biologists. The reduced network of biomolecular interactions in Marchantia NAP is not only helpful to unearth the evolutionary origin of known interactions but also offers an opportunity to study the basic design of NAP in a quantitative manner[8,9]. Therefore, in chapter 2, we presented *Marchantia polymorpha* as a suitable system to explore to quantitative aspects of NAP that can complement the available qualitative knowledge. We highlighted the quantitative parameters that are key to building a quantitative network of NAP. Determination of these parameters would provide explanation of many complex NAP outputs that are beyond the scope of qualitative data. We envision that availability of all quantitative parameter and their integration would generate a model to predict NAP output based on signal input and dynamics.

Native accumulation dynamics of NAP components

To set the foundation steps in this quantitative quest of the NAP, we generated a complete set of fluorescent knock-in lines of all core NAP proteins in Marchantia (chapter 3). These genomic knock-ins report the endogenous protein accumulation patterns, and therefore is a unique resource for analysis of native protein concentrations, dynamics, interactions, stability, complex stoichiometry, diffusion rates and so on. Among the many opportunities these lines offered, we first choose to quantitatively visualize the accumulation patterns of native proteins and follow their dynamics during gemma germination. At dormant stage when auxin concentrations are higher in gemmae (chapter 6), MpTIR1 proteasomally degrades MpAux/IAA and continuously send out an high auxin signal that is probably too high for growth. Despite the complete removal of Aux/IAA repressor, gemmae remain dormant, suggesting that other downstream elements are not permissive to growth. Upon germination, the auxin concentration decreases (chapter 6), and consequently

MpAux/IAA gains partial stabilization despite simultaneous increase in MpTIR1 protein levels. Therefore, gemmae growth coincides with two major shifts in the NAP, (1) high, inhibitory auxin levels change to lower optimal levels and (2) TIR1-Aux/IAA input module switches from a completely permissive to a more tuneable repressive status. High auxin induced dormancy was reported earlier in Arabidopsis seeds. Overexpression of auxin biosynthetic gene *iaaM* completely stops seed germination whereas loss of function mutation in *yuc1yuc6* auxin biosynthesis genes enhance germination[10]. In Marchantia, chemical inhibition of auxin biosynthesis causes germination of gemmae inside gemma cups[11]. Besides auxin, ABA (Abscisic acid) is another plant hormone involved in tissue dormancy in both angiosperm[10] and bryophytes[12]. ABA has been found to play role in seed[13] and bud[14] dormancy in angiosperms and gemmae dormancy in Marchantia[12]. The Arabidopsis ABA mediated dormancy pathway is coordinated by ARF mediated auxin function[10]. Given that both the hormones are involved in tissue dormancy across species, it is possible that high auxin and high ABA signaling dependent growth inhibition is a common mechanism across diverse tissue and generations in land plants.

Receptor dynamics in Marchantia

The opposite dynamics of auxin and MpTIR1 receptor is an interesting phenomena in young gemmalings. While the auxin level decline could be due to interruption of auxin supply form the gemma cup, the increase in MpTIR1 accumulation cannot be simply explained by transcription which is rather downregulated after germination. Since miRNA mediated gene silencing is present in bryophytes[15] and miRNA393 is known to post-transcriptionally regulate AtTIR1/AFBs[16], it is possible that MpTIR1 is regulated by small RNAs. However, in Marchantia miRNA conservation is very limited with only 7 homologs identified from other lands plant species making it unlikely that miRNA393 controls MpTIR1. Given that there are uncharacterized Marchantia specific novel miRNAs present, we cannot be certain that MpTIR1 is not controlled by another miRNA. Apart from miRNA regulation, AtTIR1 levels are post translationally regulated by its auto-degradation, in absence of Aux/IAA[17]. It is more likely that complete lack of MpAux/IAA in dormant gemmae, triggers MpTIR1 auto-degradation. This can be tested easily by treating MpTIR1-mScarlet knock-in dormant gemmae with proteasomal inhibitor.

The TIR1-Aux/IAA auxin perception complex relays the signal to MpARF1 which regulates auxin dependent transcription[18]. MpARF2 antagonizes MpARF1 function by competing for same DNA binding motif[6]. We found that both MpARFs are expressed at dormant stage (chapter 3) and are probably required in early gemma development. Earlier characterization of MpARF1 function showed that gemmae fail to maintain dormancy and start germinating inside gemma cups in *Mparf1* knock-out mutant[18]. High accumulation of MpARF1 in dormant gemmae and premature germination phenotype of *Mparf1* mutant, indicates a possible function of MpARF1 in dormancy maintenance. On the contrary, our data showed that accumulation of a stable MpARF2 leads to gemmae germination inside cups, suggesting ARF2 as a negative regulator of dormancy. Based on these data, it is possible that gemma dormancy is promoted by auxin and MpARF1 but antagonised by MpARF2. In Arabidopsis, both class-A and B ARFs are known to regulate seed dormancy. AtARF10 and AtARF16 binds to the promoter of ABA dependent transcription factor gene *ABI3* and promotes its expression to maintain dormancy[10]. Since both class-A and B MpARFs have their highest expression in dormant stage, an induction of ABA dependent gemma dormancy by ARFs, could override the upstream permissive signal from TIR1-Aux/IAA.

MpARF stoichiometry is a key factor for gemma germination

If high ARF levels are indeed required for dormancy, germination would not be possible without a negative regulation of ARF levels. While investigating the dynamics of ARFs in germination gemmae we found a support for this hypothesis and noticed a significant decline in ARF concentrations (chapter 4). As the transcript levels were static and reports of a few AtARF proteasomal regulation were known, we tested and found a proteasomal regulation of MpARF1 and 2. This proteasomal degradation of ARFs probably releases transcriptional inhibition and allow germination. In chapter 5, by a systematic dissection of MpARF2 domains, we identified a degron region in dimerization domain (DD2) of DNA binding domain (DBD). Furthermore, we showed that this degron is accessible only in ARF2 monomers, since dimers occlude the degron located in DBD interface. ARFs are well known to bind DNA mostly as dimers[19], which provide specificity in their function. We propose this mutual exclusion of MpARF2 dimerization and degradation as an additional mechanism to ensure specific DNA binding. Degradation of ARF2 monomers prevent non-specific ARF-DNA interactions and mis-regulation of genes. Loss of DNA binding specificity has severe growth defects manifested in the stable MpARF2 monomer mutant lines (chapter 5). Since ARF-DBDs

are highly conserved domains, it is quite possible that MpARF1 or ARFs in other species may have retained this ancestral degron.

Apart from enhanced DNA binding specificity for MpARF2 dimers, proteasomal degradation impacts the relative stoichiometry of MpARF1 and MpARF2, a key parameter in regulation of auxin dependent transcription. In dormant stage, class-A and B ARFs maintain a lower relative ratio which increases sharply after germination (chapter 4). This parameter is relevant for genes that are co-regulated by both ARF classes. A lower ARF1/2 ratio may prevent auxin dependent growth even though Aux/IAA levels are permissive in dormant gemmae. On the contrary, in germinated stage, higher ARF1/2 ratio permits growth whereas TIR1-Aux/IAA control turns more rigorous and allows growth based on auxin input only. The importance of relative ARF-A/B stoichiometry was also realized in earlier studies in Marchantia. Overexpression of either MpARF altered auxin sensitivity and growth whereas near stoichiometric expression of both ARFs restored normal auxin response[6]. We validated these results initially by computational simulations of blocked ARF2 degradation and tested its impact on a hypothetical gene co-regulated by both MpARF1 and 2. Later on we decreased ARF1/2 ratio *in vivo*, by inducible and constitutive expression of ARF2. Both computational and *in vivo* manipulations of ARF ratio negatively influenced auxin response and highlighted the importance of native ARF1/2 ratio.

The major source of auxin in dormant gemmae is the gemma cup[20]. This "external" supply of high auxin is distributed throughout the tissue which prevents formation of any auxin gradient. The even distribution of auxin is confirmed by the complete degradation of Aux/IAA throughout dormant gemmae. Post germination development is dependent on local auxin synthesis and therefore suitable for differentiation by auxin gradient formation. Depending on the levels of auxin in different cell types, TIR1-Aux/IAA can control the response amplitude. Although these speculations are strongly based on the observations in Arabidopsis auxin reporters, development of a transcriptional reporter for Marchantia would help to definitively confirm this. Although dormant gemmae does not grow, it does show signs of auxin dependent differentiation such as formation of rhizoid initial cells or maintenance of apical meristem. Since the auxin levels and TIR1-Aux/IAA permissive signals are mostly uniform throughout dormant gemmae, these basic differentiation must be controlled by other NAP components. A conceivable candidate for such regulation would be ARFs which express highly at this stage.

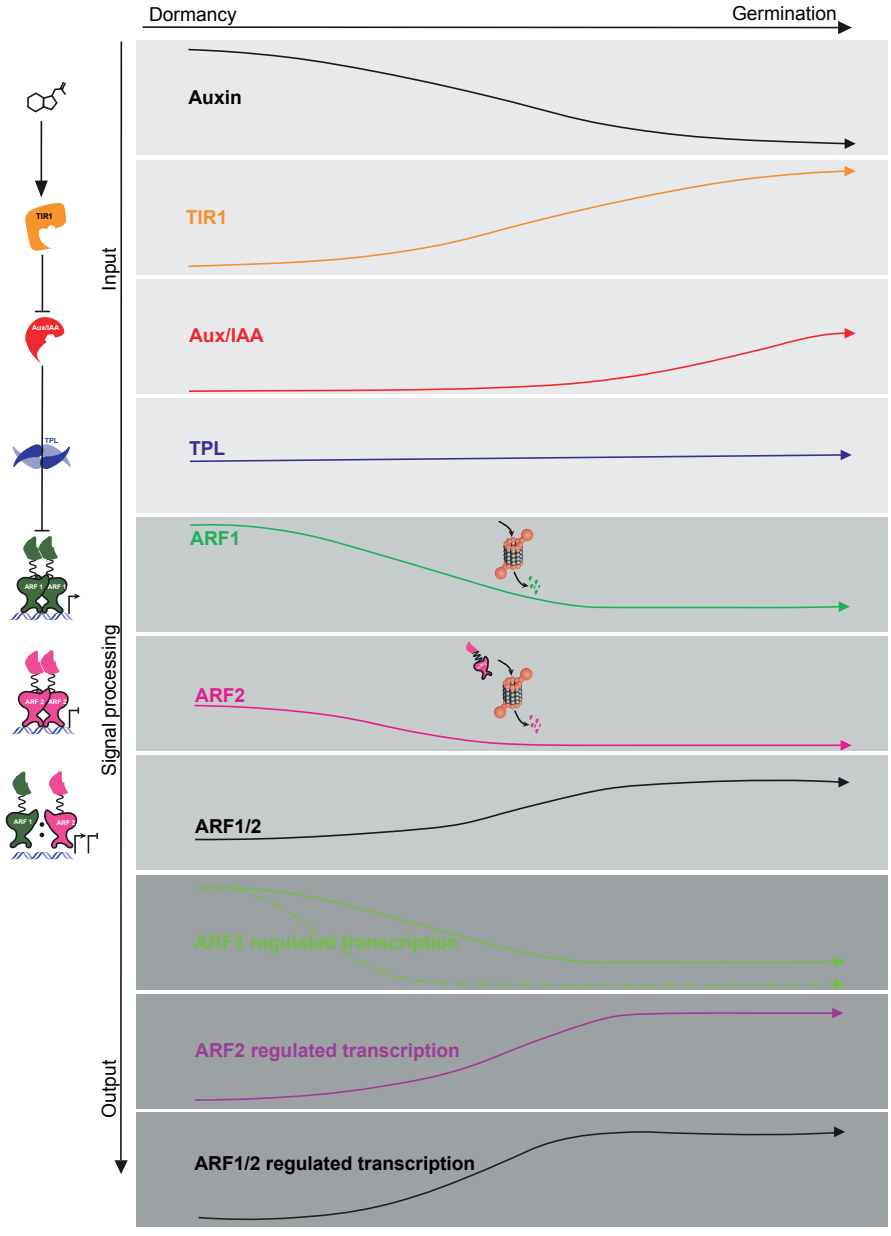

Figure 1: A schematic overview of nuclear auxin signaling pathway dynamics during gemmae germination. In the input module, TIR1-Aux/IAA receptor complex becomes more sensitive with a gradual decline in auxin levels. The signal processing unit undergoes major reorganization as both ARF1 and ARF2 are proteasomally degraded. This impacts ARF1/2 ratio in favour of ARF1 mediated gene activation. A wide range of transcriptional output is returned in response to the signal and dynamics.

Furthermore, class A and B ARFs accumulate in a pattern that creates differential relative ARF1/2 ratio in the three major cell types of gemmae (chapter 3). In future studies it would be interesting to investigate if these unique combinations of ARFs and probably an auxin gradient across gemmae could act as an instructive signal in cell differentiation in gemmae. A transcriptional auxin reporter suitable for Marchantia would again be crucial here to test whether these differential ARF1/2 ratio overlaps with distinct auxin responses.

Remodelling of auxin-dependent transcription during gemma germination

The final outcome of biologically meaningful NAP interactions and dynamics is expressed at the level of transcription[21]. We found transcriptional dynamics of majority of auxin regulated Marchantia genes suggesting an increased auxin response output after germination (chapter 6). Genes which follow a progressive pattern of up or down regulation are probably uniquely controlled by either ARF2 or ARF1 levels respectively (Figure 1). As ARF2 levels decline, ARF2 mediated repression would be released. Likewise, decreased ARF1 levels would dampen the level of uniquely ARF1 activated genes. This downregulation due to dampened ARF1 levels could be further reinforced by relatively more restrictive TIR1-Aux/IAA input signal. Among the auxin upregulated genes, a significant set displays a bell shaped expression profile with a peak expression at 3.5 hours. This is beyond a simple regulation by absolute levels of either ARFs, as degradation of ARFs cause a progressive decline in their concentrations. The heightened peak of transcription at 3.5 hours, rather coincides with a rise in relative ARF1/2 levels. Thus, this could be the set of genes commonly regulated by MpARF1 and MpARF2. A low ARF1/2 ratio at dormant stage keeps their expression basal, while an increased ratio post-germination induces transcription by MpARF1. If these genes are indeed co-regulated by both MpARFs and if monomer specific ARF2 degradation permits DNA binding competition only on inverted repeat (IR) elements, the promoter regions of the genes with peak expression at 3.5 hours could be enriched in IR type auxin responsive elements (AuxRE). Among the genes upregulated after germination, the auxin biosynthesis gene *MpYUCCA2* was identified[22]. Auxin concentration driven transcriptional feedback on *YUCCA* genes are well known in Arabidopsis[23]. Since auxin concentration in gemmae decreases during germination, it induces *MpYUC2* to initiate local auxin biosynthesis. Whether *MpYUC2* induction is executed either by higher MpARF1/2 ratio or by a release of repression from MpARF2, requires further investigation.

It is important to bear in mind that the above-mentioned possible outcomes of individual ARF mediated transcription levels are built on the concept that class-A ARFs are transcriptional activators and class-B ARFs are repressors. However, this categorization may not be universal and deviation from this categorical function is possible. For instance, AtARF5 (MONOPTEROS), a well characterized activator of many auxin dependent genes, has been shown to act as a negative regulator of cytokinin signaling by repressing transcription of A-type *ARR* (*ARABIDOPSIS RESPONSE REGULATOR*) transcription factor genes in in shoot apical meristem[24]. In Marchantia, MpARF1 is considered an activator and MpARF2 as a repressor. At high auxin concentrations, growth is inhibited in both wild-type and MpARF1 overexpressing (enhanced inhibition) plants, whereas MpARF2 overexpression lines grow uninhibited. Similarly, nondegradable ARF2 mutant also grows normally in high auxin treatment. It can be argued that MpARF2 acts as a repressor in lower, physiologically optimal auxin concentrations, whereas in repressive, high auxin environment ARF2 promotes growth. While a concrete evidence for this argument is yet to be provided, these observations indicate that ARF functions could be context dependent and might not be assigned to a certain category.

Although we were able to study NAP protein concentrations, dynamics and stoichiometry at sub-cellular resolution, a major limitation of this study is that the auxin inputs and response outputs were measured in a global manner. We quantified auxin concentrations and transcriptome from whole gemmae, and thus lack any spatial cues such as auxin gradients and differential auxin outputs. Implementation of direct auxin sensors and development of transcriptional reporters may be first steps in eliminating these limitations. With the rapid advancements in single cell sequencing, it is probably not far in future that we would be able to analyse transcriptomes of different cell types of gemmae and compare it with differential auxin and ARF1/2 stoichiometries.

Proteasomal degradation controls MpARF accumulation

An important finding in this thesis is the selective proteasomal degradation of MpARF2 monomers. Proteasomal degradation is a major pathway for targeted removal proteins in eukaryotes[25]. Specificity of proteasomal degradation is determined by an interaction between E3 ligase and a degron motif in the target protein[26]. Since we have identified the MpARF2 degron motif, an important follow up would be to use this motif as a bait to identify the E3 ligase interactor. The only known E3 ligase for ARF (AtARF1 and 19) degradation

is the recently identified AFF1(AUXIN RESPONSE FACTOR F-BOX1), an F-box domain containing protein in Arabidopsis[27]. However, AFF1 seems to be an Arabidopsis specific protein, as homologs in Marchantia are absent. If multiple functionally diverse *At*ARF members are proteasomally regulated, it is possible that they co-evolved separate E3 ligases evolved from a monophyletic origin. Finding the E3 ligase degrading MpARFs would then reveal the common ancestor of ARF degrading E3 ligases. However, another possibility is that there is no single common ancestor ARF degrading E3 ligase, rather a convergent evolution of ARFs gave rise to multiple different E3 ligases interactors for different ARFs in angiosperms. Lack of any Marchantia homolog of ARF19 targeting AFF1 E3 ligase indicates more towards the second hypothesis. The most dramatic increase in MpARF degradation is observed in the early hours after gemmae dormancy release. An interesting coincidence is that in the same time frame, we found the MpTIR1 concentration to increase. This strong temporal correlation in the pattern of MpARF degradation and rise in the level of MpTIR1 F-box protein, prompts a question if these two phenomena are interlinked. One possibility is that MpARF stability is directly regulated by MpTIR1. In line with this hypothesis, the *Mptir1* knock-out mutant[28] and plants carrying non-degradable ARF2 monomer (ARF2$^{G286I+Degron\ swapped}$) are phenocopies of each other. Both the mutants fail to develop thalli and grow slowly as callus like undifferentiated tissue. In addition, both mutants are strongly insensitive to auxin and incapable of rhizoid formation, an auxin dependent developmental process. It will be interesting to see if the non-degradable ARF2 monomer mutant cell mass also has a larger vacuolated cell in the inner region and smaller cells at the periphery, like the *Mptir1* knock-out mutant. Analysing MpARF degradation profile in *Mptir1* knock-out mutant would help to answer if TIR1 really has any influence on ARF stability.

Taking advantage of a natural developmental transition in gemmae, we captured the entire NAP in motion. Despite the simplicity of Marchantia NAP, we found a wide diversity of auxin response outputs which requires a holistic analysis to explain most of them. Still a fraction of outputs do not comply with the observed NAP dynamics and to justify them we probably need to consider other auxin mediated transcriptional pathways. The recently discovered MARK/RAF (MAP AUXIN RESPONSIVE KINASE/RAF) kinase mediated rapid phosphorylation driven pathway has been shown to influence a set of transcriptome that is uncommon to the known transcriptome of NAP[29] . Apart from diverse response outputs, the fact that MpARF levels are not controlled

by auxin or other tested plant hormones, indicates that MpARF degradation is triggered by a conformational switch form dimer to monomers. Now what exactly triggers ARF2 monomerization is a new question to address. Given that the NAP network interacts with almost every other plant signaling pathway, it is possible that MpARF2 dimers are stabilized by other scaffolding partners. Release of MpARF2 from a larger protein complex might trigger dimer disruption. Another problem that ARF2 monomer instability brings in is how MpARF2 monomers are kept stable after translation, until they are in a dimer? A solution to this problem can be a co-translational complex formation[30,31] or protection by molecular chaperons. These perplexing open questions are reminders of the sheer complexity of auxin response systems and tells that our understanding of NAP is still far from saturation.

References

1. Vanneste, S. & Friml, J. Auxin: A Trigger for Change in Plant Development. *Cell* vol. 136 Preprint at https://doi.org/10.1016/j.cell.2009.03.001 (2009).
2. Kepinski, S. & Leyser, O. Plant development: Auxin in loops. *Current Biology* vol. 15 Preprint at https://doi.org/10.1016/j.cub.2005.03.012 (2005).
3. Leyser, O. Molecular genetics of auxin signaling. *Annual Review of Plant Biology* vol. 53 Preprint at https://doi.org/10.1146/annurev.arplant.53.100301.135227 (2002).
4. Leyser, O. Auxin signaling. *Plant Physiol* **176**, 465–479 (2018).
5. Lavy, M. *et al.* Constitutive auxin response in Physcomitrella reveals complex interactions between Aux/IAA and ARF proteins. *Elife* **5**, (2016).
6. Kato, H. *et al.* Design principles of a minimal auxin response system. *Nat Plants* **6**, (2020).
7. Shimamura, M. Marchantia polymorpha: Taxonomy, phylogeny and morphology of a model system. *Plant Cell Physiol* **57**, 230–256 (2016).
8. Bowman, J. L., Araki, T. & Kohchi, T. Marchantia: Past, present and future. *Plant Cell Physiol* **57**, 205–209 (2016).
9. Das, S., Weijers, D. & Borst, J. W. Auxin Response by the Numbers. *Trends in Plant Science* vol. 26 Preprint at https://doi.org/10.1016/j.tplants.2020.12.017 (2021).
10. Liu, X. *et al.* Auxin controls seed dormancy through stimulation of abscisic acid signaling by inducing ARF-mediated ABI3 activation in Arabidopsis. *Proc Natl Acad Sci U S A* **110**, (2013).
11. Eklund, D. M. *et al.* Auxin produced by the indole-3-pyruvic acid pathway regulates development and gemmae dormancy in the liverwort marchantia polymorpha. *Plant Cell* **27**, 1650–1669 (2015).
12. Eklund, D. M. *et al.* An Evolutionarily Conserved Abscisic Acid Signaling Pathway Regulates Dormancy in the Liverwort Marchantia polymorpha. *Current Biology* **28**, 3691-3699.e3 (2018).
13. Rodríguez-Gacio, M. del C., Matilla-Vázquez, M. A. & Matilla, A. J. Seed dormancy and ABA signaling: the breakthrough goes on. *Plant Signal Behav* **4**, (2009).
14. Zheng, C. *et al.* Abscisic acid (ABA) regulates grape bud dormancy, and dormancy

release stimuli may act through modification of ABA metabolism. *J Exp Bot* **66**, (2015).
15. Lin, S. S. & Bowman, J. L. MicroRNAs in Marchantia polymorpha. *New Phytologist* **220**, 409–416 (2018).
16. Bian, H. *et al.* Distinctive expression patterns and roles of the miRNA393/TIR1 homolog module in regulating flag leaf inclination and primary and crown root growth in rice (Oryza sativa). *New Phytologist* **196**, (2012).
17. Yu, H. *et al.* Untethering the TIR1 auxin receptor from the SCF complex increases its stability and inhibits auxin response. *Nat Plants* **1**, (2015).
18. Kato, H. *et al.* The roles of the sole activator-type auxin response factor in pattern formation of marchantia polymorpha. *Plant Cell Physiol* **58**, 1642–1651 (2017).
19. Boer, D. R. *et al.* Structural basis for DNA binding specificity by the auxin-dependent ARF transcription factors. *Cell* **156**, 577–589 (2014).
20. Kato, H., Yasui, Y. & Ishizaki, K. Gemma cup and gemma development in Marchantia polymorpha. *New Phytologist* vol. 228 Preprint at https://doi.org/10.1111/nph.16655 (2020).
21. Weijers, D. & Wagner, D. Transcriptional Responses to the Auxin Hormone. *Annu Rev Plant Biol* **67**, 539–574 (2016).
22. Kato, H. *et al.* Auxin-Mediated Transcriptional System with a Minimal Set of Components Is Critical for Morphogenesis through the Life Cycle in Marchantia polymorpha. *PLoS Genet* **11**, (2015).
23. Suzuki, M. *et al.* Transcriptional feedback regulation of YUCCA genes in response to auxin levels in Arabidopsis. *Plant Cell Rep* **34**, (2015).
24. Zhao, Z. *et al.* Hormonal control of the shoot stem-cell niche. *Nature* **465**, (2010).
25. Hellmann, H. & Estelle, M. Plant development: Regulation by protein degradation. *Science* vol. 297 Preprint at https://doi.org/10.1126/science.1072831 (2002).
26. Kleiger, G. & Mayor, T. Perilous journey: A tour of the ubiquitin-proteasome system. *Trends in Cell Biology* vol. 24 Preprint at https://doi.org/10.1016/j.tcb.2013.12.003 (2014).
27. Jing, H. *et al.* Regulation of AUXIN RESPONSE FACTOR condensation and nucleo-cytoplasmic partitioning. *Nat Commun* **13**, 4015 (2022).
28. Suzuki, H., Kato, H., Iwano, M., Nishihama, R. & Kohchi, T. Auxin signaling is essential for organogenesis but not for cell survival in the liverwort Marchantia polymorpha. *Plant Cell* koac367 (2022) doi:10.1093/plcell/koac367.
29. Kuhn, A. *et al.* A RAF-like kinase mediates a deeply conserved, ultra-rapid auxin response. *bioRxiv* 2022.11.25.517951 (2022) doi:10.1101/2022.11.25.517951.
30. Shiber, A. *et al.* Cotranslational assembly of protein complexes in eukaryotes revealed by ribosome profiling. *Nature* **561**, (2018).
31. Schwarz, A. & Beck, M. The Benefits of Cotranslational Assembly: A Structural Perspective. *Trends in Cell Biology* vol. 29 Preprint at https://doi.org/10.1016/j.tcb.2019.07.006 (2019).

Summary
Auxin is a central regulator of plant growth and development. Most of the long-term growth responses to auxin are driven by the nuclear auxin signaling pathway (NAP) ultimately regulating gene transcription. Extensive research in flowering species such as *Arabidopsis thaliana* have helped us to understand the basic functions the NAP proteins and the network they generate. However, much of our understanding is qualitative in nature and based on experiments performed either *in vitro*, heterologous systems or *in vivo*, at non-native protein concentrations. While these approaches provided a general overview of how NAP proteins function and their possible biomolecular interactions, it is important to note that these protein functions and interactions are meaningful only if they occur at their natural concentration *in vivo*. This PhD thesis describes the use of fluorescent knock-in lines to gain a quantitative view of how the NAP operates at the endogenous concentration of each signaling component. Such approach will not only validate and complement the qualitative knowledge but will also provide quantitative insights into NAP. For a quantitative analysis, it is suitable if the functional complexities are at minimum, especially for a system like NAP which is involved in diverse developmental processes. The bryophyte species *Marchantia polymorpha* has the simplest but complete NAP system in terms of the number of components, and molecular genetic tools for Marchantia are recently established. Therefore, in **chapter 1** we advocated Marchantia as an appropriate model for quantitative analysis of NAP. An emphasis has been placed on the use of gemmae as it offers multiple benefits, especially in a fluorescence imaging-based quantitative analysis. This introductory chapter sets the background, presents the state of the art of NAP and some open questions, followed by the scope of this thesis.

In **chapter 2**, we prescribed the recipe of a quantitative model by highlighting the key parameters that are essential for a complete quantitative view of NAP. Why and how these parameters can be determined is also discussed in detail. We propose that on determination and integration of these parameters it is possible to have a quantitative understanding of NAP and predict auxin response outputs more accurately.

By following the roadmap provided in chapter 2, we developed a full set of fluorescent genomic knock-in lines for core NAP proteins in Marchantia. The generated lines described in **chapter 3** form an important resource for the rest of this thesis and beyond. With the use of fluorescence confocal live

cell imaging on knock-in lines, a complete view of NAP protein expression domains in dormant gemmae was obtained. Each NAP component showed nuclear expression but distinct patterns of accumulation throughout gemmae. In dormant gemmae, the MpTIR1 auxin receptor is broadly expressed, whereas its substrate MpAux/IAA repressor was not detected at all. Among the three MpARFs, MpARF1 and MpARF3 accumulate throughout dormant gemma, with MpARF1 showing a relatively higher accumulation. MpARF2 showed a relatively lower accumulation among all ARFs and was completely absent in the rhizoid initial cells. Furthermore, we analysed colocalization of the MpARF1 (class-A) and MpARF2 (class-B) in double knock-in lines and identified distinct zones of cells in gemmae with different ARF-A/B stoichiometries.

Next, we investigated in the dynamics of NAP proteins in actively growing gemmae. In **chapter 4**, we first focussed on the MpARFs and followed their natural dynamics during transition from dormancy to germination. Time-lapse confocal image quantification showed a gradual decline in the level of class-A and -B ARFs, whereas the class-C ARF expression remained constant. Further investigation confirmed an active proteasomal regulation on MpARF1 and MpARF2, but not on MpARF3. To understand the necessity of MpARF2 degradation, we blocked MpARF2 degradation in a computational model that simulates auxin and ARF dependent transcription in Marchantia. The simulations indicated a transcriptional repression in absence of MpARF2 degradation. An *in vivo* overexpression of MpARF2 also suggested that higher level of ARF2 prevents optimal auxin response and plant growth. Thus, taking advantage of the inactive to active growth transition of gemmae, we captured a natural dynamic in the MpARF levels, actively regulated by proteasome and highlighted its importance in growth.

Little is known about ARF degradation in any plant species, and therefore we further investigated MpARF2 degradation. **Chapter 5** reports on a systematic dissection of MpARF2 protein to identify the degradation signal in the protein sequence. By *in vivo* deletion analysis of MpARF2 domains, we identified a small degron region in the dimerization domain 2 of the DNA-binding domain. Further mapping of this degron onto the structure of MpARF2 dimer revealed that the degron is positioned at the dimerization interface of the DBD and hence presumably inaccessible in the dimeric form of the protein. To test this hypothesis, we generated a series of ARF2 dimerization mutants and found an enhanced degradation of the monomer in all stages of gemma

growth. This confirmed a mutual exclusivity of MpARF2 dimerization and degradation. To understand the biological significance of a system that would selectively degrade ARF monomers, we tested the effect of stabilizing a monomeric MpARF2 *in vivo*. This resulted in a strong negative effect on auxin sensitivity and plant growth, suggesting that monomeric MpARF2 strongly interferes with development. We propose that the strong growth retardation could be due to the low intrinsic DNA binding specificity of monomeric MpARF2 proteins, which mis-regulates transcription of a large number of genes.

To complete our survey of NAP dynamics, in **chapter 6**, we quantified free auxin levels in germination gemmae and found a gradual decline in auxin concentration. In the same time frame, we monitored the expression patterns of MpTIR1 auxin receptor and MpAux/IAA repressor in the knock-ins. While MpTIR1 levels increased with the decreasing auxin levels, Aux/IAA gained slightly increased stability, probably due to the concomitant decline in auxin concentration. We validated auxin-dependency of Aux/IAA degradation and quantified its half-life, an important parameter for quantitative view of NAP. To investigate the outcome of all signaling dynamics observed during germination, we compared the transcriptomes of different stages of germinating gemmae and found a clear pattern of increased auxin response. We conclude that as gemmae transit from dormancy to active growth, internal auxin levels drop while auxin sensitivity and transcriptional response increases due to stronger regulation by TIR1-Aux/IAA and a permissive signal by ARF1/2 relative quantities.

Finally in **chapter 7**, we discuss the key results of this thesis in a broader perspective. Besides integrating the main conclusions, we point out the limitations of the work described in this thesis and recommend future directions in auxin research.

Acknowledgements

On the list of things that positively impacted my life the most, the opportunity to work on this thesis is all the way up there. In early 2018, I was trying my best to find a Ph.D. position that suits my interests and offers me to work in an established lab. After many applications, failures, and reapplications, I managed to receive some opportunities. During the interview week of the Ph.D. programme in Max Plank Institute in Potsdam, Germany I met a fellow candidate Federico who told me about a project available on auxin signaling in Laboratory of Biochemistry at Wageningen University. In fact, he had an offer to join this position, but the project was not overlapping with his interests. Months after coming back to India, I received an offer to join the Max Plank Ph.D. programme but on a project that did not trigger my interests and I had only 2 weeks to respond. In the same programme, Federico also received a project offer that matched his interest. A little desperate to find an interesting project, I asked Federico for the details of the auxin project that he would be declining to join this new offer. He was happy to give me the details and luckily the project for the most part (except the mathematical modelling!) was in line with my interest to work on plant development. I emailed Dolf immediately, inquiring about this position. After submission of a formal application and explaining my urgency to make a quick decision, Dolf and Jan Willem were very understanding. Within two weeks, they finished a few interviews including mine and came back with a decision that was in my favour. It was a great moment relief for me. I wholeheartedly thank Jan Willem and Dolf for this and thank my parents, friends, family who knew my struggles in those days and were supportive. I also thank Federico for not accepting this Ph.D. position!

On my first day in Wageningen, Jan Willem came to Ede-Wageningen train station to pick me up! From that day onwards I knew, I will have a supervisor who is exceptionally caring. Throughout my time in Biochemistry, I received a warm and personal guidance from Jan Willem. We developed a friendly and open relationship where we could share anything professional or personal. I think I was lucky enough to have you as my daily supervisor and I will miss it for sure. Your caring nature worked as the perfect cushion while I was struggling to handle the cultural shocks in a new environment. Thank you for making me feel at home. Other than the lab life, we have many memories of getting together either at your home or in your nice boat. Again, I feel lucky to have supervisor who sails with his students! It was the stories of your kind gestures that took away the worries of my parents who were initially cautious

to let me go in an unknown part of the world alone. More than just the scientific guidance in daily lab work, I thank you the most for being a fantastic personal mentor. I am sure we will stay in good contact, and I wish you and Tanja a healthy life ahead.

I believe that inspiration is an important part of supervision and if that inspiration comes from your supervisor, then it becomes easier to keep going. In Dolf, I found that inspiration that kept fuelling my initial motivation that I came with. Dolf, you are a great scientist who is extremely understanding, accommodating and openminded. I admire your patience and tolerance that makes you a great leader. You are a Professor who manages like an MBA. There is a lot to learn from how you manage a team of diverse people. Thank you for believing in me and providing the opportunity to grow in my career. I will miss your scientific advices that always helped me direct my goals and prepare me for the future. It was a pleasure to work with you and I will cherish these years of my career.

During my thesis, I had the opportunity to guide many students. I have learnt a lot from you all and it was an experience that I enjoyed for the most part. Iris, you were an amazing student who is independent, accurate and skillful. I could always trust you with the experiments. Thank you for taking care of my experiments when I was away. My wishes are for your good career ahead. I am thankful to Martijn, who initially joined my project as a master's student and continued as a Ph.D. student in the group. It was all my pleasure to have you in the team. We performed so many imaging experiments together and our collaboration was really a good experience for me. Thank you for everything that you brought into this project. The last stretch would not have been the same if you were not there to help me out. Martijn, you are a great learner, and I am sure you will flourish in your career ahead.

My paranymphs Ping and Sumanth, you both were a continuous support during the last 4.5 years. Ping you are a friendly, kind, and caring mate who joined the lab just about the same time with me. I thank you for all your quick checks on me, if everything was alright in lab and in life. I will miss our chats on "what really matters in life?". Wish you good luck with the last stretch of your Ph.D. Sumanth, you were always there to help me. Be it my doubts in the lab or any practical matters in daily life, I always had you like a big brother. I am already missing all the evening meets, stayovers, and trips that we had together with you, Spoorthi and Gowtham. You guys have become like

a family specially in the last two years. We will certainly keep in touch and please visit us whenever you are in Kolkata in future. Best wishes for you and your entire family and good luck with the new professional challenge.

Like most Ph.D. students, I did have my share of imposter syndrome in the initial years, but some people in the lab helped me recover. Prasad, you were a great place for me to share my problems and get mental support despite all the personal and scientific doubts I was having. Thank you for being there. I am grateful to Hiro and Cathy who gave me the training in the initial days and taught me how to work with Marchantia. I would also like to thank Willy for all the technical support. Thank you, Willy, for making the competent cells which I used for all of my clones. Thank you, Simon, for the lab organization and Mark for help with my TurboID trials. I sincerely thank Laura who made life easy with her quick and easy solutions for every paperwork I had do. You are amazing at your job!

I thank all other members of the Biochemistry department for creating a great atmosphere to work. Thank you Juriaan for all the time-to-time updates on Marchantia and help with ARFs modelling (also for the one on the cover of this thesis), Polet and Mariska for being for being amazing bench mates in the lab. Ramakanth and Jorge for helping to get started with the proposal writing. Joao, Cecelia, Sjoerd, Andry, Vera, Andre, Feras, Evegeniya thank you for being great colleagues to work with. Thank you, Mellissa, for helping me in last few experiments while I am away. Daan, Elwira, Pilar, Viren, Bel, Sergio, Liao, Bas, Patrick, Jente, it was great to have you all as colleagues.

I am lucky to have my family and friends without whom I would not be here. I know how proud you all are to see me cross this finishing line. I thank my Maa for this life. You have been the one constant source of love and support throughout my life. Baba, I know how proud you would have been today if you were here. I will regret the rest of my life that I could not be with you in the last moments of your life. I miss you.

Dada, Boudi, it is only because of you all that I could come abroad without worrying a lot about home. Thank you for taking care of Maa and Baba while I was away. Didi, Jamaibabu, you both have always supported me in my career choices. It was you who helped me financially on my first journey to the Netherlands. Thank you for being such a great support. Surjo, Arjo, and Tojo love you all. I hope each one of you will shine in life in your own unique way.

I am grateful to my wife Mili, for continuously supporting me from the early days of my career. Thank you for believing in me and making my life more meaningful. I would also like to thank my extended family; my parents-in-laws, brother, and sister-in-law. Thank you for making me feel home and offering all the great food whenever I visit you!

My school buddies Soumya and Munna, you both were always there whenever I needed some break from the regular routine of life. I am sure our 14 years of friendship will go on forever. I also thank my college mates Debojyoti, Arindam and Saumashish for the beautiful memories of my hostel life. Thank you guys for being who you are and best wishes for your personal lives in the coming years.

Curriculum Vitae

Shubhajit Das was born on the 15th of November 1993 in Kumirpara, Purba Bardhaman, West Bengal, India. He completed his secondary (2009) and higher secondary (2011) education from Parulia K.K. High School. After a year of break to prepare for medical sciences entrance exams, he pursued B.Sc. in Biotechnology from Institute of Genetic Engineering in Madhyamgram, West Bengal. In 2015, he went to University of Hyderabad for his M.Sc. in Plant Biology and Biotechnology. During his master's thesis he worked on rice ribosomal proteins and their role in abiotic stress tolerance. This experience helped him to decide for a research career in science. In 2017, he joined National Institute of Plant Genome Research in New Delhi as a Ph.D. student and worked on Arabidopsis root development in nutrient deficient conditions. After a short stay, he decided to go abroad for Ph.D. and in 2018 he arrived in Netherlands to start as a Ph.D. student in Laboratory of Biochemistry at Wageningen University. Here he worked on auxin signaling in *Marchantia polymorpha.* His research resulted in a better understanding of the native expression patterns of auxin signaling components and their stability. Shubhajit, wants to continue his research career working on auxin signaling and from March 2023 he has joined as a post-doctoral researcher in the Institute of Science and Technology in Austria.

Publications

Shubhajit Das, Martijn de Roij, Simon Bellows, Wouter Kohlen, Etienne Farcot, Dolf Weijers, Jan Willem Borst (2022) Selective degradation of ARF monomers controls auxin response in Marchantia. bioRxiv: https://doi.org/10.1101/2022.11.04.515187

Shubhajit Das, Dolf Weijers, Jan Willem Borst (2021) Auxin response by the numbers. Trends in Plant Sciences. 26: 442-451

Hirotaka Kato, Sumanth K Mutte*, Hidemasa Suzuki*, Isidro Crespo*, **Shubhajit Das***, Tatyana Radoeva*, Mattia Fontana*, Yoshihiro Yoshitake, Emi Hainiwa, Willy van den Berg, Simon Lindhoud, Kimitsune Ishizaki, Johannes Hohlbein, Jan Willem Borst, D Roeland Boer, Ryuichi Nishihama, Takayuki Kohchi, Dolf Weijers (2020) Design principles of a minimal auxin response system. Nature Plants. 6: 473-482

Anusree Saha, **Shubhajit Das**, Mazahar Moin, Mouboni Dutta, Achala Bakshi, M. S. Madhav, P. B. Kirti (2017) Genome-Wide Identification and Comprehensive Expression Profiling of Ribosomal Protein Small Subunit (RPS) Genes and their Comparative Analysis with the Large Subunit (RPL) Genes in Rice. Frontiers in Plant Sciences. 8: 1553

*These authors contributed equally

Education Statement of the Graduate School

Experimental Plant Sciences

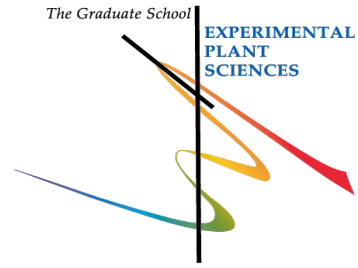

Issued to: **Shubhajit Das**
Date: **03 May 2023**
Group: **Laboratory of Biochemistry**
University: **Wageningen University and Research**

1) Start-Up Phase		*date*	*cp*
►	**First presentation of your project**		
	Integrative quantitative understanding of auxin response network	15 January, 2019	1.5
►	**Writing or rewriting a project proposal**		
►	**Writing a review or book chapter**		
	Das S, Weijers D, Borst JW. Auxin Response by the Numbers. *Trends Plant Sci*. 2021 May;26(5):442-451. doi:10.1016/j.tplants.2020.12.017	May, 2021	6.0
►	**MSc courses**		
	Subtotal Start-Up Phase		7.5
2) Scientific Exposure		*date*	*cp*
►	**EPS PhD days**		
	EPS PhD days 'Get2Gether', Soest (NL)	11-12 February, 2019	0.6
	EPS PhD days 'Get2Gether', Soest (NL)	03-04 May, 2022	0.6
►	**EPS theme symposia**		
	EPS theme 1 "Developmental Biology of Plants", Leiden (NL)	31 January, 2019	0.3
	EPS theme 1 "Developmental Biology of Plants", Wageningen (NL)	5 February, 2020	0.3
	EPS theme 1 "Developmental Biology of Plants", Wageningen (NL)	14 June, 2022	0.3
►	**Lunteren Days and other national platforms**		
	Annual Meeting "Experimental Plant Sciences", Lunteren (NL)	08-09 April, 2019	0.6
	Annual Meeting "Experimental Plant Sciences", Lunteren (NL)	11-12 April, 2022	0.6
►	**Seminars (series), workshops and symposia**		
	Seminar by Prof.Lucia Strader	10 September, 2018	0.1
	Seminar by Prof. Alexis Maizel	17 December, 2018	0.1
	Seminar by Prof. Jiří Friml	18 December, 2018	0.1
	Seminar by Prof Wolf Frommer	17 January, 2019	0.1
	Seminar by Prof Ari-Pekka Mähönen	19 June, 2019	0.1
	Seminar by Prof. Enrico Scarpella	19 June, 2019	0.1
	Seminar by Prof. Minako Ueda	04 September, 2019	0.1
	Seminar by Prof. Joe Kieber	30 May, 2022	0.1

	Seminar by Prof. Thorsten Hamann	14 June, 2022	0.1
	Mini symposium on Marchantia Biology, Wageningen (NL)	18 February, 2019	0.2
	Symposium "Land Plant Evolution & Improving Photosynthesis and Crops", Wageningen (NL)	20 June, 2019	0.3
	EPS Mendel mini-symposium, Wageningen (NL)	08 June, 2022	0.2
►	**Seminar plus**		
►	**International symposia and congresses**		
	Auxin 2022, Cavtat (HR)	02-07 October, 2022	1.2
	EMBO Workshop: An integrated view of early land plant evolution, online	08-11 November, 2022	0.9
►	**Presentations**		
	Poster presentation: Annual Meeting "Experimental Plant Sciences", Lunteren (NL)	08 April, 2019	1.0
	Oral Presentation: Plant Development and Adaptation cluster meeting, online	04 February, 2022	1.0
	Oral presentation: Annual Meeting "Experimental Plant Sciences", Lunteren (NL)	11 April, 2022	1.0
	Oral presentation: Auxin 2022, Cavtat (HR)	07 October, 2022	1.0
►	**IAB interview**		
►	**Excursions**		
	PhD trip to University of Bremen (DE)	03 December, 2018	0.3
	EPS online company visit Rijk Zwaan	16 June, 2021	0.2
	Subtotal Scientific Exposure		11.5
3) In-Depth Studies		*date*	*cp*
►	**Advanced scientific courses & workshops**		
	FEBS advanced course "Microspectroscopy: Functional Imaging of Biological Systems", Nijmegen & Wageningen (NL)	11-20 September, 2018	3.0
	EPS course "Transcription factors and Transcriptional Regulation", Wageningen (NL)	10-12 December, 2018	1.0
	PE&RC course "Basic Statistics", Wageningen (NL)	10-18 May, 2022	1.5
►	**Journal club**		
	Laboratory of Biochemistry	2018-2022	3.0
►	**Individual research training**		
	Subtotal In-Depth Studies		8.5
4) Personal Development		*date*	*cp*
►	**General skill training courses**		
	EPS Introduction Course, Wageningen (NL)	11 June, 2019	0.3
	WGS course "Project and Time Management", online	September - November, 2021	1.5
	WGS course "Adobe Indesign - From Dissertation Layout to Poster Design", online	November, 2021	0.6
	WGS course "Scientific Writing", online	May - July, 2022	1.8

	WGS workshop "Writing propositions for your PhD", online	10 June, 2022	0.0
	WGS workshop "Last stretch of PhD programme", online	10 June, 2022	0.0
►	**Organisation of meetings, PhD courses or outreach activities**		
►	**Membership of EPS PhD Council**		
	Subtotal Personal Development		4.2
	TOTAL NUMBER OF CREDIT POINTS*		**31.7**
Herewith the Graduate School declares that the PhD candidate has complied with the educational requirements set by the Educational Committee of EPS with a minimum total of 30 ECTS credits.			
** A credit represents a normative study load of 28 hours of study.*			

The research presented in this thesis was performed at the Laboratory of Biochemistry, Wageningen University & Research, and was financially supported by a grant from the Netherlands Organization for Scientific Research (NOW: ALWOP.402)

Financial support from the Laboratory of Biochemistry for printing this thesis is gratefully acknowledged.
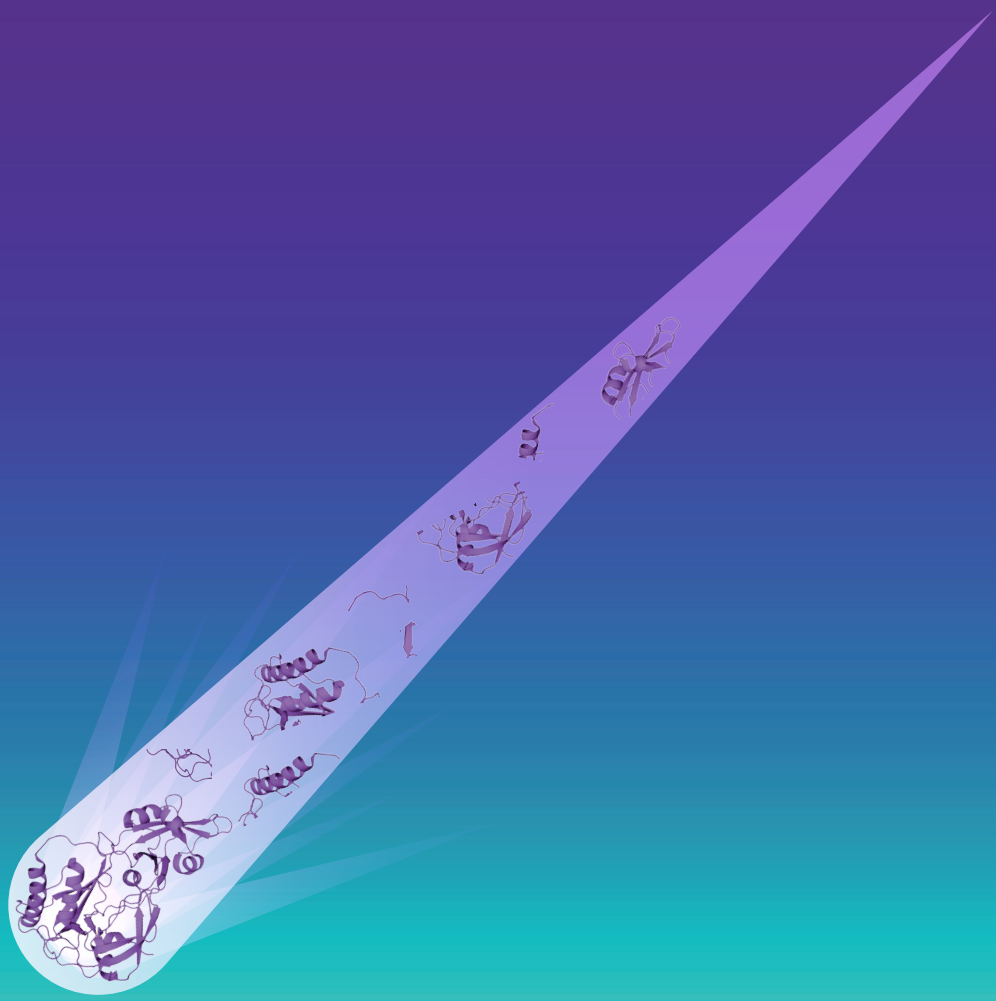
Cover design by Shubhajit Das
Layout by Shubhajit Das and ProefschriftMaken.nl
Printed by ProefschriftMaken.nl